

**Expression and Localisation of the *Mycobacterium marinum*
Potential Virulence Factor, MPM70 during Infection:
Evidence for a Post-Phagosomal Role in Pathogenesis**

Thesis submitted for the degree of
Doctor of Philosophy
University of Leicester

By
Alistair Ray, BSc Hons. (Bath)
Department of Biochemistry
University of Leicester

September 2010

Abstract

During infection, MPT70 is one of the most highly upregulated *Mycobacterium tuberculosis* genes, implying an important role in virulence. To track expression of MPT70 during macrophage infection, a *Mycobacterium marinum*: J774A.1 macrophage infection model was used with a custom polyclonal antibody raised against purified full-length, folded MPM70 without its N-terminal signal sequence (88% homology to *M. tuberculosis* MPT70). Immunofluorescence studies showed that MPM70 is localised in large, non-uniformly arranged buttresses along the mycobacterial cell surface. Analysis of representative confocal microscopy images revealed that MPM70 expression was lowest at initial infection levels of 1-5 mycobacteria per host cell, but was greatly upregulated at mycobacterial densities of over 6, where expression remained constant in around 20% of the infected cells up to mycobacterial densities of greater than 35. This implies that MPM70 expression is independent of mycobacterial density following the initial stages of infection and may be triggered by individual mycobacteria contacting a specific cytoplasmic host cell factor. Cytoplasmic tracks of MPM70 were a rare observation, but suggest that the protein may act as a molecular intermediate between the mycobacterial surface and a cytoplasmic host cell protein. Structural analyses and comparisons to eukaryotic homologues such as fasciclin and β ig-H3 reveal two potential interaction faces on opposite sides of MPT70, which supports the hypothesis that MPT70/MPM70 may act as a 'molecular bridge' between two proteins. Evidence of MPM70 production in cell infections using a Δ RD1 strain of *M. marinum* showed that MPM70 expression is RD1 independent. We used the lysosomal marker LAMP-1 and the lipophilic dye DiIC₁₈(5)-DS to show that expression of MPM70 occurs after mycobacteria have escaped from the phagolysosome. A possible role for MPM70 in the modulation of host cell actin was investigated, but fluorescent phalloidin staining showed no co-localisation with expressed MPM70.

Acknowledgements

This thesis is dedicated to my Dad. I hope you'd be proud of my achievements here, and would be interested in some of my findings. You're missed greatly.

I would like to thank the Biotechnology and Biological Sciences Research Council and the Wellcome Trust for their funding in this project.

My thanks also go to Dr. Thierry Soldati and especially Dr. Monica Hagedorn at the University of Geneva, who provided me with *Mycobacterium marinum* strains. The fluorescent *Mycobacterium marinum* strains were originally engineered by Dr. Lalita Ramakrishnan at the University of Washington. Cambridge Research Biochemicals also deserve thanks for producing the polyclonal antibodies that made much of this research possible, and for a level of customer service that was far in excess of my expectations.

Prof. Mark Carr has been a fantastic supervisor throughout my time at Leicester, and I'd like to extend my thanks to him for his support and ideas throughout the project. Dr. Richard Williamson and Dr. Bernie Burke have also been excellent committee members, full of ideas to push myself and my project in a positive direction. Dr. Kirsty Lightbody and Dr. Philip Renshaw have been fundamental to my development and the success of this project. Thanks to Dr. Lorna Waters for the NMR spectra in this thesis, Dr. Vaclav Veverka for structural analyses of MPB70 and MPM70 substitution mutations, and to Dr. Andrew Bottrill for the mass spectroscopy data. Many thanks to Dr. Kees Straatman for his help and endless patience with me on the confocal and Scan^R microscopes.

I'd like to thank everyone in the MDC group for their help and friendship over the years, you guys have been a great example of just how good an academic group can be, in terms of your scientific knowledge, team spirit and ability to have a laugh too!

Thanks also, Mum, Adi and all my family. You guys have been supportive helpful and positive. I know you'll all see this as an achievement to feel proud of. To my friends Jamie, Sammy, Rob, Alan and Charlie to mention a few; you've been a great source of distraction over the years. You guys are true legends.

And finally, my thanks go to Ruby. You've been loving, fun and inspirational during my PhD, all while doing your own research at the same time.

Alistair Ray, Leicester, September 2010.

Contents

Abstract	2
Acknowledgements	3
Chapter 1, Introduction	10
1.1 Tuberculosis, the disease and current situation.....	10
1.2 The Organism.....	13
1.3 Tuberculosis Infection, and Host-Pathogen Interactions	18
1.4 Cell Biology of Tuberculosis Infection.....	21
1.4.1 Mycobacteria escape the phagosome during early infection	23
1.4.2 Modulation of host cell actin by mycobacteria.....	27
1.4.3 Granuloma formation	30
1.5 Secreted Mycobacterial Proteins.....	31
1.6 MPT70/MPB70, MPT83/MPB83 and MPM70 proteins.....	32
1.7 Aims of this project.....	36
Chapter 2, Production of anti-MPM70 polyclonal antibodies and characterisation of the <i>Mycobacterium marinum</i> : J774A.1 infection model	41
2.1 Introduction	41
2.2 Methods	42
2.2.1 Bacterial strains, Cell lines and Media.....	42
2.2.2 DNA Analysis by Agarose Gel Electrophoresis	43
2.2.3 SDS Polyacrylamide Gel Electrophoresis (SDS-PAGE).....	43
2.2.4 Cloning of MPB70 and MPM70 with a C-terminal His tag	45
2.2.5 Expression trials of C-terminally His tagged (cHis) MPB70 and MPM70	49
2.2.6 Purification of cHis MPB70 and cHis MPM70	49
2.2.7 Mass spectroscopy analysis of the cHIS MPB70 and cHIS MPM70 purified proteins.....	51
2.2.8 ¹ H NMR analysis of the cHIS MPB70 and cHIS MPM70 purified proteins.....	52
2.2.9 Production of rabbit anti-MPM70 polyclonal antibodies 4060 and 4061	52
2.2.10 Purification of polyclonal antibodies from rabbit 4060 and 4061 sera.....	52
2.2.11 Dot-blot to test the sensitivity of polyclonal antibodies 4060 and 4061 to purified MPM70.....	53
2.2.12 Enzyme-Linked Immunosorbent Assay (ELISA) to determine the sensitivity of polyclonal antibodies 4060 and 4061 to purified MPM70.....	54
2.2.13 J774 macrophage infections with fluorescent <i>M. marinum</i>	55

2.2.14 Confocal fluorescence microscopy/slide preparation	55
2.3 Results	57
2.3.1 Cloning of MPB70 and MPM70 with a C-terminal HIS tag	57
2.3.2 Expression trials of C-terminally His tagged (cHis) MPB70 and cHis MPM7061	
2.3.3 Purification of cHis MPB70 and cHis MPM70	64
2.3.4 Mass spectroscopy analysis of purified MPM70	67
2.3.5 ¹ H NMR to assess physical properties of purified MPB70 and MPM70	
proteins.....	69
2.3.6 Purification of polyclonal antibodies from rabbit 4060 and 4061 sera.....	71
2.3.7 Dot-blots to test the sensitivity of polyclonal antibodies 4060 and 4061 to	
purified MPM70.....	74
2.3.8 Enzyme-Linked Immunosorbent Assay (ELISA)	75
2.3.9 Characterisation of the <i>Mycobacterium marinum</i> : J774 macrophage infection	
model.....	76
2.4 Discussion	81
Chapter 3, Localisation and quantification of MPM70 expression during infection	
.....	85
3.1 Introduction	85
3.2 Methods	86
3.2.1 J774A.1 macrophage infections with fluorescent <i>Mycobacterium marinum</i>	86
3.2.2 Western blot analysis of the expression of MPM70 in <i>Mycobacterium Marinum</i>	
in infected macrophages.....	86
3.2.3 Confocal fluorescence imaging of MPM70 expression during infection	87
3.2.4 Quantification of MPM70 expression from fluorescent microscope slides.....	89
3.2.5 Immobilised MPB70/MPM70-based screens for host cell interaction targets... 89	
3.3 Results	92
3.3.1 Global MPM70 expression in <i>Mycobacterium marinum</i> infected macrophage	
cells.....	92
3.3.2 MPM70 expression is localised closely to the outer surface of <i>Mycobacterium</i>	
<i>marinum</i>	94
3.3.3 Characterisation of the <i>M. marinum</i> :J774A.1 macrophage infection model and	
MPM70 expression	99
3.3.4 MPM70 expression is not associated with phagolysosomal <i>Mycobacterium</i>	
<i>marinum</i>	105
3.3.5 MPM70 expression is not associated with actin polymerisation	108

3.3.6 Phagosomal escape and MPM70 expression are RD1 independent in <i>Mycobacterium marinum</i>	110
3.3.7 Immunoprecipitation confirms that MPM70 is strongly associated with the mycobacterial surface.....	112
3.3.8 Assessment of pull-down experiments to identify MPB70 and MPM70 binding targets.....	113
3.4 Discussion	117
Chapter 4, Conclusions and future work	123
4.1.1 Cloning of MPB70, MPM70 and the production of anti-MPM70 polyclonal antibodies.....	123
4.1.2 Characterisation of the <i>Mycobacterium marinum</i> :J774A.1 macrophage infection model.....	124
4.1.3 Characterisation of MPM70 expression and localisation during infection.....	125
4.2 Future directions	129
References	132

Abbreviations

Single and Three-Letter Codes for Amino Acids:

Alanine	A	Ala	Leucine	L	Leu
Arginine	R	Arg	Lysine	K	Lys
Asparagine	N	Asn	Methionine	M	Met
Aspartic Acid	D	Asp	Phenylalanine	F	Phe
Cysteine	C	Cys	Proline	P	Pro
Glutamine	Q	Gln	Serine	S	Ser
Glutamic Acid	E	Glu	Threonine	T	Thr
Glycine	G	Gly	Tryptophan	W	Trp
Histidine	H	His	Tyrosine	Y	Tyr
Isoleucine	I	Ile	Valine	V	Val

DNA Bases:

Adenine	A	Guanine	G
Cytosine	C	Thymine	T

Abbreviations:

AEBSF	4-(2-Aminoethyl) benzenesulfonyl fluoride hydrochloride
AIDS	Acquired immunodeficiency syndrome
Amp	Ampicillin
ATP	Adenosine-5'-triphosphate
B-cell	Bursa dependent lymphocyte
Bis-Tris	2-[bis(2-hydroxyethyl)amino]-2-hydroxymethyl-propane-1,3-diol
BSA	Bovine serum albumin

bp	Base pair
CFP-10	Culture filtrate protein, 10kDa
Da	Dalton
dH ₂ O	De-ionised water
DNA	Deoxyribonucleic acid
dNTP	Deoxynucleotide triphosphate
DOTS	Direct observed therapy short-course
DTH	Delayed-type hypersensitivity
DTT	1,4,-dithiothreitol
EDTA	Ethylene diaminetetraacetate
ESAT-6	Early secreted antigenic target, 6kDa
ESAT-6/CFP-10	The ESAT-6 CFP10 complex
FCS	Foetal calf serum
HIV	Human immunodeficiency virus
IFN γ	Interferon gamma
IL	Interleukin
INH	Isoniazid
IPTG	Isopropyl-1-thio- β -D-galactoside
Kan	Kanamycin
kDa	kilo Dalton
LB	Luria-Bertani
LDS	Lithium dodecyl sulphate
MDR	Multiple drug resistant
MMP9	Matrix metalloproteinase 9
MMAR	<i>Mycobacterium marinum</i>
MPB	<i>Mycobacterium bovis</i> protein

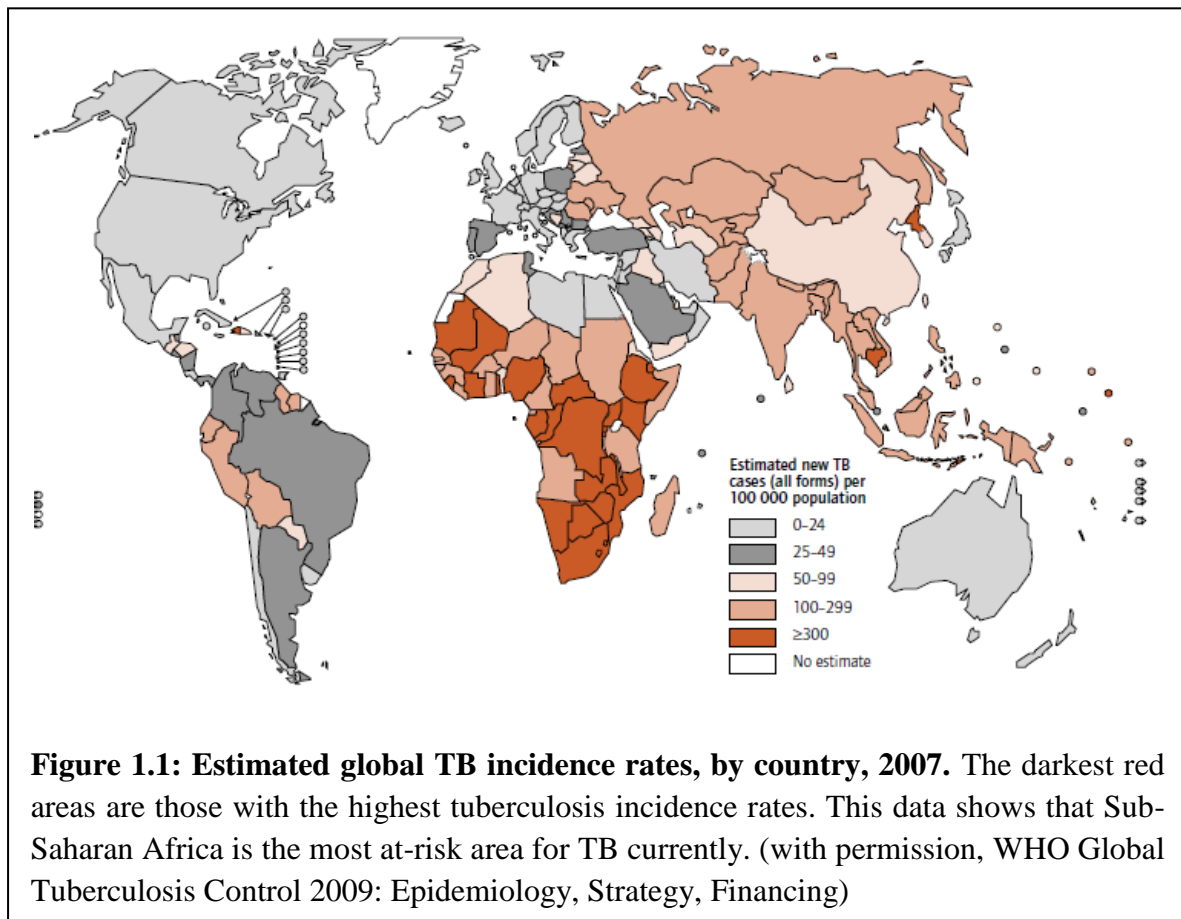
MPM	<i>Mycobacterium marinum</i> protein
MPT	<i>Mycobacterium tuberculosis</i> protein
MTB	<i>Mycobacterium tuberculosis</i>
MW	Molecular weight
OADC	Oleic acid-albumin-dextrose-catalase
OD	Optical density
PAGE	Polyacrylamide gel electrophoresis
PBS	Phosphate buffered saline
PCR	Polymerase chain reaction
PFA	Paraformaldehyde
<i>Pfu</i>	<i>Pyrococcus furiosus</i>
RD	Region of difference
RIF	Rifampicin
RPM	Revolutions per minute
SDS	Sodium dodecyl sulphate
TAE	Tris-acetate
TB	Tuberculosis
T-cell	Thymus-dependent lymphocyte
TE	Tris HCL-EDTA buffer
TNF α	Tumour necrosis factor alpha
Tris	2-amino-2-hydroxymethyl-propane-1,3-diol
UV	Ultraviolet
v/v	Volume per volume
w/v	Weight per volume
WCL	Whole Cell Lysate
WHO	World Health Organisation

Chapter 1

Introduction

1.1 Tuberculosis, the disease and current situation

The World Health Organisation (WHO) estimate that one person is infected with TB every second, and that in 2007 there were 9.27 million new cases, compared to 9.24 million new cases in 2006. The countries of highest incidence, from first to fifth, were India, China, Indonesia, Nigeria and South Africa (figure 1.1), and many of these areas show a correlation between HIV prevalence and TB incidence, as shown in figure 1.2 (World Health Organisation, 2009)



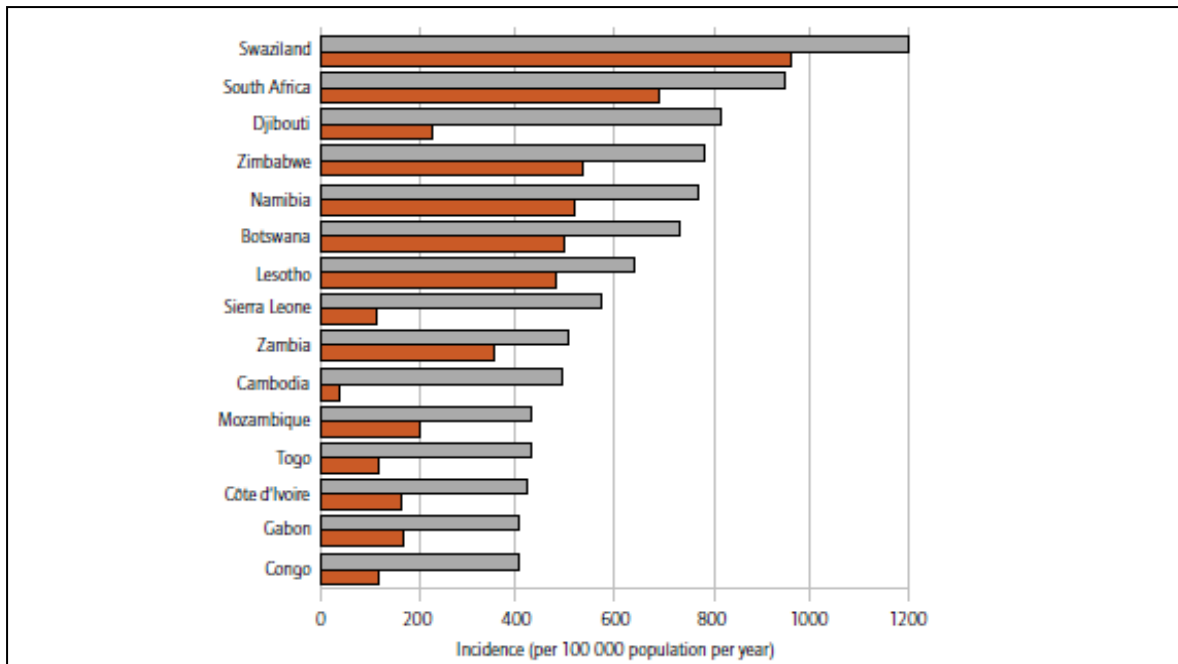


Figure 1.2: TB Incidence rates and HIV. Fifteen countries with the highest estimated TB incidence rates (all forms of TB, grey bars) and corresponding HIV-related TB incidence (red bars) 2007. The highest HIV rates often correlate with higher rates of tuberculosis. (with permission, WHO Global Tuberculosis Control 2009: Epidemiology, Strategy, Financing)

Worldwide, there is a growing link between HIV/AIDS and TB infection. An estimated 1.32 million HIV-negative people died from TB in 2007, and there were a further 456,000 deaths in HIV-positive people. TB accounts for around 23% of all HIV-related deaths, of which there are an estimated 2 million annually (World Health Organisation, 2009).

Another complication in the fight against TB is the emergence of Multi-Drug Resistant TB (MDR-TB), which is resistant to at least the main two first-line drugs used to treat TB infection; Isoniazid (INH) and rifampicin (RIF). Extensively Drug Resistant TB (XDR-TB) resistant to at least INH and RIF, as well as to any member of the quinolone family and at least one of the following second-line drugs: kanamycin, capreomycin, or amikacin (World Health Organisation, 2006).

RIF acts on many bacteria, and functions as a bactericidal agent by binding tightly, and inhibiting, the bacterial DNA-dependent RNA polymerase (Hartmann *et al.*, 1967). RIF resistance arises almost exclusively from mutations in the *rpoB* gene which encodes for the beta-subunit of the RNA polymerase core, and 95% of tested RIF-resistant MTB strains were found to share the same missense mutation in the beta subunit as found in RIF-resistant *Escherichia coli*, with the remaining strains showing a novel A381V substitution in the N-terminal region of the protein (Taniguchi *et al.*, 1996).

Isoniazid is a prodrug which requires bacterial cellular processing before reaching its active form, and the enzyme governing this reaction is the catalase-peroxidase katG. (Rattan *et al.*, 1998). The drug acts to inhibit mycolic acid synthesis, which is thought to make the mycobacteria more susceptible to environmental stresses, like reactive oxygen species, and deletion of katG from the chromosome was found to be associated with INH resistance in two clinical isolates of *Mycobacterium tuberculosis* (Zhang *et al.*, 1992). However, the most common mutation in the activating KatG enzyme is a serine-threonine substitution at residue 315 (S315T) and this occurs in around 30-60% of all resistant mutants (Musser *et al.*, 1996; Slayden *et al.*, 2000). INH and RIF are mainly used in combination to give the best chance of clearing the infection. These drugs are administered over a 6-8 month course of treatment, known as Direct Observed Therapy Short-course (DOTS) which was outlined by the WHO in 2004. This therapy course treats sputum smear-positive patients, and ensures that they are supervised, taking each dose of chemotherapy for the full 6-8 month treatment course. DOTS also comprises a full monitoring and patient record system as well as a commitment to establish and maintain a consistent supply of essential anti-tuberculosis drugs (World Health Organisation, 2004).

The most common preventative way of dealing with the problem of tuberculosis is via vaccination with *M. bovis* BCG. *M. bovis* BCG is an attenuated form of *Mycobacterium bovis*, and was derived between 1908 and 1921 at the Pasteur institute. It provided effective TB protection in animal models and has been adapted to human vaccination programs. It has been found that this attenuated mycobacterium is avirulent because it lacks around 13 genomic regions, or RDs (Regions of Difference 1-13). However, the only shared Region of Difference between all BCG strains is RD1 (Behr *et al.*, 1999). H37Rv TB with the RD1 region knocked out showed an infection profile much the same as the original BCG infection, and furthermore, BCG could be complemented with a WT RD1 region, which gave rise to a full necrotic infection (Junqueira-Kipnis *et al.*, 2006). This shows that the virulence proteins encoded by the RD1 region, including ESAT-6 and CFP-10, are required for full virulence of the organism.

1.2 The Organism

In humans, tuberculosis is mainly caused by *Mycobacterium tuberculosis* and *Mycobacterium africanum*. These two organisms are part of a larger, highly genetically similar group of organisms known as the *Mycobacterium tuberculosis* Complex (MTB Complex) (Sreevatsan *et al.*, 1997). This group comprises of the aforementioned *M. tuberculosis* and *M. africanum* (the main causative agent of tuberculosis in Africa), as well as *Mycobacterium bovis*, a broad-range pathogen which affects animals like cattle, as well as humans. One important point to note is that *M. bovis* carries an intrinsic resistance to the front-line antibiotic pyrazinamide, which must be considered during treatment of a patient infected with this bacillus (Allix-Beguec *et al.*, 2010). *M. bovis* BCG is a laboratory-attenuated vaccine strain of *M. bovis*. It carries a number of genetic

deletions that render it avirulent, known as Regions of Difference. Furthermore, it has been proposed that Single Nucleotide Polymorphisms (SNPs) may play a significant part in the attenuated virulence in *M. Bovis* BCG. Full-genome comparison studies revealed 736 SNPs between virulent *M. Bovis* and *M. Bovis* BCG Pasteur (Brosch *et al*, 2007, Garnier *et al*, 2003), and further work comparing 21 virulent *M. Bovis* strains with 13 BCG strains revealed only 186 SNPs shared between all BCG strains, 115 of which affect important functions such as global regulators, transcription factors and central metabolism, which may give rise to attenuated virulence (Carmen Garcia Pelayo *et al*, 2009).

M. microti is a rodent pathogen, mainly affecting voles and shrews, but has recently been found to inhabit the feline host. *M. microti* is distinguished from other members of the MTB Complex in that it has an RD1 deletion, like *M. bovis* BCG, but has intact RD4 and RD12 loci, which are otherwise missing in the vaccine strain (Smith *et al*, 2009). *M. canettii* is a rare causative agent of human tuberculosis (Pfyffer *et al*, 1998), and is identified by its smooth colony morphology and differing sequence of the gene *recA*, which encodes a DNA recombinase (van Soolingen *et al*, 1997).

Members of this complex are classified as acid-fast, which means that their cell wall is resistant to acid destaining during staining procedures. When Gram stained they produce an abnormal Gram-positive result due to the mycolic acid present in the cell wall. As such, acid-fast stains such as the Ziehl-Neelsen stain have been devised, which stain backgrounds blue and the acid-fast bacilli pink (Madison, 2001).

In the study presented here, *M. marinum* is adopted as a model organism for mycobacterial infection. *M. marinum* is a pathogen of fish and amphibians, and is closely related to *M. tuberculosis*. The genome encodes 3000 *M. tuberculosis*

orthologues with an average amino acid identity of 85% (Stinear *et al.*, 2008). However, *M. marinum* is a more broad-range pathogen with a larger genome, of around 6000 genes compared to *M. tuberculosis*, which has only around 4000 (Cole *et al.*, 1998). This is thought to represent significant downsizing and lateral gene transfer in order to make *M. tuberculosis* a human/primate-specific pathogen (Stinear *et al.*, 2008). The *M. marinum* infection itself causes a wasting disease in infected fish, and is aptly named ‘Fish Tuberculosis’, but is unable to infect humans in the same way as *M. tuberculosis* due to its poor growth at 37°C. *M. marinum* can only infect at the skin surface of infected human patients, where it can grow at a more favourable temperature of 25-35°C (Tobin *et al.*, 2008).

The result is a granuloma formed under the skin, which is strikingly similar in pathology to the lesions found in the lung during *Mycobacterium tuberculosis* infection.

Mycobacterium marinum is widely used in the field of tuberculosis research, and is beneficial to our particular study for a number of reasons. Firstly, it is much safer to work with than *M. tuberculosis*, being a Biological Laboratory Safety classification 2 organism. Secondly, many studies have shown that in a range of model organisms, it forms granulomas analogous to those formed in the human lung by *M. tuberculosis* (Cosma *et al.*, 2004; Ramakrishnan *et al.*, 2004; Cosma *et al.*, 2006; Davis *et al.*, 2009).

The last reason for using the *M. marinum* infection model in our experiments lies within the genome of the pathogen itself, and the proteins of interest to this thesis, MPB70, MPB83 and MPM70 (see Section 1.6). In previous MPB70 studies in *M. tuberculosis* and *M. bovis* BCG, antibodies have been unable to distinguish between MPB70 and MPB83 due to their 88% homology (70% identity). However, *M. marinum* has no homologue for MPB83 within its genome, and has a single MPB70 homologue,

MPM70, which has an 88% homology (67.5% identity) to MPB70 (Cole *et al.*, 1998, Stinear *et al.*, 2008). The multiple sequence alignment in Figure 1.3 shows the strong homology between all three of these proteins, with the main difference being the N-terminal region where MPB83 is glycosylated for mycobacterial cell surface localisation. This means that an antibody raised against MPM70 should identify the single protein we are looking for, and give a clear idea of its localisation during infection.

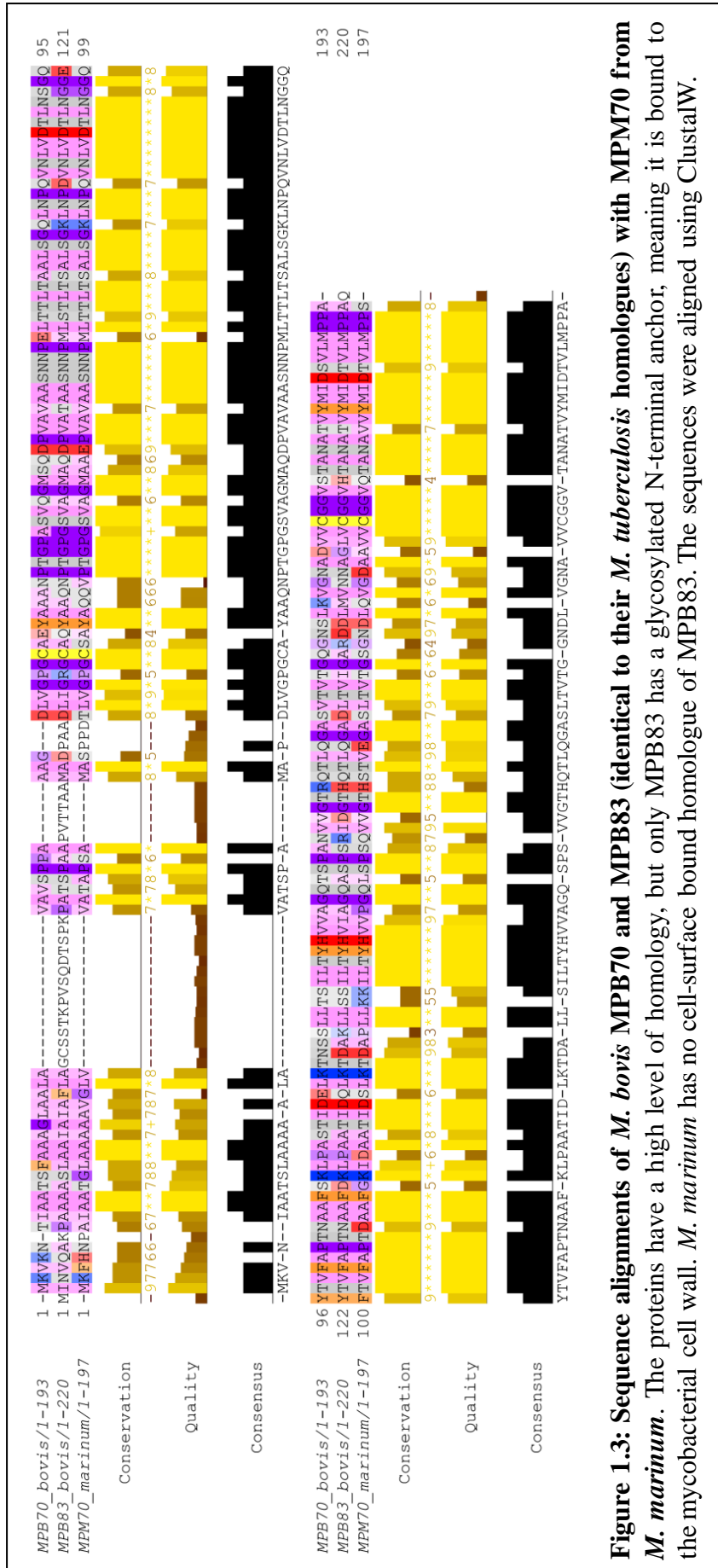


Figure 1.3: Sequence alignments of *M. bovis* MPB70 and MPB83 (identical to their *M. tuberculosis* homologues) with MPM70 from *M. marinum*. The proteins have a high level of homology, but only MPB83 has a glycosylated N-terminal anchor, meaning it is bound to the mycobacterial cell wall. *M. marinum* has no cell-surface bound homologue of MPB83. The sequences were aligned using ClustalW.

1.3 Tuberculosis Infection and Host-Pathogen Interactions

The tuberculosis infection starts when mycobacteria inhaled in air droplets are uptaken by alveolar macrophages. From here, the course of infection can proceed in a number of directions, as summarised in Figure 1.4.

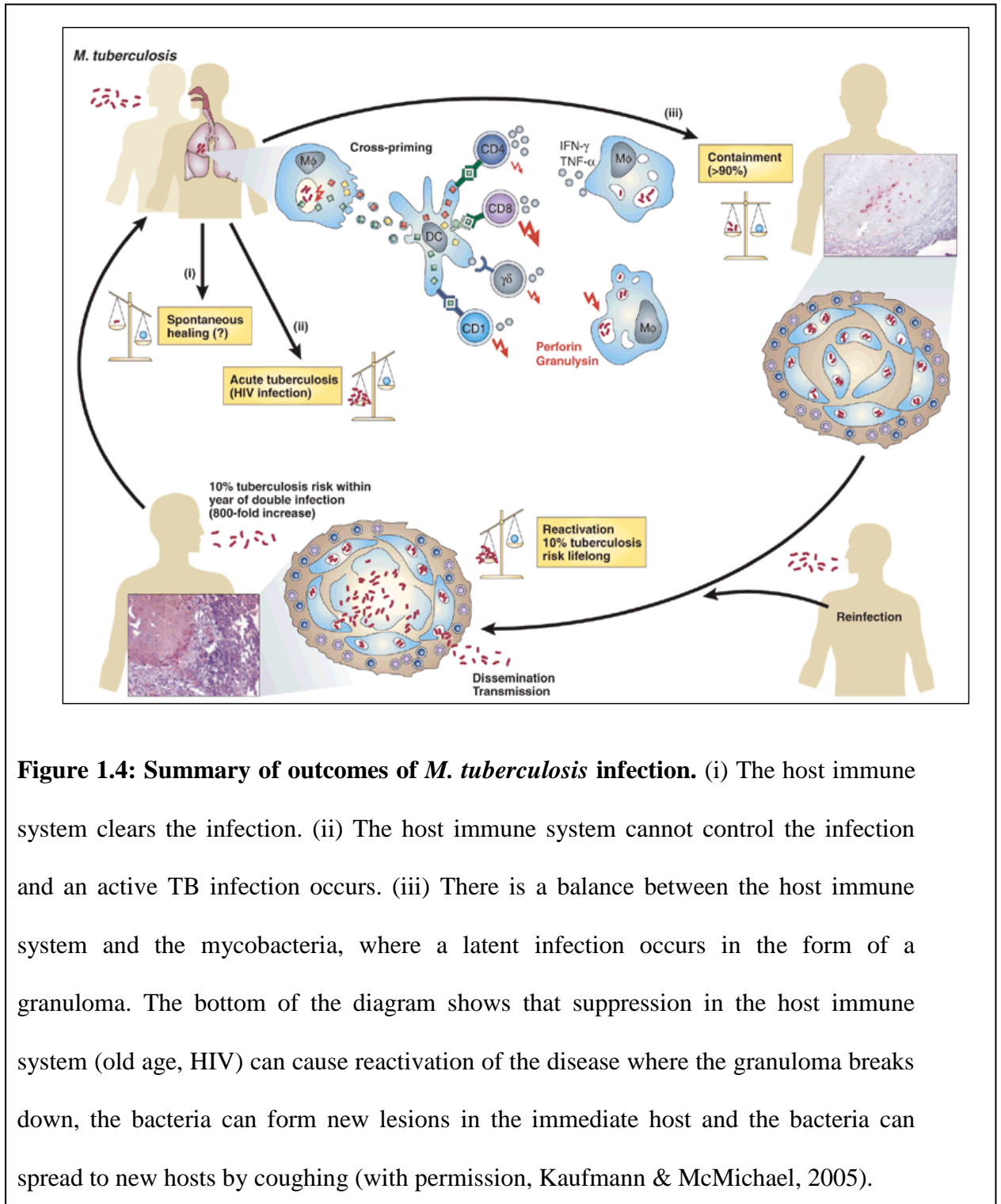


Figure 1.4: Summary of outcomes of *M. tuberculosis* infection. (i) The host immune system clears the infection. (ii) The host immune system cannot control the infection and an active TB infection occurs. (iii) There is a balance between the host immune system and the mycobacteria, where a latent infection occurs in the form of a granuloma. The bottom of the diagram shows that suppression in the host immune system (old age, HIV) can cause reactivation of the disease where the granuloma breaks down, the bacteria can form new lesions in the immediate host and the bacteria can spread to new hosts by coughing (with permission, Kaufmann & McMichael, 2005).

Only around 10% of TB infections result in the active, wasting disease associated with the active tuberculosis infection (World Health Organisation, 2009). The majority of airborne bacilli are cleared from the upper respiratory tract before they reach the lung. Once in the lung, the bacilli are phagocytosed by alveolar macrophages and dendritic cells. These phagocytes are unable to kill the pathogen due to the mycobacteria's ability to prevent phagosome/lysosome fusion (Malik *et al.*, 2000; Fratti *et al.*, 2003.)

The majority of TB infections (80-90%) lead to the formation of an asymptomatic latent infection. This type of TB infection arises when the alveolar macrophages phagocytose the bacilli, and then recruit mononuclear cells from the surrounding vasculature to the site of infection. This forms an early granuloma, where the infected core is surrounded by large, multinucleate foamy macrophages, followed by a layer of individual macrophages and lymphocytes (as shown in Figure 1.5). Fibroblasts at the outer rim of the granuloma form a fibrous cuff. This type of lesion can remain in the host as 'latent', asymptomatic tuberculosis for a number of years until there is a change in the host immune system through old age, HIV/AIDS, or immunosuppressive drugs. This leads to a breakdown in the centre of the granuloma, causing spread of the mycobacteria through the host lung and causing a cough which spreads the bacteria to new hosts (Russell, 2007).

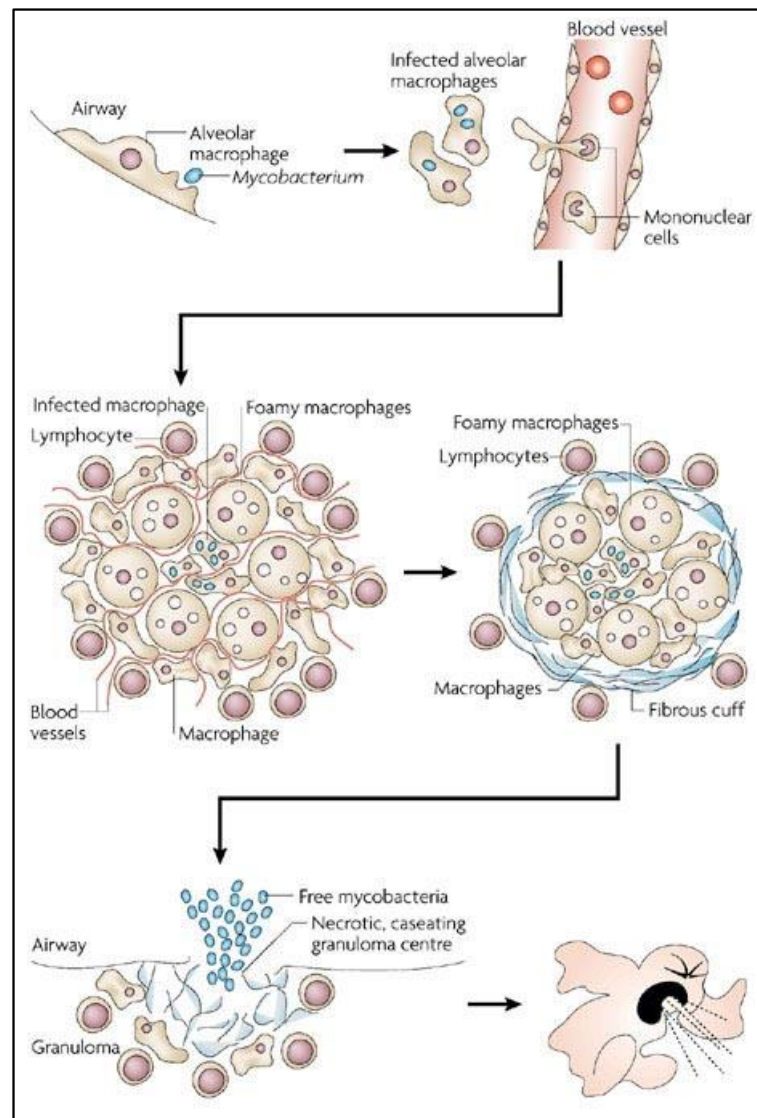


Figure 1.5: A diagrammatical representation of early, latent and reactivated TB infection stages. The mycobacteria are first uptaken by alveolar macrophages, and monocytes from the bloodstream are targeted to the infection site where a granuloma is formed. The infected macrophages in the centre of the granuloma are surrounded by multinucleate foamy giant cells, single macrophages and lymphocytes. A fibrous cuff forms around the outside of the granuloma where it can remain as a latent infection for a number of years. A change in the immune system through old age, disease, or immunosuppression can lead to a breakdown of the granuloma where free mycobacteria are spread via liquid droplets as the host coughs (with permission, Russell, 2007).

1.4 Cell Biology of Tuberculosis Infection

In order to understand the TB infection at a cellular level, it can be studied using modern molecular biology and biochemical techniques. This is achieved using various model organisms and cell lines in order to replicate the different stages and conditions of a tuberculosis infection.

Many recent advances in the field of mycobacterial infection were made using immunofluorescence and confocal microscopy, such as phagosomal escape during early infection, and the formation of actin tails (Stamm *et al.*, 2003; van der Wel *et al.*, 2007; Hagedorn *et al.*, 2009). For immunofluorescence in this study (Chapter 3), secondary antibodies and phalloidin were conjugated to a range of AlexaFluor dyes, including AlexaFluors 488, 555 and 633. AlexaFluor dyes have well-differentiated spectra which allow use of multiple dyes together with minimal bleed-through. The dyes are pH insensitive between pH 4 and 10, water soluble and are more fluorescent and photostable than alternative fluorescent dyes like Fluorescein, while keeping almost identical excitation and emission spectra (Panchuk-Voloshina *et al.*, 1999). The structure of AlexFluor 488 and comparative fluorescence with Fluorescein-EX is shown in Figure 1.6.

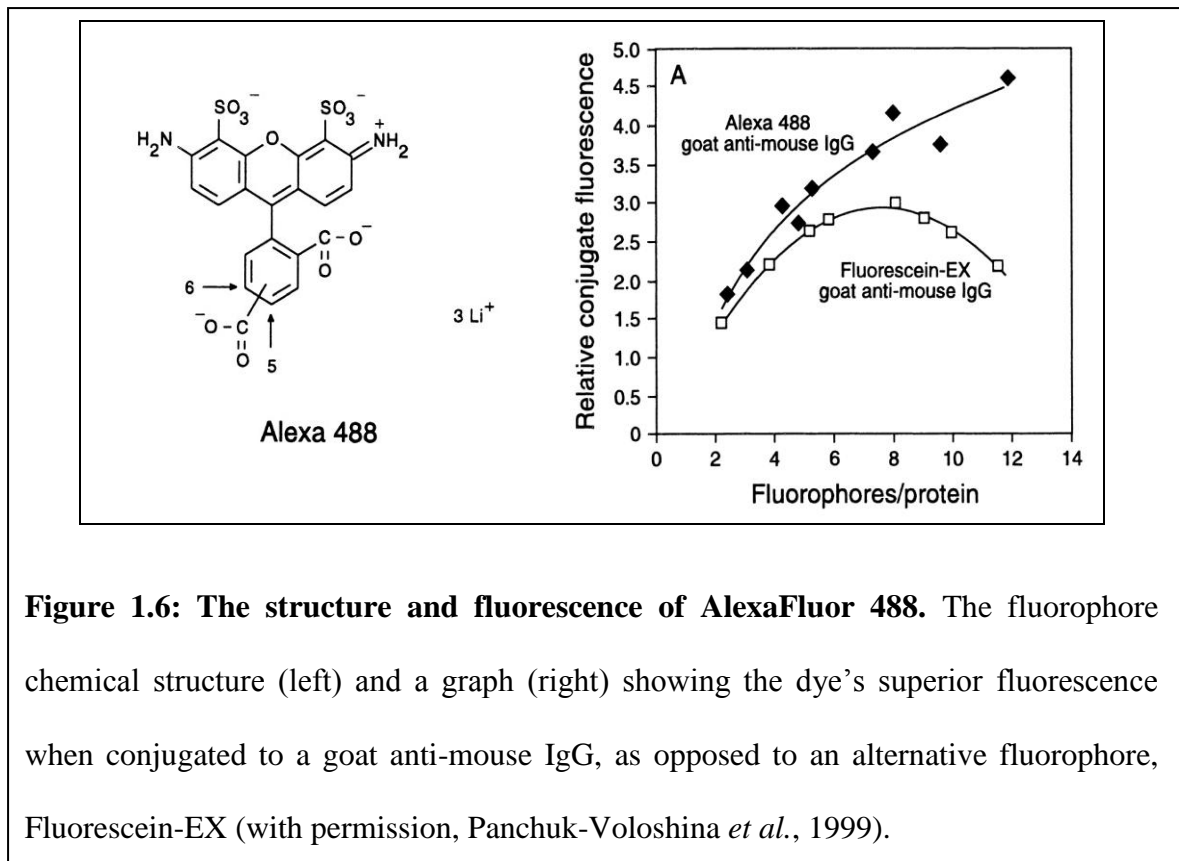


Figure 1.6: The structure and fluorescence of AlexaFluor 488. The fluorophore chemical structure (left) and a graph (right) showing the dye's superior fluorescence when conjugated to a goat anti-mouse IgG, as opposed to an alternative fluorophore, Fluorescein-EX (with permission, Panchuk-Voloshina *et al.*, 1999).

Fluorescent mycobacteria have been used in a number of studies (Cosma *et al.*, 2004; van der Wel *et al.*, 2007), and are usually rendered fluorescent via expression of GFP or DsRed in an extrachromosomal plasmid, driven by a mycobacterial promoter, such as *msp12* (Valdivia *et al.*, 1996; Cosma *et al.*, 2002; Cosma *et al.*, 2004). These plasmids confer constitutive expression of the fluorescent proteins, allowing visualisation of the mycobacteria in confocal microscopy. AlexaFluor Phalloidin is a commonly-used fluorescent F-actin stain that is used to observe the various states of host actin polymerisation by *M. marinum* once they have escaped the phagosome. This includes actin tail formation (Stamm *et al.*, 2003) and ejectosome formation to facilitate non-lytic cell-cell spread in the social amoeba *Dictyostelium* (Hagedorn *et al.*, 2009).

1.4.1 Mycobacteria escape the phagosome during early infection

There is some controversy as to the cellular localisation of mycobacteria during infection. It has been proposed that throughout the course of infection mycobacteria remain, and replicate, within the phagosome. They are thought to do so by preventing full maturation of the phagosome to avoid intracellular killing (Malik *et al.*, 2000; Fratti *et al.*, 2003). The mechanism by which mycobacteria block phagosome maturation and lysosome fusion remains elusive, however, in *M. avium* it has been shown to be dependent on an adequate iron supply to the mycobacteria and the potential blocking of the GTPase Rab5, which regulates early endosome fusion (Kelley and Schorey, 2002). This blocking of endosome/lysosome fusion may also be dependent upon certain mycobacterial cell wall components, such as lipoarabinomannan (LAM), which blocks the acquisition of late endosomal/lysosomal constituents in early endosomes (Vergne *et al.*, 2003b) and phosphatidylinositol mannoside (PIM), which facilitates endosome fusion with early endosomal compartments, effectively halting full phagosome/lysosome maturation (Vergne *et al.*, 2003b). The blocking of phagosomal maturation has also been shown in *M. marinum*, where live, infecting mycobacteria in murine macrophages localised to non-acidified vesicles, but heat-killed organisms and latex beads were seen in fully acidified lysosomes (Barker *et al.*, 1997).

The first evidence of mycobacteria escaping the phagosomal compartment and localising to the host cell cytoplasm came from electron microscopy studies on *M. tuberculosis* H37Rv-infected rabbit alveolar macrophages. Phagosomal membrane disruption was seen only in fully virulent *M. tuberculosis* H37Rv, but not with the avirulent H37Ra strain or *M. bovis* BCG (Myrvik *et al.*, 1984; Leake *et al.*, 1984). Further electron microscopy work later defined that a small population of both *M.*

tuberculosis H37Rv and H37Ra may escape into the host cell cytoplasm, but may be contained in tightly-apposed membrane compartments that are difficult to resolve, even by electron microscopy (McDonough *et al.*, 1993). Electron microscopy on *Rana pipiens* (Northern leopard frog) infected with *M. marinum* also showed that intracellular mycobacteria within granulomas were always found within host cell-membrane structures, rather than being free in the cytoplasm (Bouley *et al.*, 2001). More recent electron microscopy studies have since shown that *M. tuberculosis*, *M. bovis* and *M. bovis* BCG are found exclusively within phagosomal membrane compartments in both human and murine macrophages, up to six days post-infection (Jordao *et al.*, 2008).

Contrary to these observations, other microscopy evidence has shown that virulent mycobacteria migrate into the cytosol of infected non-apoptotic cells where they can replicate, free from the bactericidal environment of the phagosome (van der Wel *et al.*, 2007). Bacteria lacking the RD1 locus were unable to escape the into the host cytoplasm (van der Wel *et al.*, 2007). Figure 1.7 shows green fluorescent, fully virulent *M. tuberculosis* at both 4 h post-infection (hpi) in dendritic cells, where the mycobacteria are localised with the lysosomal markers LAMP-1 and cathepsin D, and at 96hpi, where the mycobacteria grow rapidly and are no longer localised with these phagosome/lysosome markers. LAMP-1 and Cathepsin-D are markers of late endosomes and lysosomes and can localise mycobacteria to the phagolysosome. van der Wel *et al.* used LAMP-1 and Cathepsin D to identify *M. tuberculosis* phagosomal escape at 48 hpi in both confocal immunofluorescence and immunogold electron microscopy (van der Wel *et al.*, 2007). Phagosomal escape is not seen in avirulent *M. bovis* BCG. Figure 1.8 shows that at 7 days post-infection, *M. bovis* BCG was co-

localised with the phagosomal/lysosomal markers cathepsin D and LAMP-1. This was further clarified using an anti-LAMP-1 antibody in electron microscopy.

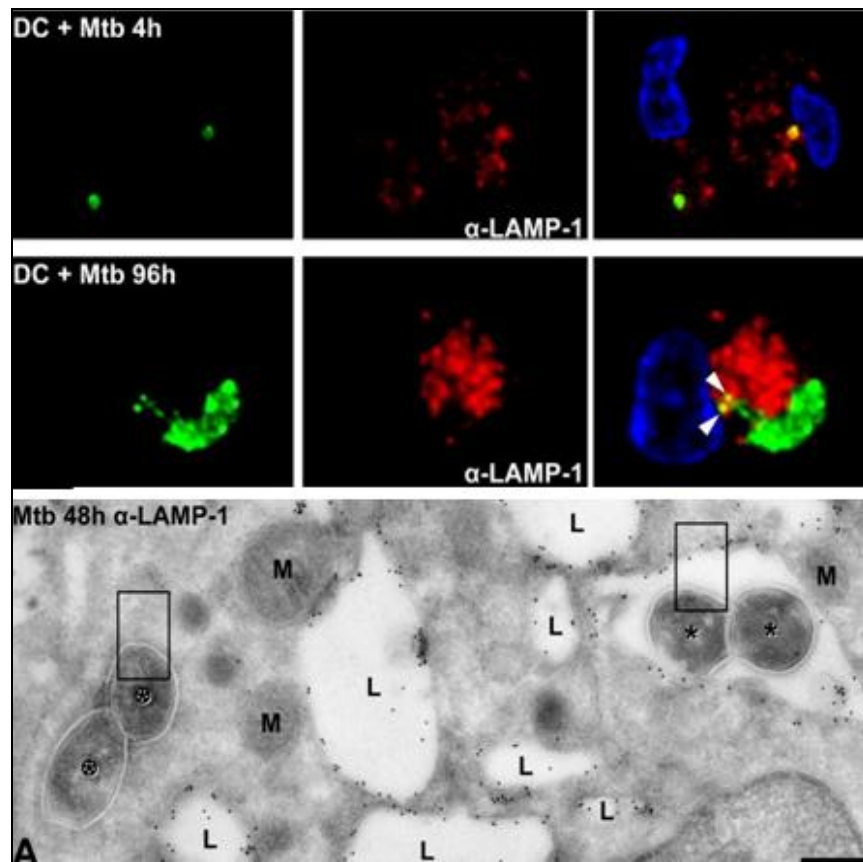


Figure 1.7: Confocal microscopy showing wild-type (WT) *Mycobacterium tuberculosis* (green) cellular localisation in dendritic cells at 4hpi and 96hpi. The phagosome/lysosome markers used is LAMP-1 (red), and by 96hpi, the majority of rapidly-growing *M. tuberculosis* are not associated with the two markers, bar a small fraction of the total population (white arrows). Host cell nuclei are DAPI-stained (blue). The bottom panel is an immunogold electron micrograph of *M. tuberculosis* (asterisks) both in the cytoplasm (left box) and contained within the phagosome (right box). The phagosomal space can be seen as a white area around the mycobacteria. The dots mark LAMP-1 on phagosome membranes. L - lysosomes, M - mitochondria (with permission, van der Wel *et al.*, 2007).

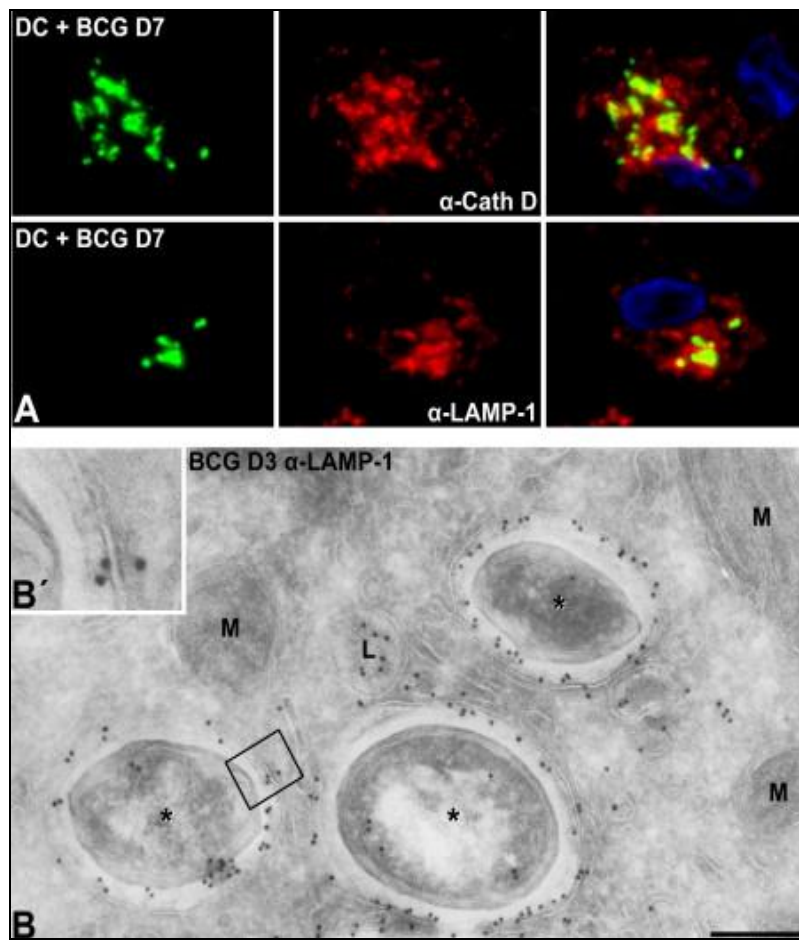


Figure 1.8: *M. bovis* BCG is unable to escape the phagosome, unlike fully-virulent MTB. Panel A shows dendritic cells infected with green fluorescent *M. bovis* BCG, and after 7 days infection still co-localises with the phagosomal/lysosomal markers cathepsin D and LAMP-1 (red). Host cell nuclei are DAPI stained (blue). B and B' show single mycobacteria (marked with asterisks) in the phagosome 3 days post infection. The membrane marker used was LAMP-1. B' shows the LAMP-1 positive phagosomal membrane surrounding the mycobacteria (with permission, van der Wel *et al.*, 2007).

Further evidence to suggest that virulent mycobacteria escape the phagosome and localise to the host cell cytoplasm include the polymerisation of host cell actin to form tails (Stamm *et al.*, 2003), which is covered in more detail in Section 1.4.2.

Mycobacteria must be able to contact cytoplasmic actin in order to effect polymerisation, and actively recruit host cytoplasmic actin-interacting proteins arp2/3, WASP and N-WASP in order to form actin tails, enabling intracellular motility (Stamm *et al.*, 2005).

1.4.2 Modulation of host cell actin by mycobacteria

It has recently been shown that infecting *M. marinum* can modulate host cell actin once they have escaped the phagosomal environment. AlexaFluor Phalloidin is a commonly-used fluorescent F-actin stain that is used to observe the various states of host actin polymerisation by *M. marinum* once they have escaped the phagosome. This includes actin tail formation (Stamm *et al.*, 2003) and ejectosome formation to facilitate non-lytic cell-cell spread in the social amoeba *Dictyostelium* (Hagedorn *et al.*, 2009). The bacteria may need polymerised actin tails in order to reach the inner plasma membrane for cell-cell transfer. This has been studied in a number of intracellular pathogens, like *Burkholderia* (Stevens *et al.*, 2005), and *Listeria* (Welch *et al.*, 1997), and has recently been studied in the *Mycobacterium marinum* infection model (Smith *et al.*, 2008; Collins *et al.*, 2009). *M. marinum* were shown not only to escape the phagosome, but some in the cytosol formed long actin tails, not unlike those made by *Listeria*. The mycobacteria were able to move around in the cytosol using the actin tails, and this may be how they reach the plasma membrane for cell-cell transfer.

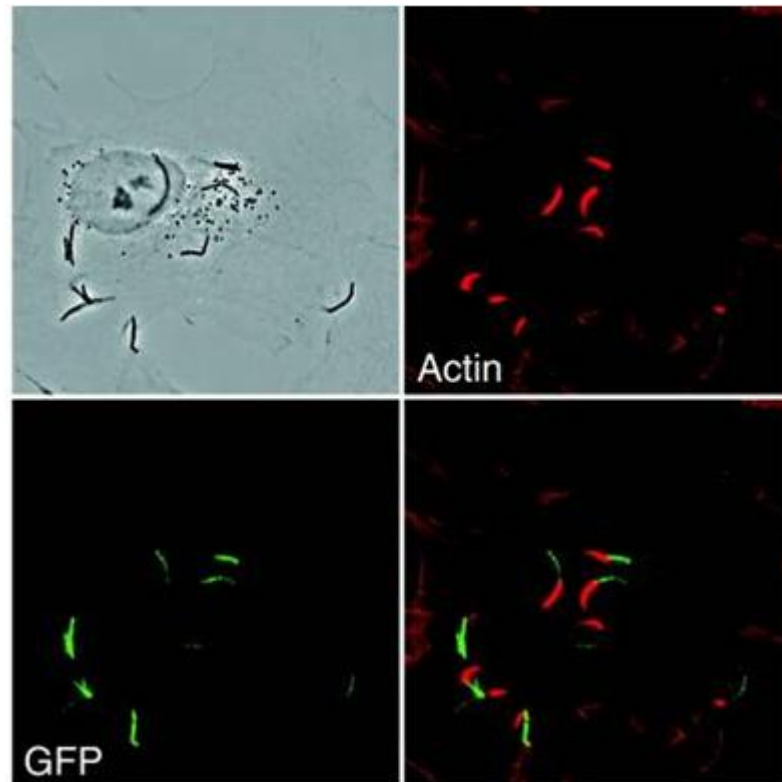


Figure 1.12: Actin tail formation in *Mycobacterium marinum*. The top-left image shows a brightfield image of an infected macrophage. Actin is shown in red, and the mycobacterial cells produce GFP. The merged image shows the long tails polymerised at the mycobacterial poles. Only mycobacteria that have escaped the phagosome can contact actin to form polymerised tails, however; not all cytoplasmic mycobacteria form actin tails (with permission, Stamm *et al.*, 2003).

Hagedorn *et al.* observed in the social amoeba *Dictyostelium* that fully-virulent *M. marinum* were able to spread from host cell to host cell using actin to propel them through the host membrane. The polymerised actin could be seen in ring structures around ejecting mycobacteria, ‘sealing’ the host membrane as the mycobacteria left the host, without lysing the *Dictyostelium*, as shown in Figure 1.13 (Hagedorn *et al.*, 2009).

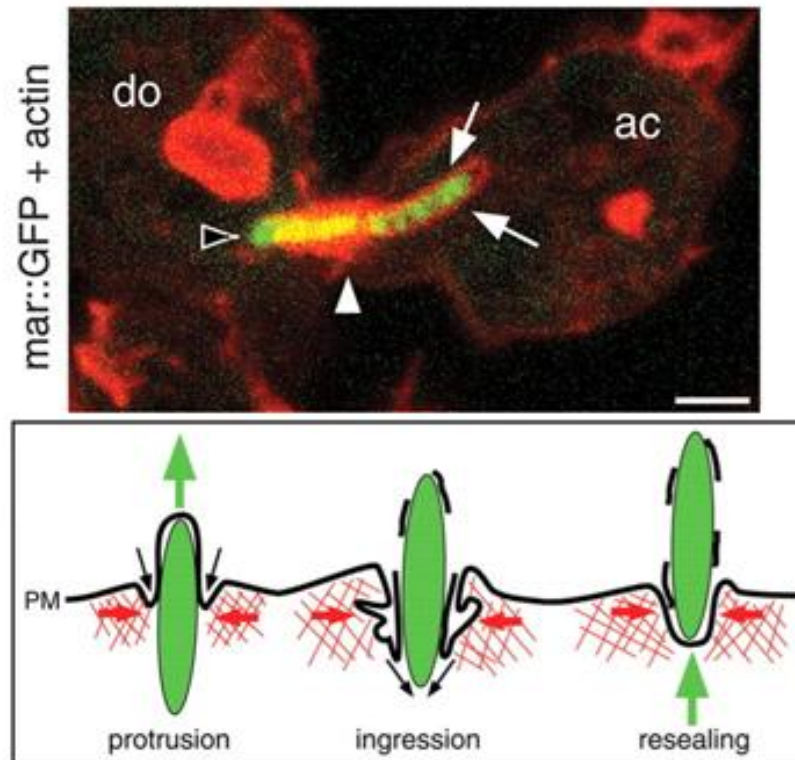


Figure 1.13: Cell-cell spread of *M. marinum* via actin ejectosomes. The top panel shows GFP-*M. marinum* escaping from a donor (do) Dictyostelium cell to an acceptor (ac) cell. Phalloidin staining (red) shows a concentrated ring of F-actin used as an ejectosome. (Black arrowhead – back of mycobacterial cell, white arrowhead – actin ejectosome ring, white arrows – phagocytic cup of the acceptor Dictyostelium. The bottom panel is a model to show how ejectosomes may work, propelling the mycobacterium out of the host and sealing up the membrane (with permission. Hagedorn *et al.*, 2009).

Phagosomal escape and actin polymerisation are important new areas in the field of tuberculosis research, and may help us to understand the intracellular mechanisms of mycobacteria which give rise to an infection. This may also show the similarities of these organisms to other intracellular pathogens such as *Listeria* and *Burkholderia*, and potentially lead to new drug targets and therapeutics.

1.4.3 Granuloma formation

Studies using *Mycobacterium marinum* in macrophage cell lines and zebrafish and have proven to be successful in elucidating the molecular mechanisms of TB pathogenesis, for example granuloma formation. Recent fluorescence studies have shown that fully-virulent mycobacteria appear to be required for granuloma formation (Davis *et al.*, 2009) using a *Mycobacterium marinum* infection model in zebrafish embryos. It was shown that host macrophages were rapidly recruited to the granuloma in an RD1-dependent fashion, as shown in Figure 1.9 (Davis *et al.*, 2009).

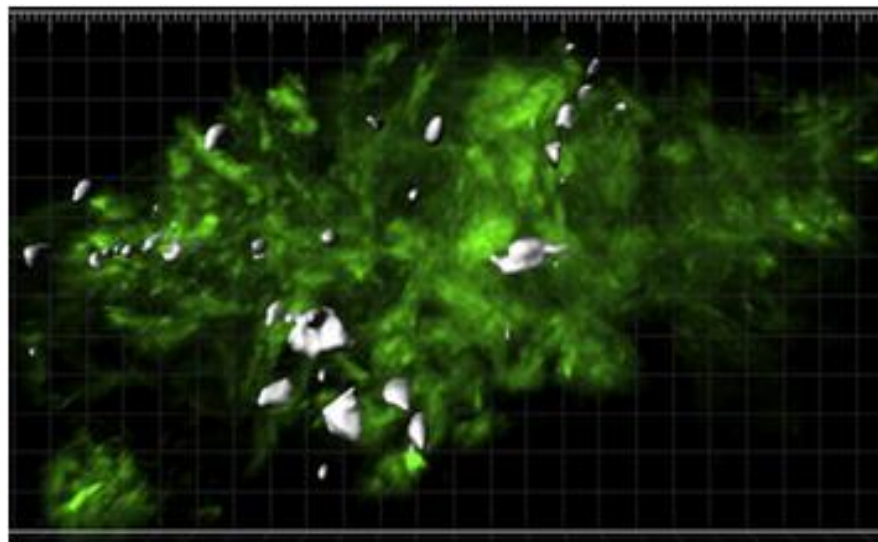


Figure 1.9: A false-colour representation of a granuloma in a zebrafish embryo hindbrain. The granuloma is shown in green. The white areas are a 3D surface reconstruction of recruited Hoescht-positive nuclei recruited to the granuloma from the bloodstream. Hoescht dye was injected into the zebrafish embryo caudal vein, and cannot pass the blood-brain barrier. Any Hoescht-positive cells found in hindbrain granulomas were recruited from the bloodstream. This was not observed in Δ RD1 *M. marinum* granulomas. (with permission, Davis *et al.*, 2009)

1.5 Secreted Mycobacterial Proteins

The recent advances in the molecular mechanisms of TB infection (actin tails and ejectosome-mediated escape), coupled with discoveries that mycobacteria may not be withheld in the phagosomal compartment (van der Wel *et al.*, 2007), help us to understand how mycobacterial infections work on a cellular level. The next step in this molecular understanding is finding the role of individual, important secreted protein factors which potentially play a role in virulence.

ESAT-6 and CFP-10 are two secreted mycobacterial proteins encoded for in the RD1 region. They are thought to be virulence factors because *M. tuberculosis* RD1 deletion mutants and *M. bovis* BCG do not possess the genes to express these proteins, and are attenuated strains. Structural and biophysical characterisation suggests that they form a tight, 1:1 heterodimer which is required for their molecular function as virulence factors (Lightbody *et al.*, 2004; Renshaw *et al.*, 2005).

The role of ESAT-6/CFP-10 is unclear and widely debated. Earlier findings by Tan *et al.* observed, in confocal microscopy studies, that wild-type (WT) *M. marinum* did not co-localise with the lysosomal marker LAMP-1 or LysoTracker (acidified lysosome indicator). This was not observed in the attenuated *M. marinum* mutant strain MRS1459, which has a transposon insertion in an ATPase gene thought to be part of the RD1 ESX secretion machinery, or *M. smegmatis*, which completely lacks the RD1 region, and is avirulent. Lack of the ATPase meant that ESAT-6/CFP-10 was not secreted, and this correlated with full phagosome maturation, implying a potential role for the complex (Tan *et al.*, 2006). It has been shown that *M. tuberculosis* phagosomal escape was RD1 dependent, and also a $\Delta cfp10$ mutant was unable to escape from the phagosome (van der Wel *et al.*, 2007). This implies that the ESAT-6/CFP-10 complex

may be required for phagosomal escape. Recent observations reported that direct injection of purified ESAT-6 protein was enough to induce MMP9 (matrix metalloproteinase 9) expression in host epithelial cells neighbouring infected a result that was not observed with CFP-10 or a mixture of ESAT-6 and CFP-10 together. MMPs matrix metalloproteinases, zinc-dependent endopeptidases which can digest a range of extracellular matrix proteins (Alo-aho and Kahari, 2005). In the tuberculous infection, MMP9 expression may contribute to the remodelling of host cell tissue for full granuloma formation. This has led to the conclusion that ESAT-6 acts alone as a mycobacterial factor to induce granuloma formation via a mechanism involving host MMP9 (Volkman *et al.*, 2010). However, structural studies from our research group have conclusively shown that ESAT-6 and CFP-10 form a tight 1:1 complex and are resistant to low pH (Renshaw *et al.*, 2002; Lightbody *et al.*, 2008), which implies that they do not dissociate to have individual roles in virulence.

1.6 MPT70/MPB70, MPT83/MPB83 and MPM70 Proteins

MPT70 is a 19 kDa, highly soluble secreted protein with a relative electrophoretic mobility of 0.70 by native polyacrylamide gel electrophoresis at pH 9.4 (Daniel and Janicki, 1978). The term ‘MPT’ is derived from ‘**M**ycobacterial **P**rotein from *M. tuberculosis*’ (MPB is derived from ‘**M**ycobacterial **P**rotein from *M. bovis*’, and MPM70 is ‘**M**ycobacterial **P**rotein from *M. marinum*’). MPT70 and MPT83 are secreted by SecA, shared in many bacteria (Braunstein *et al.*, 2001), which is dependent upon a 30 residue signal sequence that is cleaved upon secretion. See Figure 1.3 for a sequence alignment of MPB70, MPB83 and MPM70 with intact N-terminal signal

sequences (Hewinson and Russell, 1993). This differs from ESAT-6 and CFP-10, which are secreted through a novel Type-VII secretion system (Abdallah *et al.*, 2007).

MPT70 is encoded by a non-essential gene, as shown by transposon mutation (Sasseti *et al.*, 2003), found as part of a six-gene operon from Rv2871-Rv2876 (Cole *et al.*, 1998). The operon also contains the close homologue, *mpt83*, which encodes a protein with 70% amino acid identity to MPT70. MPT83 is glycosylated at the N-terminus and localised to the mycobacterial surface upon expression (Hewinson *et al.*, 1996). Another gene of interest within this operon is *dipZ*, thought to encode an enzyme needed for disulphide bond formation due to its C-terminal hydrophilic domain, which contains a disulphide isomerase/thioredoxin-like motif (Juarez *et al.*, 2001). This enzyme may be important in the folding of MPT70 and MPT83 proteins upon their expression. *In vitro* expression of MPT70 and MPT83 proteins is low in *M. tuberculosis*, high in *M. bovis* (where these proteins are annotated as MPB70/MPB83) and varies depending upon the strain of *M. bovis* BCG. Low MPB70/MPB83 expressers include BCG Pasteur, Glaxo, Tice and Denmark. High expressing strains include BCG Tokyo, Russia, Birkhaug, Moreau and Sweden (Charlet *et al.*, 2005). In *M. tuberculosis* infection, MPT70 is one of the most upregulated genes in the *M. tuberculosis* genome along with its close homologue MPB83, as shown in a murine model infection and qRT-PCR studies on *M. tuberculosis* infected murine bone marrow derived macrophages (Schnappinger *et al.*, 2003). This is a marked upregulation compared to very low *in vitro* MPT70 expression (Said-Salim *et al.*, 2006), and implies that the protein must play an important role in virulence.

The expression of genes in the MPT70/MPB70 operon are controlled by the sigma factor SigK (Charlet *et al.*, 2005). A point-mutation in the start codon of this sigma

factor has been attributed to the low MPB70 and MPB83 expression seen in *M. bovis* BCG strains such as BCG Pasteur and BCG Glaxo. This low MPB70 and MPB83 expression could subsequently be restored by complementation with a fully functional SigK (Charlet *et al.*, 2005). The amino acid sequence of both the *M. tuberculosis* (MPT70) and *M. bovis* (MPB70) proteins are identical (Harboe *et al.*, 1986), but *M. bovis* has constitutively high expression of this protein *in vitro* and *M. tuberculosis* does not. This has been attributed to SNP mutations at 320 bp and 550 bp within the genome sequence of *Rv0444c*, which encodes the anti-sigma factor RskA (Said-Salim *et al.*, 2006). An attenuated anti-sigma factor leaves SigK to act constitutively, and accounts for the high *in vitro* MPB70/MPB83 expression seen in *M. bovis*.

M. marinum has a single MPT70 homologue: MPM70, and lacks an MPB83 homologue (Stinear *et al.*, 2008). MPM70 is found as part of a two-gene operon within the *M. marinum* genome containing only *mpm70* and *dipZ*, and the encoded protein has 68% identity to MPB70 and MPB83. This high level of homology suggests that MPM70 must play a similar role during infection to MPT70 in *M. tuberculosis* (Stinear *et al.*, 2008). In the interests of the research in this thesis, *M. marinum* is a desirable model as any immunofluorescent microscopy should identify only MPM70. The high level of homology between MPT70 and MPT83 in *M. tuberculosis* could have cross-reaction problems, particularly with polyclonal antibodies, as used in the course of this thesis (see Chapter 3).

Early studies on MPB70 identified the protein as an immunodominant mycobacterial antigen (Lind, 1965) and was found to be highly expressed *in vitro* by the Tokyo strain of *M. bovis* BCG (Nagai *et al.*, 1981). The protein was purified from BCG Tokyo culture filtrate and was found to elicit a strong, delayed-type hypersensitive response in

guinea pigs that had been exposed to high MPB70-expressing BCG strains such as BCG Tokyo, but not low-expressers like BCG Pasteur, or heat-killed BCG cells (Miura *et al.*, 1982). The high expression of MPB70 by *M. bovis* and strong immunogenic response by test animals placed this protein as a key indicator of bovine tuberculosis, and led to the development of ELISA-based tests for diagnostic use in cattle farming (Harboe *et al.*, 1990; Fifis *et al.*, 1992).

The high level of immune response to these proteins has led to them being considered potential vaccine components. However, MPB70 and MPB83 have been tested as DNA vaccines with mixed success (Vordermeier *et al.*, 2000). DNA vaccines have the advantage of not giving a false-positive tuberculin skin-test, which is a known problem with live BCG vaccination (Vordermeier *et al.*, 2000). An MPB70 vaccine tested in mice was shown to have a therapeutic effect rather than a protective effect in mice that were already infected with *M. tuberculosis*. Results indicated a drop in lung and spleen colony forming unit counts that was rivalled only by an IL-12 DNA vaccine, which would directly activate CD4⁺ T-cells known to be effective in the immune response to tuberculosis (Lowrie *et al.*, 1999). This clearing of an existing infection may be due to the delayed-type hypersensitivity response, a memory T-cell mediated response characterised by monocytic infiltration to the lesion site and localised swelling (Harboe *et al.*, 1986).

Although no specific function for MPT70/MPB70 is known, the structure of the protein and its homologues may give some idea as to its role in virulence. The solution structure of MPB70 was solved using NMR spectroscopy and consists of a seven-stranded beta barrel beta-barrel with eight alpha helices above and to one side (Carr *et al.*, 2003). The protein contains a novel fold, previously unseen in bacterial proteins, with high

homology to the FAS1 domains of the eukaryotic proteins fasciclin 1 (Figure 1.14), β ig-H3 and periostin. FAS1 domains are extracellular modules of around 140 amino acids, and are thought to be ancient cell adhesion domains that are common in all phyla, for example: β ig-H3 in animals, (Kim *et al.*, 2000), Algal-CAM of *Volvox* and *Arabidopsis* arabinogalactans in plants (Huber and Sumper, 1994; Faik *et al.*, 2006) and MPB70/MPB83 in bacteria (Matsumoto *et al.*, 1995; Carr *et al.*, 2003.). The structure of FAS1 domains 3 and 4 from *Drosophila melanogaster* revealed a novel domain fold consisting of a seven-strand beta wedge and five alpha-helices (Clout *et al.*, 2003), the backbone structure of which is closely conserved in MPB70, as shown in Figure 1.14 (Carr *et al.*, 2003).

FAS1 domain containing proteins play important roles in mediating interactions between the cell surface and the extracellular matrix (ECM). When non-adherent S2 cells were transiently transfected with fasciclin 1 cDNA, they formed aggregates. The effect could be subsequently blocked by addition of anti-fasciclin 1 antiserum (Elkins *et al.*, 1990).

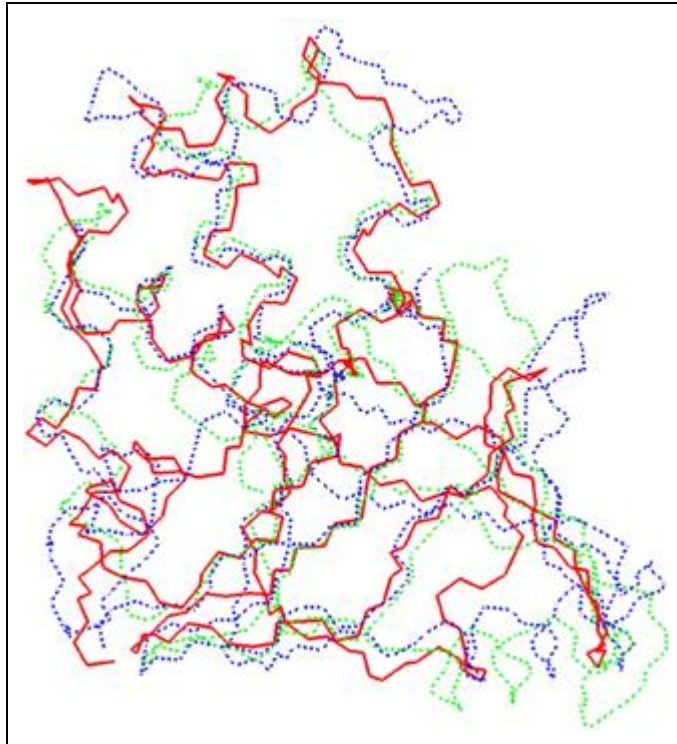


Figure 1.14: Structural homology of MPB70 to FAS1 domain-containing proteins.

MPB70 has close backbone structural homology to FAS1 domains of fasciclin I from *Drosophila melanogaster*. The MPB70 FAS1 domain backbone (red) superimposed onto the FAS1 domains 3 (green) and 4 (blue) of fasciclin 1 (with permission, Carr *et al.*, 2003).

In humans, FAS1 containing proteins include β ig-H3 and periostin. β ig-H3 was first localised to the human cornea (Escribano *et al.*, 1994; Klintworth *et al.*, 1994), and binds fibronectin and collagen I in the ECM of the eye, as fibroblasts can adhere onto β ig-H3 coated plates, forming actin stress fibres. The protein was shown to bind fibronectin in the collagen/gelatine binding region at the N-terminal domain (Billings *et al.*, 2002). Different mutations of the gene were attributed to various different inherited corneal diseases (Kannabiran *et al.*, 2006), where denatured kerato-epithelin (the β ig-H3 gene product) forms amyloid deposits, giving rise to corneal dystrophy (Munier *et al.*,

1997). Periostin is another FAS1 domain containing eukaryotic protein. It is a bone-specific protein that has an export signal to secrete it into the ECM around MC3T3-E1 osteoblast-like cells. This is necessary for regulation of adhesion, and differentiation of osteoblasts (Horiuchi *et al.*, 1999).

The main function of these proteins appears to be as a molecular intermediate between the eukaryotic cell surface and the ECM. The work in this thesis suggests that the cell-wall localisation of MPM70 may mean it is playing a similar role as a molecular intermediate between the mycobacterial cell and a host-cell cytoplasmic structure. This is further supported by the structure of MPB70 and related FAS1 proteins. When the conserved residues, between MPB70, MPB83, FAS1 and those mutated in β ig-H3 in patients with corneal dystrophies are superimposed onto the MPB70 structure, they reveal two distinct interaction faces on the protein (Carr *et al.*, 2003), as shown in Figure 1.15. This implies that MPB70 and MPM70 may have a similar function as a 'bridging molecule', analogous to that of FAS1 and β ig-H3 in eukaryotic tissues. However, evidence in this report shows that instead of binding to an ECM component, MPM70 is most likely a molecular intermediate between the mycobacterial surface and a host cytoplasmic protein.

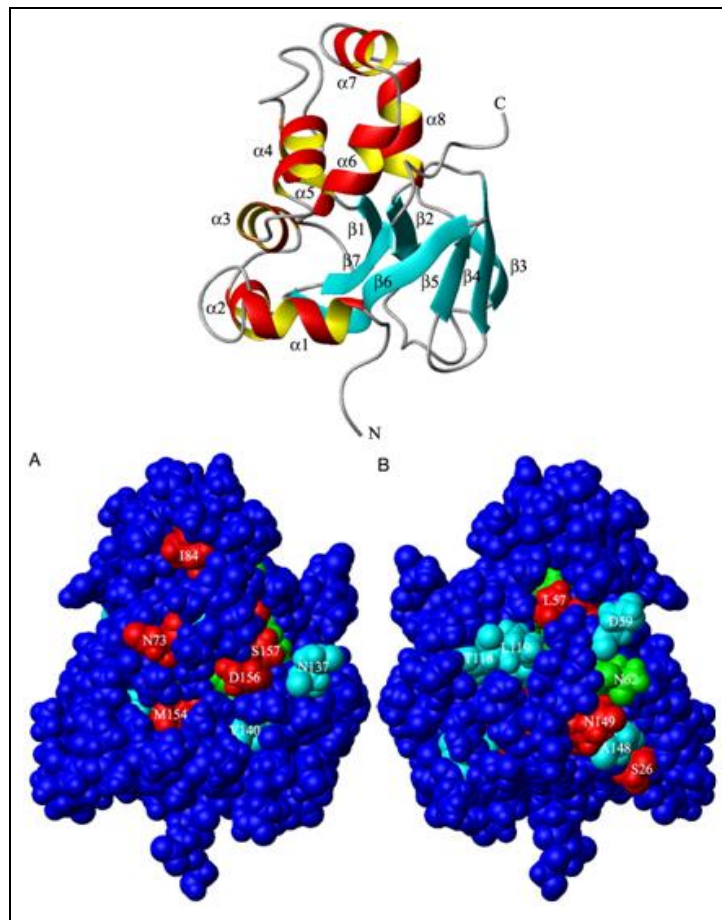


Figure 1.15: Structure of MPB70 and comparison to related proteins MPB83, fasciclin and β ig-H3. The top image shows the ribbon structure of MPB70, and panel A shows a filled-space model in the same orientation as the top image. Panel B shows a filled-space model of the opposite face of the protein. Colour-coded residues are: red – residues mutated in β ig-H3 in corneal dystrophies (which may also be important in protein-protein interactions on homologues such as MPB70), green – identical residues in MPB70, MPB83, FAS1 domains 3 and 4 of fasciclin, and FAS1 domain 4 of β ig-H3, cyan – residues closely structurally conserved in the above proteins (with permission, Carr *et al.*, 2003).

1.6 Aims of the Project

The aim of this project was to provide insight into the role of the *Mycobacterium tuberculosis* potential virulence factor MPT70 and its homologues in mycobacterial infection and TB pathogenesis.

The focus of this project was to use a *Mycobacterium marinum* infection in the murine macrophage line J774A.1 for use as an infection model for *M. tuberculosis* infection. The project focussed on tracking the intracellular localisation and expression of the *M. marinum* MPB70 homologue, MPM70. Confocal microscopy studies have revealed the localisation of the protein to the mycobacterial surface, suggesting that the protein may be acting as a 'molecular bridge', an intermediate between the mycobacterial surface and an as-yet unknown host cell cytoplasmic factor. This may be analogous to the way in which MPB70 and MPM70 homologues in eukaryotes (fasciclin1 and β ig-H3) act as molecular intermediates between the eukaryotic cell surface (via NCAMs and integrins, respectively) and extracellular matrix components such as collagen and fibronectin.

Chapter 2

Production of anti-MPM70 polyclonal antibodies and characterisation of the *Mycobacterium marinum* : J774A.1 infection model

2.1 Introduction

This chapter describes the systems and reagents generated for the production of detailed *in vivo* studies of MPM70 expression reported in Chapter 3. One of the key goals within this project was to clone and express MPB70 into an inducible expression system to produce highly purified, natively folded MPM70 protein for the production of highly specific antibodies. A ligation-free system was successfully employed to clone and express c-terminally His tagged MPB70, and its *M. marinum* homologue MPM70. Expression optimisation produced soluble, mature, natively folded proteins which could be purified using a two-step method consisting of a Ni-NTA column and a Sephadex gel filtration column. Highly purified proteins were provided to Cambridge Research Biochemicals for the production of two batches of rabbit polyclonal antibodies (4060 and 4061). These antibodies were purified, and their sensitivity and specificity assessed using a range of immunological tests. Antibody 4061 was found to be more sensitive and was selected for use in the experimental work in Chapter 3. This Chapter also reports the characterisation of the *Mycobacterium marinum*:J774 murine macrophage infection model which was exploited for the studies of MPM70 expression in infected cells, as described in Chapter 3. A range of conditions, such as initial mycobacterial load (MOI) and temperature were assessed in order to obtain a representative infection time-course over four days. This allowed both low and high host cell mycobacterial densities to be observed, in order to track secreted MPM70s potential role in both early and late-stage events, as detailed in Chapter 3.

2.2 Methods

2.2.1 Bacterial strains, Cell lines and Media

DH5 α and BL21 (DE3) *Escherichia coli* strains were used for cloning and protein expression. These were grown in LB liquid and LB agar (solid) media at 37°C, supplemented with the appropriate antibiotics.

Fluorescent *Mycobacterium marinum* strains expressing the red fluorophore DsRed (pMSP12:DsRed, selected for by addition of 50 μ g/ml kanamycin), and a Δ RD1 mutant strain expressing GFP (pR2Hyg – selected for by 50 μ g/ml hygromycin) were kindly provided by the Thierry Soldati group at the University of Geneva, courtesy of the Lalita Ramakrishnan group, University of Washington, Seattle. All strains were grown in 7H9 liquid media (BD Biosciences) supplemented with Middlebrook oleic acid-albumin-dextrose-catalase (OADC) enrichment (BD Biosciences) at 32°C without shaking or 7H10 solid media at 32°C, supplemented with OADC (BD Biosciences).

U937 human monocytes (85011440, ECACC) were grown in RPMI liquid media (Sigma-Aldrich) supplemented with 10% foetal calf serum and 2 mM L-glutamine (Sigma-Aldrich). U937 cells were used at 2×10^5 cells/ml for cell infections with *M. marinum* and at 1×10^6 for lysate preparation in pull-downs against MPB70.

J774A.1 murine macrophages (91051511, ECACC) were grown in Dulbecco's Modified Eagle's Media (Sigma-Aldrich) supplemented with 10% foetal calf serum and 2 mM L-glutamine (Sigma-Aldrich).

2.2.2 DNA Analysis by Agarose Gel Electrophoresis

PCR products were analysed by electrophoresis on a 1% (w/v) agarose gel run at a constant 100 V for 30 mins. The PCR products were prepared for analysis by combining 5 µl of the PCR reaction samples with 5 µl dH₂O and 2 µl 6x Blue/Orange Loading Dye (Promega). SYBR[®] Safe DNA Gel Stain (Invitrogen) was used to visualise the PCR products under ultraviolet light. For gel extraction and purification, the amount loaded onto the agarose gel was increased to 20 µl. For PCR analysis, a 100 bp ladder (Promega) was used to indicate PCR product size. For Colony PCR experiments, a 100 bp ladder (Promega) and λ DNA/*Eco*RI + *Hind*III marker (Promega) were used to indicate PCR product size.

2.2.3 SDS Polyacrylamide Gel Electrophoresis (SDS-PAGE)

Protein expression and purification were analysed by SDS-PAGE. Unless stated, 20 µl protein samples were combined with 10 µl 200 mM dithiothreitol (DTT) and 10 µl 4x NuPAGE LDS sample buffer. Samples were heated for 10 minutes at 70 °C before being loaded on 4 – 12 % acrylamide gradient, pre-cast NuPage[®] Bis-Tris gels (Invitrogen). Electrophoresis was carried out in MES-SDS Running Buffer (Invitrogen) at a constant 200 V for 40 minutes. For protein expression and purification, Wide Range Molecular Weight Markers (Sigma) were used to indicate protein sizes, and ranged from 6.5 kDa to 205 kDa. For Western blotting, Novex[®] Sharp Prestained Protein Markers (Invitrogen) were used, and ranged from 3.5 kDa to 260 kDa. Protein gel staining was done using Coomassie Brilliant Blue or a SilverXpress[®] Silver Staining Kit (Invitrogen). For Coomassie staining, 2.5 g/l Coomassie Brilliant Blue was dissolved in 40 % v/v methanol and 10 % acetic acid, made up to 1 L with dH₂O and filtered through

at 0.2 μm filter. Gels were stained in this solution for 30 minutes and destained in a 40 % methanol (v/v), 10 % acetic acid solution until protein bands were visible.

Silver staining was performed in accordance with the manufacturer's protocol. The gel was fixed in 200 ml fixing solution for 10 minutes before sensitizing in two changes of 100 ml sensitizing solution for 30 mins each. The gel was then washed in two changes of 200 ml dH_2O for 10 minutes each before 15 minutes of the staining solution. The gel was again washed in two changes of 200 ml dH_2O before adding the developing solution, and the stopping solution was added when the protein bands were sufficiently visible on the gel. The gel was then washed in three 200 ml washes of dH_2O .

2.2.4 Cloning of MPB70 and MPM70 with a C-terminal His tag

Cloning of these two constructs was performed using PCR. MPB70 was amplified from a pBluescript KS⁺ template containing the full MPB70 coding sequence, and MPM70 was amplified from a *M. marinum* genomic DNA template. Both MPB70 and MPM70 constructs were put into the pLEICS-05 vector (shown in Figure 2.1), containing a sequence for a C-terminal HIS tag (cHIS MPB70 and cHIS MPM70, respectively).

Primers for MPB70

Forward primer:

5'-AGGAGATATACATATGAAGGTAAAGAACAAT-3'

Reverse primer:

5'-GAAGTACAGGTTCTC CGCCGGAGGCATTAGCAC-3'

Primers for MPM70

Forward primer:

5'-AGG AGA TAT ACA TATG AAG TTC CAC AAC CCA GCA-3'

Reverse primer:

5'-GAA GTA CAG GTT CTC GCT GGG CGG CAT CAG CAC-3'

PCR was carried out in 50 µl reaction volumes using a Techne TechGene Thermal Cycler. The PCR protocol consisted of a 1.5 min initial denaturation at 95 °C, followed by 35 cycles of seconds at 95 °C, 40 seconds at 55 °C for annealing and 1 minute 15 seconds at 72 °C for extension. The final extension was 72 °C for 5 minutes.

PCR products were visualised by agarose gel electrophoresis using a 1 % (w/v) agarose gel, with Invitrogen SYBR[®] safe DNA gel stain. PCR products were gel purified using the Promega Wizard PCR clean up/gel extraction kit. The clean PCR products were then inserted into the pre-cut pLEICS-05 vector by mixing 2 µl of PCR product, 2 µl of the cut pLEICS-05 vector and 3 µl of Dry-Down InFusion mixture (BD Clontech). The mixture was heated at 37°C for 15 mins, 50 °C for 15 mins and finally at room temperature for 5 mins. 100 µl of DH5α *E. coli* cells were added to the reaction mixture, and incubated on ice for 30 mins, followed by heat shock at 42 °C for 45 secs, and incubation on ice for a further 5 mins. 100 µl of sterile LB media was added for 30 mins at 37°C, and the cells plated onto LB agar plates supplemented with 5 % (w/v) sucrose and 100 µg/ml ampicillin.

The ligation-free cloning method employed here used the Clontech Dry-Down InFusion kit to insert the purified PCR-amplified MPB70 and MPM70 sequences into pLEICS-05 (Figure 2.1.3), which carries an ampicillin resistance gene. The presence of the insert and the plasmid are selected for by plating transformants onto LB agar supplemented with 100 µg/ml ampicillin and 20% sucrose. If the insert does not anneal into the vector, pLEICS-05 will anneal at the *BsmI* site, and the SacB gene will be functional, arising in a sucrose-lethal gene product, levans.

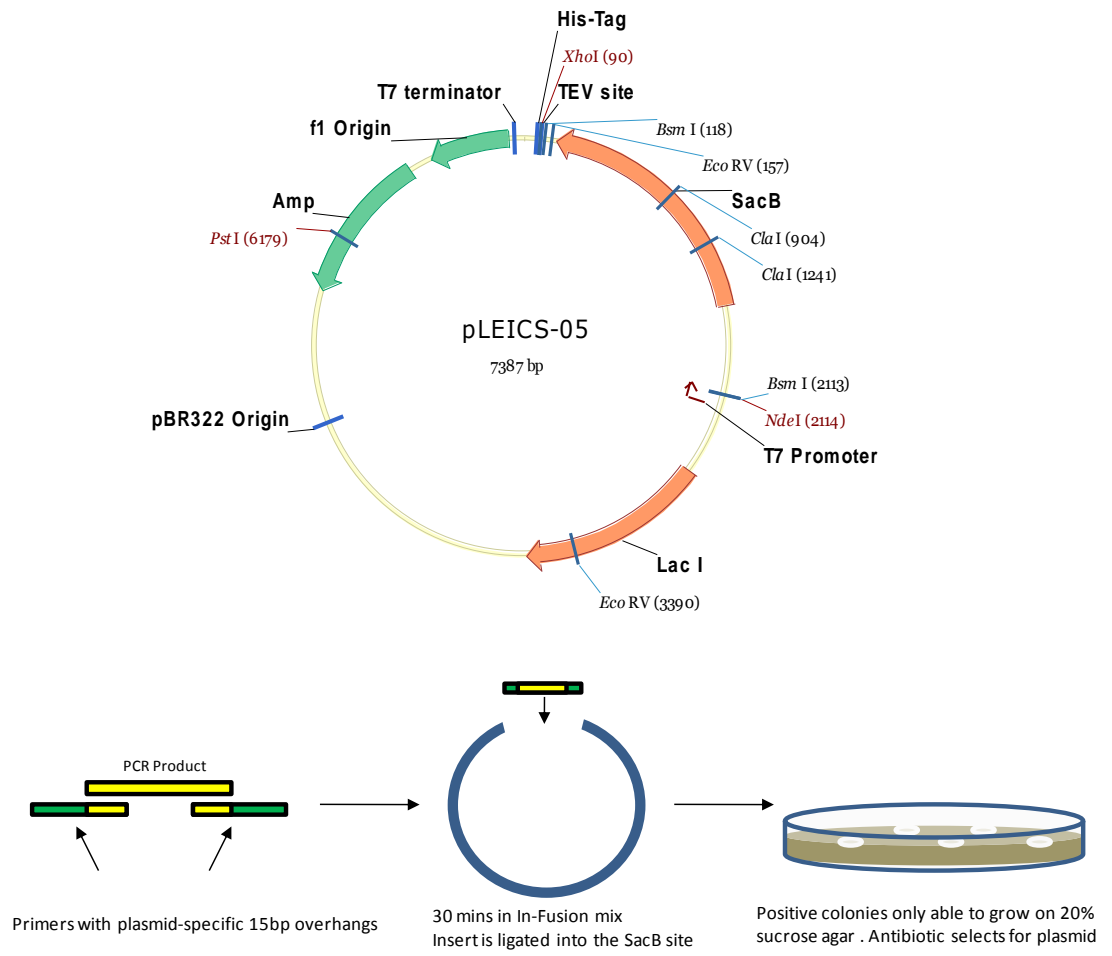


Figure 2.1: Vector map of pLEICS-05. The top diagram shows a map of pLEICS-05 vector, with the His-tag and TEV cleavage site present in the vector. The *BsmI* sites are shown (at 118 and 2113 bp) surrounding the the *SacB* gene where the plasmid is linearised for insertion of PCR products with the correct 15bp extensions. (Bottom) A diagrammatical representation of the In-Fusion Reaction, using primers with vector-specific 15 bp overhangs. Transformants with correctly inserted PCR products have a disrupted *SacB* gene, allowing them to grow on 20% sucrose agar.

Colony PCR experiments were performed by picking 3 individual transformant colonies and resuspending them in 20 µl dH₂O for use as a template, with the following primers for the T7 promoter and terminator sequences found within the pLEICS-05 vector:

Colony PCR Primers for pLEICS-05

T7 Promoter:

5'- TAATACGACTCACTATAGGTG -3'

T7 Terminator:

5'- GCTAGTTATTGCTCAGCGG -3'

The PCR reaction was carried out in a 25 µl reaction volume in a Techne TechGene Thermal Cycler. The PCR protocol consisted of a 5 min initial denaturation at 95 °C, followed by 35 cycles of 1 minute at 94 °C, 1 minute at 50 °C for annealing and 2 minutes at 68 °C for extension. The final extension was 68 °C for 10 minutes. PCR products were identified and verified by electrophoresis using 1 % (w/v) agarose gel electrophoresis.

Plasmid DNA was isolated using a Promega Wizard miniprep kit to isolate the pLEICS-05 plasmid, which was sequenced by The University of Leicester Protein and Nucleic Acid Chemistry Laboratory (PNACL). 4 µl of the pLEICS-05 plasmid (containing the correct MPB70 or MPM70 sequence, respectively) was mixed with 100 µl of competent BL21 (DE3) *E. coli* cells, and the same heat-shock protocol was carried out as above with the DH5α cells. Selection of transformants into BL21 (DE3) was done using LB agar plates, with 100 µg/ml ampicillin as a selective agent.

2.2.5 Expression trials of C-terminally His tagged (cHis) MPB70 and MPM70

In order to assess and optimise the expression of cHis MPB70 and cHis MPM70 50 ml LB expression trials for both constructs were performed. Protein expression trials involved growing the *E.coli* to mid-log phase (optical density of 0.6-0.7 at 600 nm) in 50 ml of LB broth with 100 ug/ml ampicillin, shaking at 200 rpm at 37°C before adding the appropriate Isopropyl β -D-1-thiogalactopyranoside (IPTG) concentration to induce the production of C- terminally His-tagged (cHis) MPB70 or cHis MPM70. In order to maximise the soluble protein yield, a number of conditions were tested; 0.45 mM IPTG and 0.045 mM IPTG, and post induction temperatures of 37 °C and 15 °C were trialled in combination with each other. The culture was induced, and samples taken every hour for 4 h post-induction, before being allowed to grow and express the induced protein overnight. A 1ml sample was taken after the overnight culture, as well as the LB culture supernatant. The samples were normalised according to cell density and analysed by SDS-PAGE for protein production.

2.2.6 Purification of cHis MPB70 and cHis MPM70

E. coli BL21(DE3) cells transformed with the pLEICS-05 expression vector for either cHis MPB70 or cHis MPM70 were grown in LB broth containing 100 ug/ml ampicillin. The cells were grown at 37 °C in an orbital shaker at 200 rpm until they reached mid-log phase (optical density of 0.6-0.7 at 600 nm) and induced with 0.045 mM IPTG. The cells were then incubated at 15 °C overnight. The next day the cells were harvested at 4000 xg for 15 minutes at 4 °C (Beckman JA 10.500 rotor, Beckman Coulter Avanti J-30I centrifuge). The cell pellet was lysed in 20 mM Tris-HCl, 150 mM NaCl, 30 mM imidazole, 5 mM MgCl₂ pH8.0, with 1 mg/ml hen egg albumin lysozyme (Sigma)

added, incubated for 30 minutes on a rocker at room temperature. The lysate was sonicated using a Misonix sonicator at full power, 20 seconds on, 20 seconds off for a total of two minutes. Any remaining DNA was digested using bovine DNase I (Sigma), added at 1 mg/ml and incubated for 30 minutes at room temperature on a rocker. Insoluble material was removed from the lysate by centrifugation at 48,000 xg for 30 minutes, and the soluble supernatant loaded into a 50 ml Superloop (GE Healthcare) for purification on an Akta FPLC system.

cHis MPB70 and cHis MPM70 recombinant proteins were purified using a 5 ml Ni-NTA column (GE Healthcare). Ni-NTA purification was carried out by using a base buffer of 20 mM Tris-HCl, 150 mM NaCl and 30 mM imidazole, pH8 with the elution buffer comprising of the same Tris-HCl and NaCl concentrations but with 500 mM imidazole. The elution buffer was applied to the column as a linear gradient to elute the bound protein. A constant flow-rate of 2 ml/min was applied to the column during the purification. Eluted proteins were analysed on NuPAGE SDS-PAGE gel using Coomassie Brilliant Blue Staining. Fractions containing cHis MPB70 or cHis MPM70 were pooled and dialysed into a gel filtration buffer of 25 mM Na₂HPO₄ and 100 mM NaCl, pH 6.5.

A 120 ml Sephadex 70 gel filtration column (GE Healthcare) was used to remove high and low molecular weight contaminants. The buffer used was 25 mM Na₂HPO₄, 100 mM NaCl, pH 6.5 at a constant flow rate of 1 ml/min. The final purification product was analysed by NuPAGE SDS-PAGE gel, with Coomassie Brilliant Blue staining, and protein concentrations were calculated using the absorbance at 280 nm.

In order to remove the His tag, TEV protease cleavage was performed. His tagged TEV protease was kindly provided by Dr. Xiaowen Yang at the University of Leicester. 1

A_{280} unit of TEV protease was added to 10 A_{280} units of cHis MPM70 overnight. This was dialysed in 20 mM Tris-HCL, 200 mM NaCl, pH8. A 5 ml Ni-NTA column was pre-equilibrated in 20 mM Tris-HCL, 200 mM NaCl, pH8 and used to remove the His tag cleaved from MPM70 and to remove the His tagged TEV protease. Untagged MPM70 was collected in the flow-through and the protein content analysed by SDS-PAGE. The protein concentration was measured at 280 nm.

2.2.7 Mass spectroscopy analysis of the cHis MPB70 and cHis MPM70 purified proteins

SDS-PAGE gel samples of purified cHis MPB70 and cHis MPM70 (after gel filtration) were excised from their respective gels and the proteins digested using trypsin. MALDI-TOF mass spectroscopy was performed and the fragments analysed using Mascot Peptide Mass Fingerprint software (Matrix Science).

To ensure that the purified MPM70 protein was mature, with the N-terminal signal sequence cleaved off, an intact mass analysis of the protein was measured using electrospray mass spectroscopy. Purified MPM70 with the His tag removed by TEV protease cleavage (section 2.2.6) was supplied at a concentration of 0.7 mg/ml in 20 mM Tris-HCl, 200 mM NaCl, pH8. Electrospray mass spectroscopy was performed by the PNAFL Proteomics laboratory at the University of Leicester.

2.2.8 ¹H NMR analysis of the cHis MPB70 and cHis MPM70 purified proteins

¹H NMR was used to ascertain whether the purified proteins were correctly folded. 200 μM samples of cHis MPB70 and cHis MPM70 in 25 mM Na₂HPO₄, 100 mM NaCl, pH 6.5 were obtained by concentrating in an Amicon Ultracel MWCO 10 concentrator (Millipore), spinning at 2000 x g, and D₂O added to a final concentration of 5% (v/v). ¹H NMR spectra were acquired using a Bruker 600MHz spectrometer at 30°C.

2.2.9 Production of rabbit anti-MPM70 polyclonal antibodies 4060 and 4061

Anti-MPM70 polyclonal antibodies 4060 and 4061 were produced by Cambridge Research Biochemicals (CRB) using their custom antibody production service. The company was provided with 10 ml of purified MPM70 at 0.5mg/ml in a solution of 25 mM Na₂HPO₄, 100 mM NaCl, pH 6.5 for immunisation of two rabbits. During an 11-week immunisation course, CRB provided pre-immune sera to assess the suitability of the rabbits as candidates for antibody production, as well as test bleeds at weeks 5 and 7 of the course for sensitivity and specificity testing by Enzyme-Linked Immunosorbent Assay (ELISA, see section 2.2.12) and dot blots (see section 2.2.11). The final harvest bleeds of 120 ml were provided after 11 weeks and the IgG fraction purified using a prepacked Protein A column (GE Healthcare), as detailed in Section 2.2.10 below.

2.2.10 Purification of polyclonal antibodies from rabbit 4060 and 4061 sera

A pre-packed 5ml Protein A Sepharose column (GE Healthcare) was equilibrated with 10 column volumes (CV) of filtered, degassed Phosphate Buffered Saline, pH 7.3 (PBS, Oxoid). 7 ml of polyclonal sera from rabbits 4060 and 4061 were diluted 1:1 with PBS

and any insoluble material removed by centrifugation at 4000 *xg*, for 10 mins. The supernatant from this was then loaded onto the pre-equilibrated Protein A column and the flow-through collected. 10 CV of PBS was applied to wash any unbound material from the column, and the bound material was eluted using 5 CV of 100 mM Sodium Citrate, pH2.8. 1ml fractions were collected into 1.5ml microfuge tubes containing 450µl 1M Tris-HCL, pH 9.0. In preliminary experiments, this neutralised the pH of the eluted sample to around 7.2. The A₂₈₀ of eluted samples was used to create an elution profile and the purity of polyclonal IgGs, and the purity of the antibodies analysed on SDS-PAGE gel. The appropriate fractions were pooled together and the total IgG content quantified at A₂₈₀.

2.2.11 Dot-blot to test the sensitivity of polyclonal antibodies 4060 and 4061 to purified MPM70

In order to assess the sensitivity of polyclonal antibodies 4060 and 4061 to fully folded recombinant MPM70, dot blots were used. This is a more appropriate approach than Western blotting, as it does not denature the protein. 3 µl of purified MPM70 was pipetted directly onto nitrocellulose membrane. The MPM70 dilutions used were 250µg/ml, 25µg/ml, 2.5µg/ml, 250ng/ml and 25ng/ml. The nitrocellulose membrane was blocked using 5% Calbiochem BLOT-Quickblocker™ Reagent in PBS-Tween for 1 h and washed three times with PBS-Tween. Primary antibodies 4060 or 4061 were applied at a 1:1000 (v/v) dilution in PBS-Tween with 1% Quickblocker™ Reagent for 1 h at 4°C, washing three times with PBS-Tween before adding the secondary antibodies. The secondary antibody was goat anti-rabbit IgG (H+L) with an HRP conjugate (Invitrogen Molecular Probes), used at a 1:2500 (v/v) dilution in PBS-Tween with 1%

Quickblocker™ Reagent. The secondary antibody was applied for 1 h at room temperature, then washed three times with PBS-Tween. Protein bands were visualised using GE Healthcare ECL plus Western Blot Detection kit.

2.2.12 Enzyme-Linked Immunosorbent Assay (ELISA) to determine the sensitivity of polyclonal antibodies 4060 and 4061 to purified MPM70

ELISA was used to quantify the sensitivity of polyclonal antibodies 4060 and 4061 to fully folded recombinant MPM70. MaxiSorpELISA plates (Nunc) were coated with 10µg/ml purified MPM70 diluted in PBS, overnight at 4°C. Excess protein was washed from the plate three times with PBS-Tween (PBS with 0.01% v/v Tween-20, Sigma-Aldrich). The plate was blocked using 1% Calbiochem BLOT-Quickblocker™ Reagent in PBS-Tween for 1 h at room temperature, and washed three times with PBS-Tween again. PBS dilutions of the primary purified anti-MPM70 4060 and 4061 polyclonal rabbit antibodies were applied as follows: 1:100, 1:500, 1:1000, 1:2000, 1:5000, 1:10000, 1:20000 and 1:50000 (v/v). Negative controls of the prebleed sera from rabbits 4060 and 4061 were added in PBS dilutions of 1:100.

All primary antibodies were incubated on the plate for 1 h at room temperature, before the plate was again washed three times in PBS-Tween. The secondary antibody was an HRP conjugated goat anti-rabbit IgG (H+L) diluted in PBS-Tween at 1:2500. The secondary antibody was incubated on the plate for 1hr at room temperature. The HRP substrate, 3,3',5,5'-tetramethylbenzidine (TMB) single solution (Invitrogen) was added to each well, and the reaction quantified at 405 nm by a plate-reading spectrophotometer (BioRad).

2.2.13 J774 macrophage infections with fluorescent *M. marinum*

For cell infections, *M. marinum* cultures were grown up for 6-7 days (an OD₆₀₀ of 0.8) and centrifuged at 2700 x g for 10 mins, washed twice with sterile Phosphate Buffered Saline, pH 7.3 (PBS) (Oxoid), and resuspended in 10ml sterile PBS before being passed through a 26 gauge needle (Terumo) to break up large bacterial clumps. Clumps were removed by centrifuging twice at 1000 x g for 2 mins. This produced a single-cell mycobacterial suspension in PBS. The cells were counted using a haemocytometer and added to U937 human monocytes or J774 murine macrophages at the required multiplicity of infection (MOI). 10 ml of J774 macrophages (in DMEM supplemented with 10% foetal calf serum and 2mM L-glutamine) or U937 monocytes (in RPMI media, supplemented with 10% foetal calf serum and 2 mM L-glutamine) were used for cell infection studies at a density of 2×10^5 cells/ml, and the red fluorescent strain of *M. marinum* msp12::dsred was applied as a single cell suspension at host cell : mycobacteria ratios of 1:1, 1:5, 1:10 and 1:20 (MOIs of 1, 5, 10 and 20). These cells were then incubated at 34.5°C and 5% CO₂ over a 4 day period, and 1ml samples were taken for microscope studies every 24 hrs. For confocal microscopy slides, 2 ml of J774 cells in DMEM were seeded onto coverslips at a density of 1×10^5 cells/ml and allowed to adhere and grow for 24 hrs, before a single cell suspension of the appropriate *M. marinum* strain was applied at an MOI of 1:10 (J774 : mycobacteria).

2.2.14 Confocal fluorescence microscopy/slide preparation

Coverslip mounted, infected J774s were washed three times with PBS and fixed for 10 mins using 4 % paraformaldehyde in PBS. The paraformaldehyde was removed and the coverslip washed three times in PBS, then allowed to dry and mounted onto glass slides

using ProLong[®] Gold anti-fade reagent (Invitrogen). The mounting reagent was allowed to dry for 24 h before imaging. Successful mycobacterial infections were assessed using a Leica Confocal Scanning Laser Microscope. The infected cells were studied using a 63x oil immersion lens and DSRED expressed by the mycobacteria was excited at 561 nm.

2.3 Results

2.3.1 Cloning of MPB70 and MPM70 with a C-terminal HIS tag

PCR amplification of the full length coding sequence for MPB70 and MPM70, with their N-terminal signal sequences, was analysed by 1% agarose gel electrophoresis. The PCR products observed indicated that the amplification of the MPB70 (582 bp) and MPM70 (594 bp) coding sequences had been successful, as bands of the expected size were visualised on the gel (Figures 2.2 and 2.3).

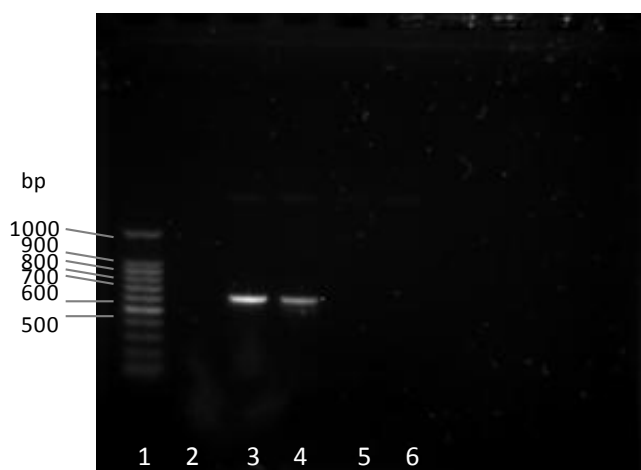
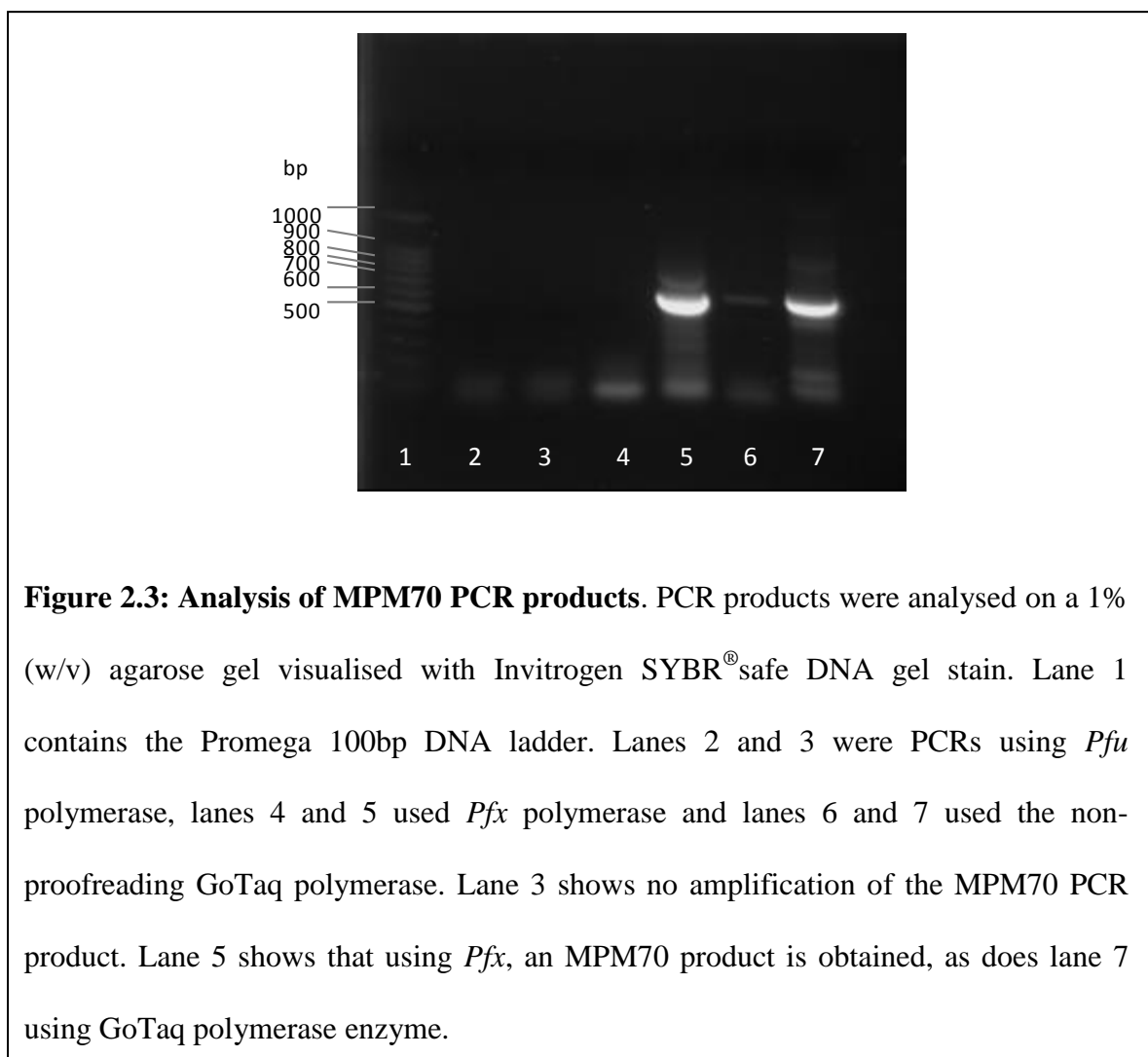


Figure 2.2: Analysis of MPB70 PCR products. PCR products were analysed on a 1% (w/v) agarose gel visualised with Invitrogen SYBR safe DNA gel stain, under ultraviolet light. Lane 1 contains the Promega 100bp DNA ladder. Lane 2 contains a control PCR reaction, where no DNA template was used. Lane 3 contains the MPB70 PCR product, at the expected size of around 582 bp. Lane 4 contains the MPB70 PCR product from a reaction containing 5% DMSO. Lane 5 shows no MPB70 product, and was a PCR reaction containing 1M betaine. Lane 6 shows no MPB70 product, and was a PCR reaction using both 5% DMSO and 1M betaine.

Cloning of the MPM70 product used *Mycobacterium marinum* genomic DNA as a template. PCR experiments were performed with the enzymes *Pfu*, *Pfx* and GoTaq. No PCR product was obtained with the *Pfu* enzyme; this may have been due to unoptimised conditions and could be remedied by increasing the Mg^{2+} concentration or adding DMSO to the reaction mix. PCR products for MPM70 were obtained with *Pfx* and GoTaq, however; each of these had high levels of contaminants. Gel purification allowed the contaminants to be removed and MPM70 products to be purified.



In order to assess the correct insertion of MPB70 and MPM70 products into the pLEICS-05 vector correctly, colony PCR was performed. 3 individual *E. coli* DH5 α

colonies were picked from each plate of transformants and a PCR reaction used to confirm that the MPB70 or MPM70 product was within the T7 region. Specific T7 promoter and terminator primers were used (see Methods 2.2.4). Colony PCR products indicated that only one of the 3 colonies picked contained MPB70 inserted within the T7 region, as shown in Figure 2.4 below, where there is a PCR product at the predicted 789 bp size. PNACL DNA sequencing confirmed that this product was of the correct sequence and orientation. PCR products obtained in the 3 MPM70 colony PCRs were all at the expected 801 bp size, indicating that all the colonies picked contained pLEICS-05 with the MPM70 PCR product correctly inserted into the T7 region. PNACL DNA sequencing confirmed that colony 1 (Figure 2.5, lane 3) contained the full MPM70 coding sequence in the correct orientation within the pLEICS-05 vector.

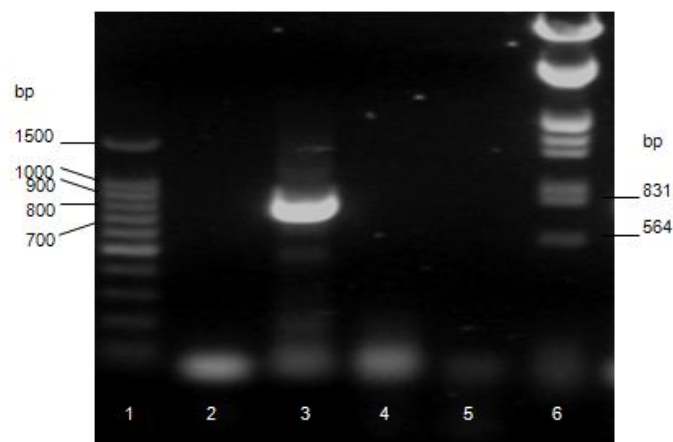


Figure 2.4: Colony PCR confirming that the MPB70 product had been successfully ligated into the pLEICS05 vector. Lane 1 contains the Promega 100bp marker, lane 2 is a control PCR reaction, where no template DNA was added. Lane 3 shows a positive result with MPB70 inserted correctly into the vector (at the predicted size of 789 bp), whereas lanes 4 and 5 do not. Lane 6 contains the Promega λ DNA/*EcoRI* + *HindIII* marker.

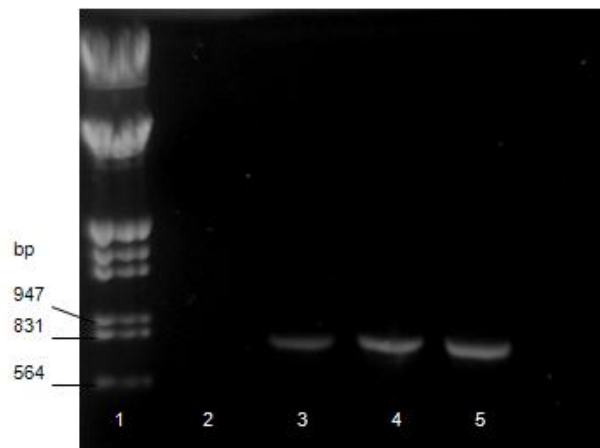
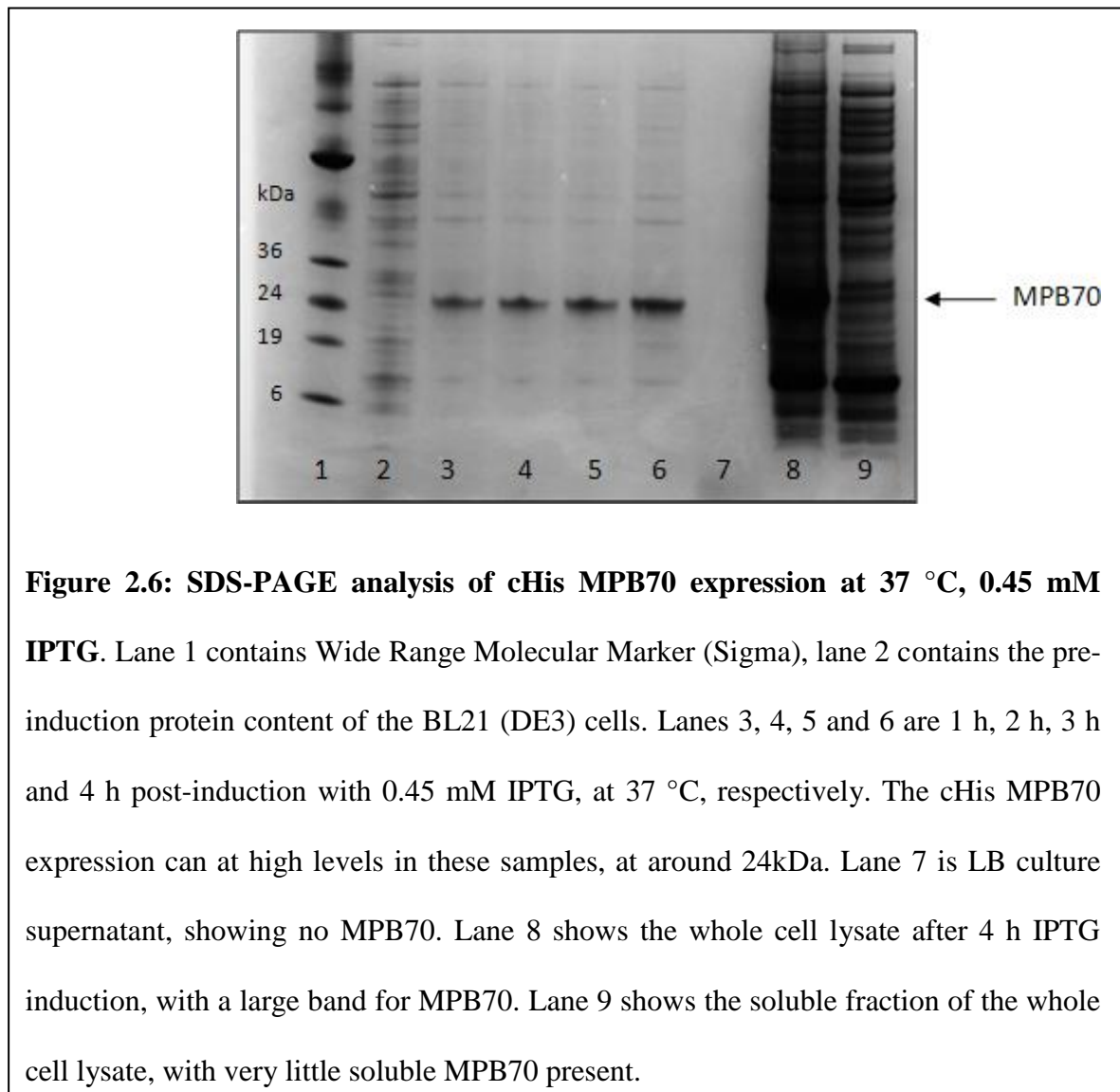


Figure 2.5: Colony PCR confirming that the MPM70 PCR product has been successfully ligated into the pLEICS05 vector. Lane 1 contains the Promega λ DNA/*EcoRI* + *HindIII* marker. Lane 2 contains a control reaction, where no template DNA was added. Lanes 3, 4 and 5 contain three different reactions using different picked colonies as DNA templates, and all three had the MPM70 PCR product ligated into the correct region, at the correct size of 801 bp.

After selecting the DH5 α colonies that contained the pLEICS-05 vectors with MPB70 and MPM70 products correctly within the T7 region, minipreps were used to isolate the plasmids for sequencing in-house by PNACL. The single colony containing a PCR product for MPB70 (Figure 2.4, lane 3) was confirmed as having a full coding sequence in the right orientation within the pLEICS-05 vector. The first colony picked containing the PCR product for MPM70 (Figure 2.5, lane 3) was confirmed as having the full MPM70 coding sequence in the correct orientation within the vector. These constructs with the correct sequences for MPB70 and MPM70 were transformed into competent BL21 (DE3) *E. coli* cells for protein expression.

2.3.2 Expression trials of C-terminally His tagged (cHis) MPB70 and cHis MPM70

The optimised expression of recombinant cHis MPB70 and cHis MPM70 required the testing of a combination of conditions, including temperatures of 37°C and 15°C, and final IPTG concentrations of 0.45 mM and 0.045 mM. Figure 2.6 shows an example of cHis MPB70 expression at 37°C and an IPTG concentration of 0.45 mM, which produces mainly insoluble protein.



Successful expression of soluble MPB70 and MPM70 required an IPTG concentration of 0.045 mM and a post-induction temperature of 15°C. Figure 2.7 shows SDS-PAGE analysis of cHis MPB70 expression, which was induced overnight to attain maximum protein yield. The results for cHis MPM70 were near-identical.

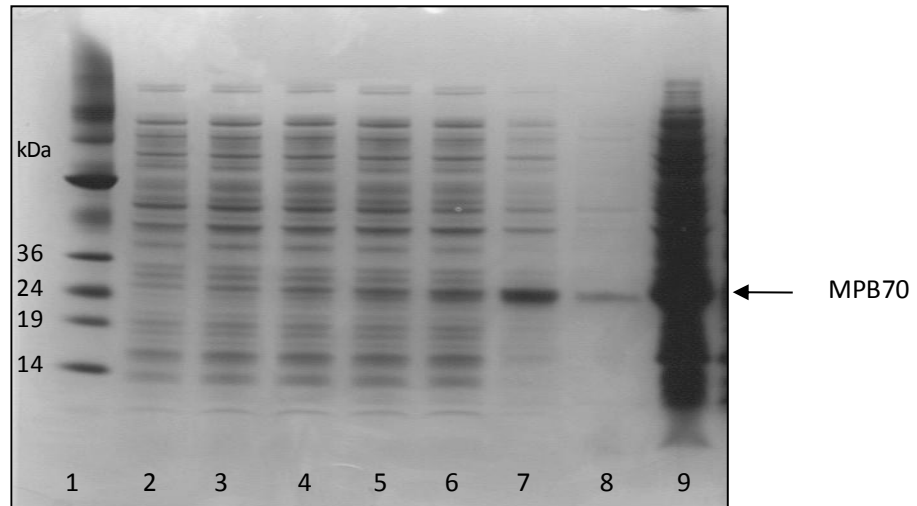


Figure 2.7: SDS-PAGE analysis of cHis MPB70 expression at 15 °C, 0.045 mM IPTG. Lane 1 contains Wide Range Molecular Marker (Sigma), lane 2 contains the pre-induction protein content of the BL21 DE3 cells. Lanes 3, 4, 5 and 6 are 1 h, 2 h, 3 h and 4 h post-induction with 0.045 mM IPTG, at 15°C, respectively. The cHis MPB70 expression can be seen increasing through these samples, at around 24kDa. Lane 7 is the overnight sample, showing high cHis MPB70 expression. Lane 8 is the culture supernatant; showing a small amount of cHis MPB70 has been secreted. Lane 9 shows the final concentration of soluble cHis MPB70 for the total culture, once the cells had been spun down and the pellet lysed into 2ml of lysis buffer.

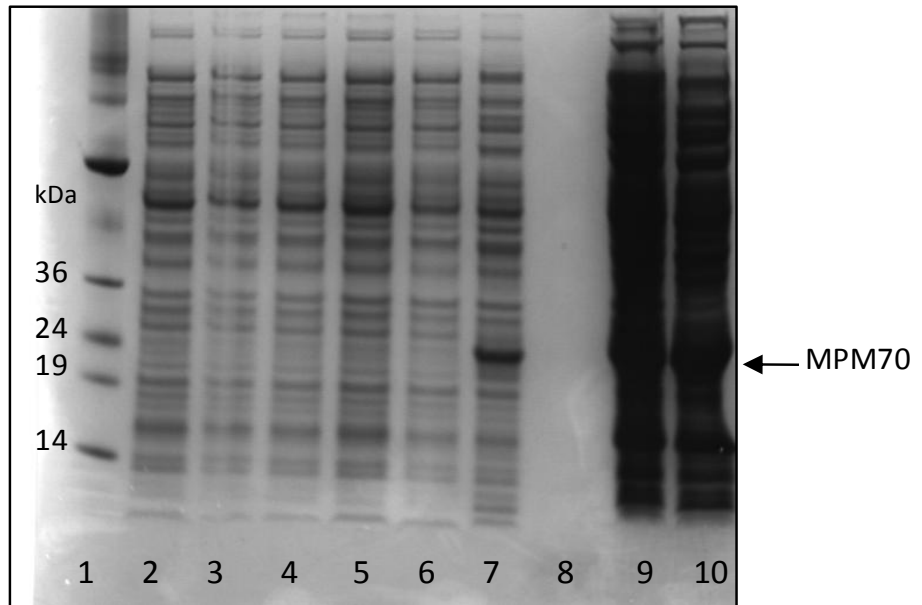
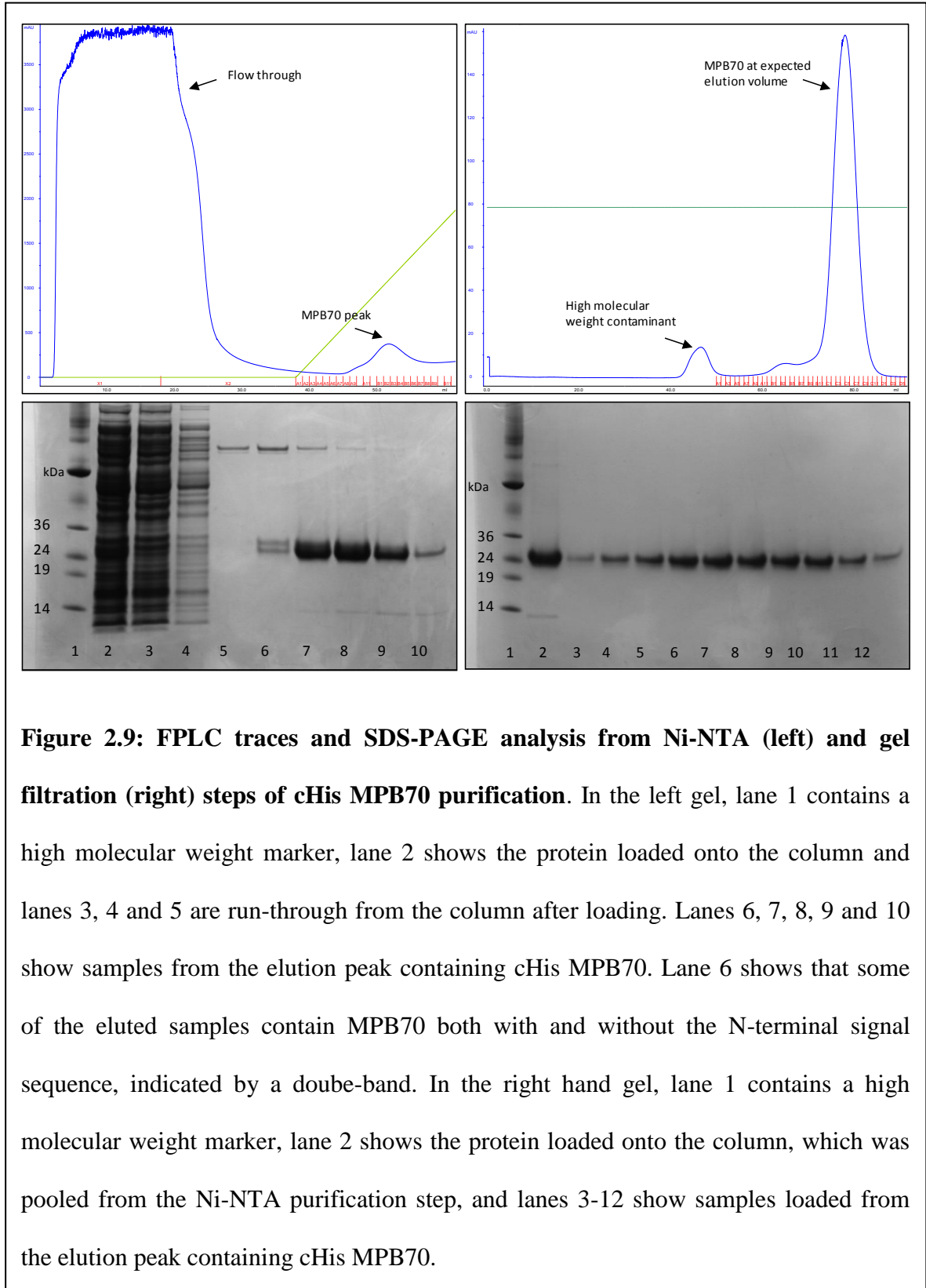
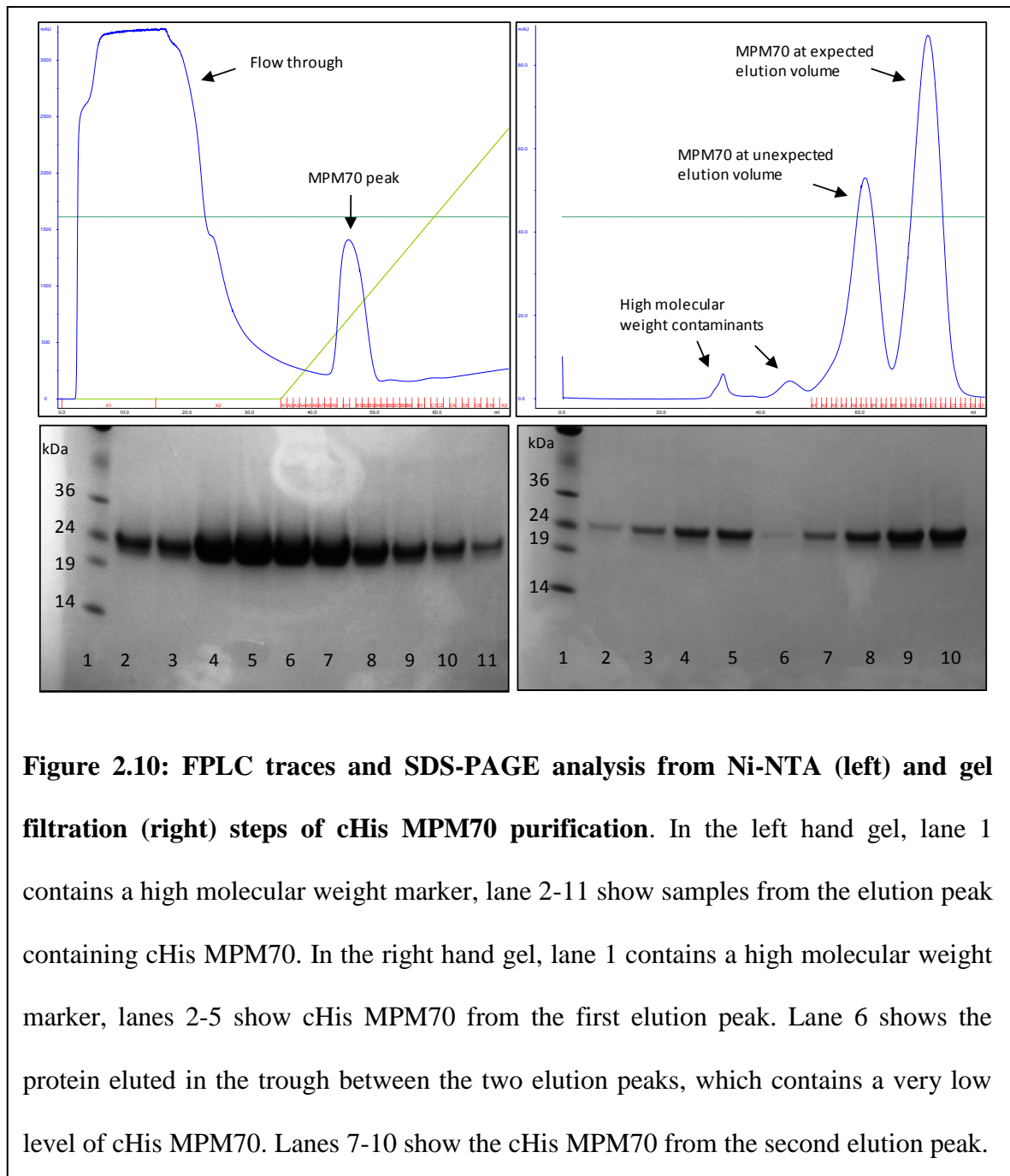


Figure 2.8: SDS-PAGE analysis of cHis MPM70 expression at 15 °C, 0.045 mM IPTG. Lane 1 contains Wide Range Molecular Marker (Sigma), lane 2 contains the pre-induction protein content of the BL21 DE3 cells. Lanes 3, 4, 5 and 6 are 1 h, 2 h, 3 h and 4 h post-induction with 0.045 mM IPTG, at 15°C, respectively. Lane 7 is the overnight sample, showing high cHis MPM70 expression. Lane 8 is the culture supernatant. Lane 9 shows the whole cell lysate, and lane 10 contains the total soluble fraction showing that there is a high level of soluble cHis MPM70.

2.3.3 Purification of cHis MPB70 and cHis MPM70

Successful purification of both cHis MPB70 and cHis MPM70 was achieved in a two-step process. The bound proteins were eluted from the Ni-NTA column via a linear imidazole gradient. The resulting SDS-PAGE analysis showed the His tagged proteins bound the column efficiently with very few contaminants present upon elution. High and low molecular weight contaminants were removed by Sephadex gel filtration. The gel filtration of cHis MPM70 produced two peaks on the FPLC trace, the larger of which eluted at the expected volume for MPM70. The other peak eluted may have contained unfolded protein or MPM70 which still had an intact N-terminal signal sequence (Figure 2.10).



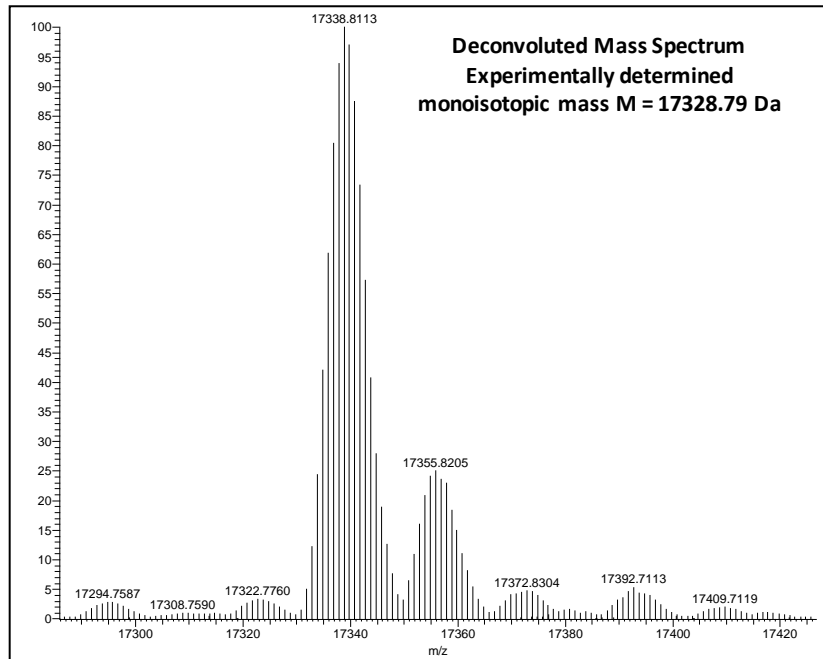


cHis MPM70 from the expected elution peak was pooled together and the concentration measure at 280 nm. This was then concentrated to 200 μ M for ^1H NMR to assess whether the protein was fully folded.

2.3.4 Mass spectroscopy analysis of purified cHis MPB70 and cHis MPM70

cHis MPB70 and cHis MPM70 were correctly identified using MALDI-TOF mass spectroscopy by excision of a band from an SDS-PAGE gel (after gel filtration Lane 9, Figure 2.10). The protein was digested with trypsin and protein fragment mass analysis using Mascot was performed, confirming that they were indeed MPB70 and MPM70, respectively (data not shown).

Electrospray mass spectroscopy confirmed that purified, native MPM70 did not have the N-terminal signal sequence attached. Samples were submitted to PNACL at the University of Leicester. The ExPASy ProtParam tool was used to calculate theoretical molecular masses for MPM70 with its N-terminal signal sequence (20218.0 Da) and without the N-terminal sequence (17412.7 Da). The experimentally determined mass was 17328.79 Da, confirming that the MPM70 species purified did not have an N-terminal signal sequence attached.



MPM70 without signal sequence:

```
ASPPDTLVGPGCSAYAQQVPTGPGSVAGMAAEPVAVAASNNPMLTTLTSAL
SGKLNQVNLVDTLNGGQFTVFAPTDAAFGKIDAATIDSLKTDAPLLKILTYH
VVPGQLSPSQVVGTHSTVEGASLTVTGSGNDLQVGDAAVVCGGVQ
TANAVVYMIDTVLMPPSENLYFQ
```

Predicted Mass = 17412.7 Da

MPM70 with signal sequence:

```
MKFHNPAIAATGLAAAAVGLVVATAPSAMASPPDTLVGPGCSAYAQQVPT
GPGSVAGMAAEPVAVAASNNPMLTTLTSALSGKLNQVNLVDTLNGGQFTV
FAPTDAAFGKIDAATIDSLKTDAPLLKILTYHVVPGQLSPSQVVGTHSTVEGAS
LTVTGSGNDLQVGDAAVVCGGVQ TANAVVYMIDTVLMPPSENLYFQ
```

Predicted Mass = 20218.0 Da

Figure 2.11: Electrospray mass spectroscopy of MPM70 confirms that the N-terminal signal sequence has been cleaved from the protein. The top spectrum shows a deconvoluted mass spectrum of submitted MPM70, with the most abundant isotopes having a mass around 17330 – 17340 Da. The sequences underneath show MPM70 with and without the N-terminal signal sequence, with calculated molecular masses from the ExPASy ProtParam tool. The N-terminal signal sequence is highlighted in red.

2.3.5 ^1H NMR to assess physical properties of purified MPB70 and MPM70 proteins

^1H NMR was employed to ensure that both MPB70 and MPM70 proteins were correctly folded. Previous NMR structural studies have provided our group with high-resolution structural data for native MPB70, making comparisons with recombinant purified MPM70 possible. The spectrum observed for MPM70 was strikingly similar to that previously reported for fully-folded MPB70, and expected, given their 85% sequence homology. This also strongly implies that the recombinant purified MPM70 is fully folded with a native structure.

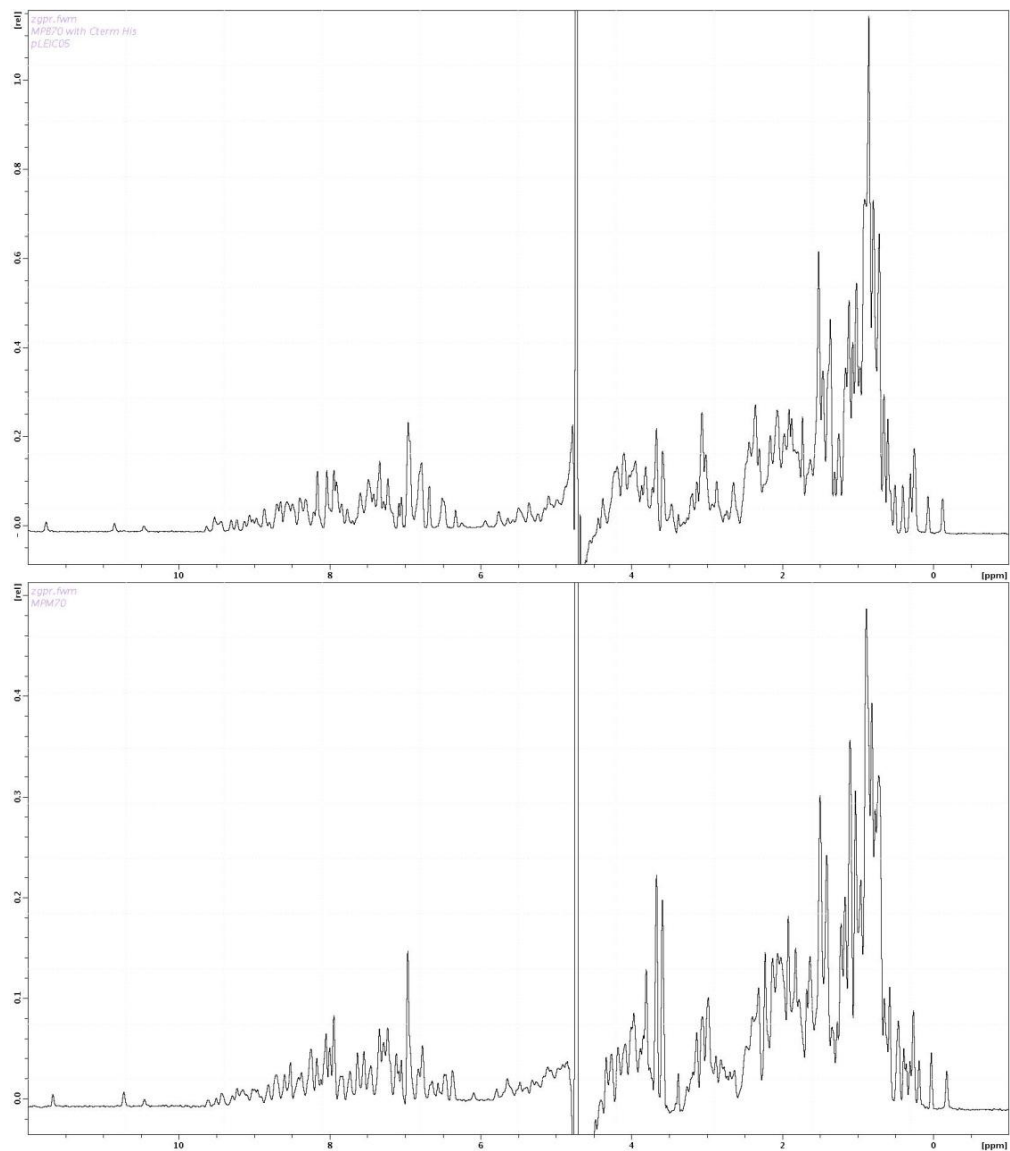


Figure 2.12: ^1H NMR spectra of purified recombinant MPB70 (top), and MPM70 (bottom). The ^1H NMR spectrum obtained for MPM70 (bottom) is essentially identical to that seen for fully-folded MPB70 previously (top), which indicates that the MPM70 produced here is fully folded. The methyl peaks on the right of the spectra are also well dispersed in both MPB70 and MPM70, which characteristic of folded proteins.

2.3.6 Purification of polyclonal antibodies from rabbit 4060 and 4061 sera

Polyclonal antibodies from the sera of both rabbits were purified in a one-step procedure using a pre-packed 5ml Protein A column (GE Healthcare). Polyclonal antisera from rabbits 4060 and 4061 were diluted 1:1 with PBS and loaded onto the column using a luer-lok syringe. The bound IgGs were eluted using a 100mM Sodium Citrate, pH2.8, and 1ml fractions collected, and the protein concentration determined from the A_{280} . The elution profiles show that in both cases, IgGs eluted after 4ml of the elution buffer was applied, and in both cases, the full elution was completed in roughly 5mls (top panels, Figures 2.13 and 2.14), meaning that the IgGs eluted were highly concentrated. Absorbance at 280 nm confirmed that both 4060 and 4061 were around 2.5mg/ml. The SDS-PAGE gel shows that the eluted IgG fractions were highly purified when compared to the initial sera samples (bottom panels, Figures 2.13 and 2.14).

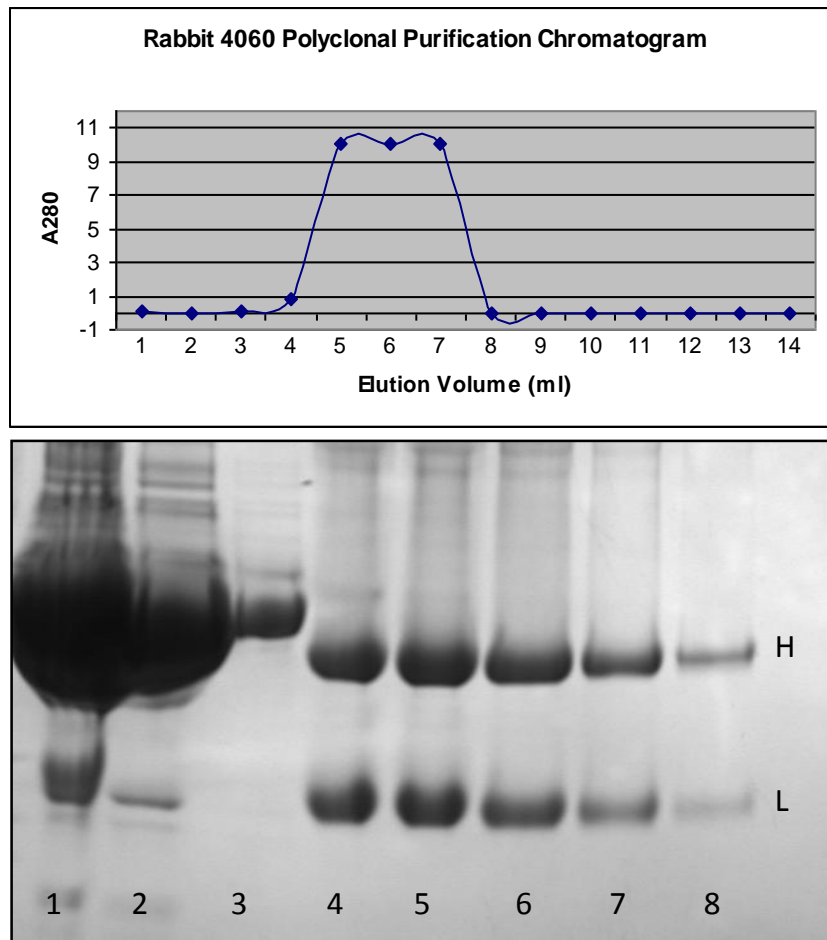


Figure 2.13: Protein A purification of anti-MPM70 rabbit 4060 polyclonal antibodies. The top image shows the A₂₈₀ elution profile of the IgGs from the Protein A column. The bottom image shows the corresponding SDS-PAGE analysis. Lane 1 contains the raw antiserum; lane 2 shows the PBS-diluted column load. Lane 3 contains the eluate after a 10 column volume PBS wash. Lanes 4-8 correspond to elution fractions from the chromatogram above, i.e. lane 4 contains a sample of the protein eluted at 4ml of elution buffer. H = Antibody heavy chain, L = Antibody light chain.

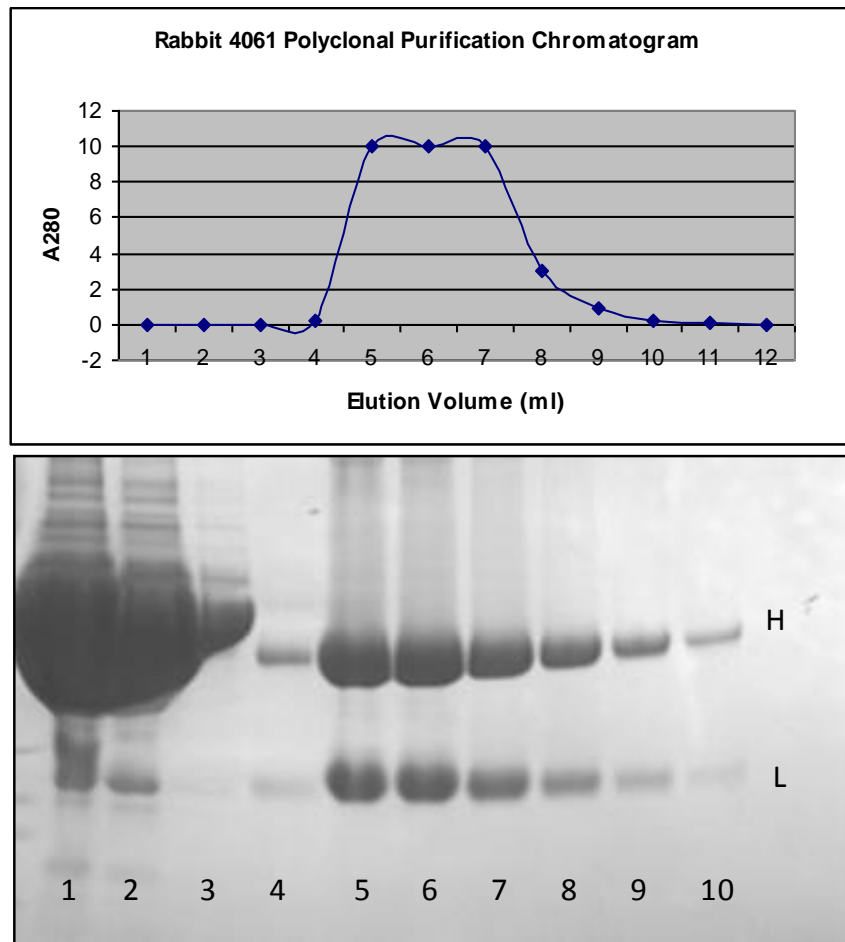


Figure 2.14: Protein A purification of anti-MPM70 rabbit 4061 polyclonal antibodies. The top image shows the A₂₈₀ elution profile of the IgGs from the Protein A column. The bottom image shows the corresponding SDS-PAGE analysis. Lane 1 contains the raw antiserum; lane 2 shows the PBS-diluted column load. Lane 3 contains the eluate after a 10 column volume PBS wash. Lanes 4-8 correspond to elution fractions from the chromatogram above i.e. lane 4 contains a sample of the protein eluted at 4ml of elution buffer. H = Antibody heavy chain, L = Antibody light chain.

2.3.7 Dot-blots to test the sensitivity of polyclonal antibodies 4060 and 4061 to purified MPM70

In order to test the sensitivity of the purified polyclonal antibodies from rabbits 4060 and 4061, a dot blot was used against decreasing concentrations of purified MPM70. The results showed that antibody 4060 could pick up as little as 2.5 $\mu\text{g/ml}$ of the purified protein, and antibody 4061 as little as 250 ng/ml . Both antibodies were applied at a final concentration of 2.5 $\mu\text{g/ml}$. From this, it was decided that the extra sensitivity of polyclonal antibody 4061 would be advantageous and therefore this antibody should be the primary antibody used in future experiments.

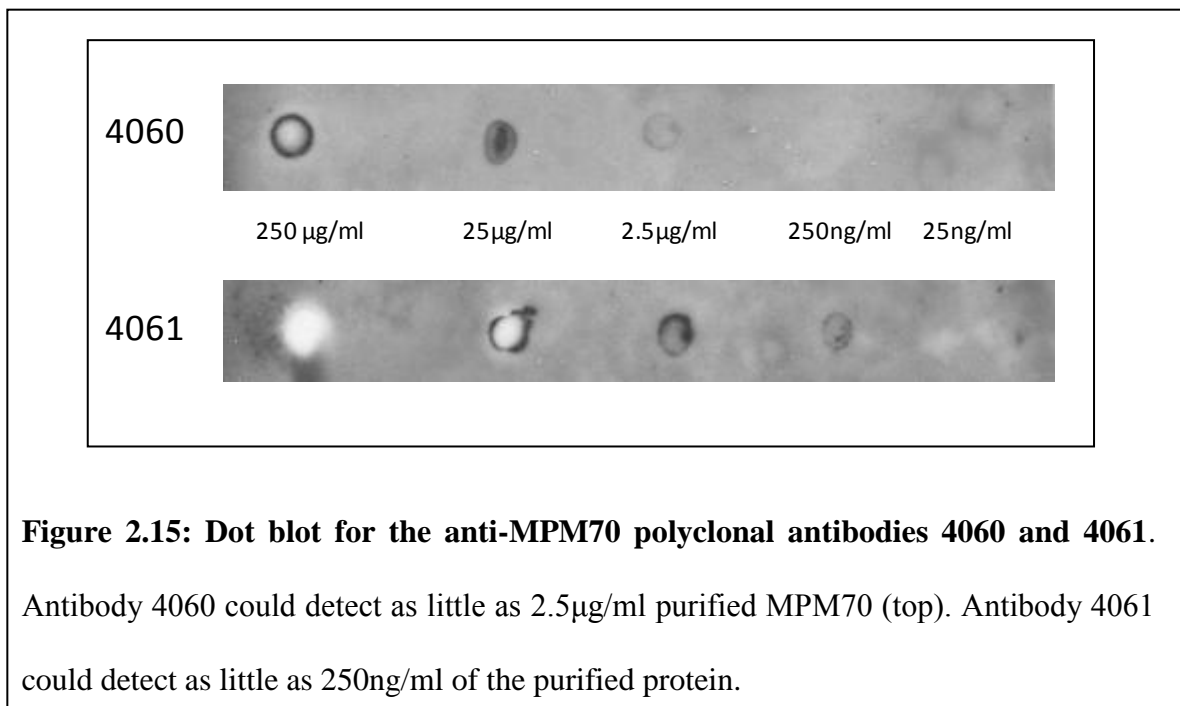


Figure 2.15: Dot blot for the anti-MPM70 polyclonal antibodies 4060 and 4061. Antibody 4060 could detect as little as 2.5 $\mu\text{g/ml}$ purified MPM70 (top). Antibody 4061 could detect as little as 250 ng/ml of the purified protein.

2.3.8 Enzyme-Linked Immunosorbent Assay (ELISA)

Enzyme-Linked Immunosorbent Assays were employed to quantify the sensitivity of the antibodies 4060 and 4061 to fully folded recombinant MPM70 protein seeded onto 96 well plates at a concentration of 10 µg/ml in PBS. The ELISA assays show that both purified polyclonal antibodies 4060 and 4061 were able to detect purified MPM70 protein at antibody dilutions of over 1:50,000 (v/v). The result for each purified antibody was repeated twice to ensure consistency. The negative controls consisted of rabbits 4060 and 4061 pre-immune sera, and showed that there was minimum reactivity to MPM70 in both rabbits' sera prior to MPM70 immunisation. The positive control consisted of the secondary antibody added directly to its TMB substrate.

	1/100	1/500	1/1000	1/2000	1/5000	1/10000	1/20000	1/50000
Rabbit 4060	3.367	3.158	2.963	2.726	2.555	2.125	1.907	1.42
Rabbit 4060	3.458	2.836	2.801	2.791	2.541	2.1	1.912	1.45
Rabbit 4061	2.978	2.955	2.833	2.754	2.68	2.528	2.374	1.922
Rabbit 4061	3.044	3.055	3.193	2.844	2.882	2.725	2.348	1.907
	0.335	0.54						1.413
Prebleed -ve controls	4060	4061						+ve control

Figure 2.16: ELISA assays to show the high sensitivity of purified polyclonal antibodies 4060 and 4061. Antibodies 4060 and 4061 were assayed for sensitivity to 10 µg/ml MPM70 recombinant protein. 4061 was shown to be consistently more sensitive than 4060, even at dilutions of up to 1:50,000 (v/v). Two repeat assays were performed for each antibody, to minimise anomalous results.

2.3.9 Characterisation of the *Mycobacterium marinum* : J774 macrophage infection model

Mycobacterium marinum is widely used as a model for *M. tuberculosis* infection, both *in vitro* (Ramakrishnan *et al.*, 1994; Stamm *et al.*, 2003) and *in vivo* (Cosma *et al.*, 2006; Davis *et al.*, 2009) and the use of fluorophore-expressing mycobacteria has been used in confocal microscopy studies to show phagosomal escape and actin polymerisation by mycobacteria during infection (Stamm *et al.*, 2003; van der Wel *et al.*, 2007; Hagedorn *et al.*, 2009). Previous studies using both *M. tuberculosis* and *M. marinum* (Stamm *et al.*, 2003; van der Wel *et al.*, 2007) have used a multiplicity of infection (MOI) around 10. Optimisation of the temperature dependency of the infection has been highlighted in previous studies (Ramakrishnan *et al.*, 1994) and had to be addressed here. Details of the effects of varying conditions on a 4 day infection course are covered in the table in Figure 2.17. Different MOIs and temperatures were tested and evaluated either by confocal microscopy, as the example images demonstrate in Figure 2.18, or by light microscopy in cell culture, as summarised in the table in Figure 2.17.

The representative images in Figure 2.18 show macrophage cells infected at MOIs of 1 (image A), 10 (image B) and 30 (image C), at 24 hpi, respectively. Image A shows that at 24 hpi, only a small fraction of cells are infected; and this is mainly with single mycobacteria. The infection then progresses slowly and late-stage infections (densities of 30+ mycobacteria per cell) are not observed by 72 hpi (data not shown). Image B shows an infection with a MOI of 10 at 24 hpi, where around 40% of cells are infected and there are between 1-10 mycobacteria per cell. At this MOI, at 72 hpi, many cells can be observed at densities of 30+ mycobacteria without high levels of host cell death.

Image C shows host cells at 24 hpi with a MOI of 30. Many cells can be observed at high infection densities, of around 20-25 mycobacteria per host cell. At 72 hpi, very few host cells were observed due to high levels of cell death, as mycobacterial counts were too high (data not shown). The effects of infection temperature are summarised in the table in Figure 2.17, and representative images are shown in Figure 2.18. Observations were made using light microscopy during cell culture, for example, at 32°C, high densities of mycobacteria were observed in the surrounding media without infecting host cells (data not shown). At 34.5°C, mycobacteria were observed mostly inside host cells, as seen in images A, B and C in Figure 2.18 with few in the surrounding media. At 37°C, light microscopy showed J774 cells growing to confluence but mycobacteria did not appear to infect host cells, presumably due to mycobacterial death at this temperature (data not shown).

Condition	Result
MOI = 1	Slow infection progress. Late-stage events are rare during a 4 day time-course. (Image A)
MOI = 10	Early, mid- and late-stage events observed during 4 day time-course. (Image B)
MOI = 30	Fast infection progress. High level of host cell death by 72 hpi. (Image C)
Temp = 32°C	High level of bacterial growth in DMEM.
Temp = 34.5°C	Mycobacteria mostly uptaken by J774 cells, very few in surrounding media.
Temp = 37°C	J774 cells grow to confluence; mycobacteria struggle to establish an infection.

Figure 2.17: Table summarising different infection conditions tested in a 4-day time-course. The table gives an example of observations made using light and fluorescent confocal microscopy with varying infection conditions, including initial mycobacterial load (MOI) and temperature. Example images A-C for MOI variations are shown in Figure 2.18.

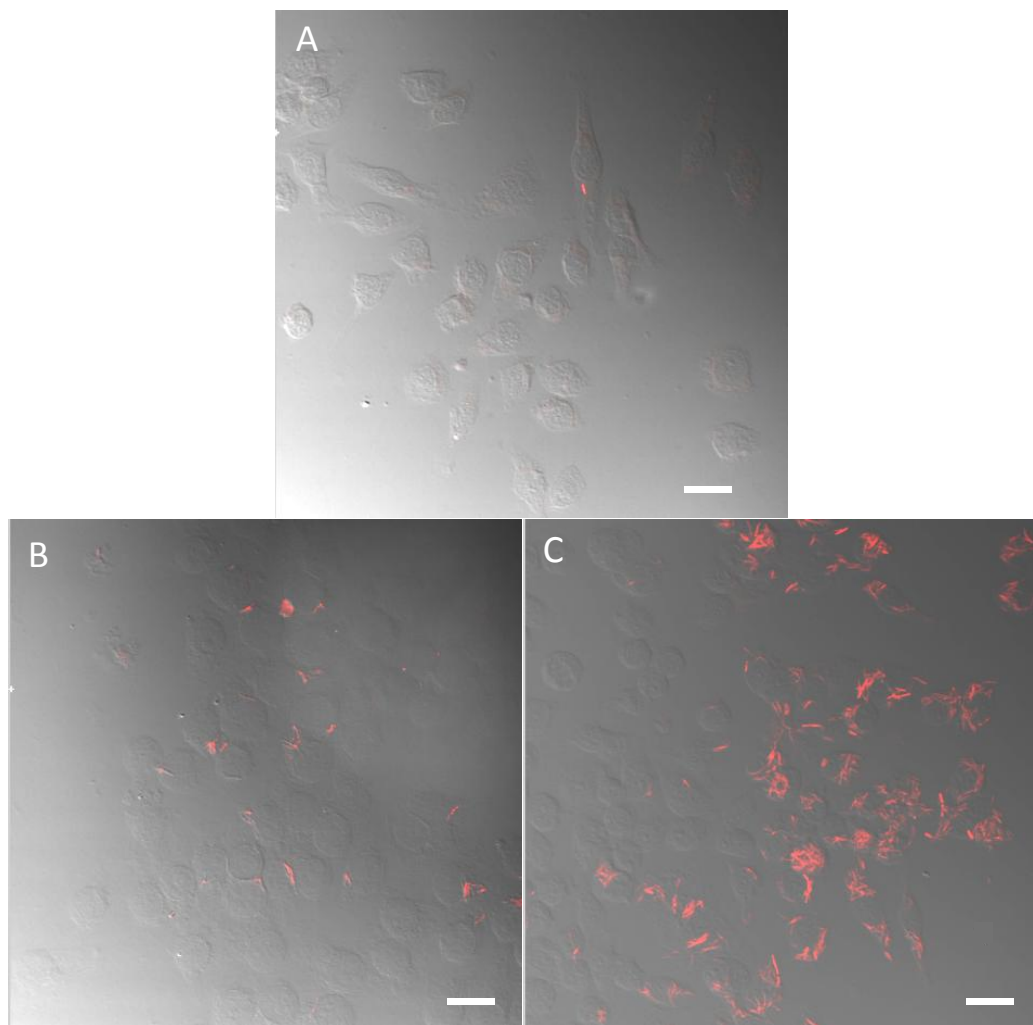
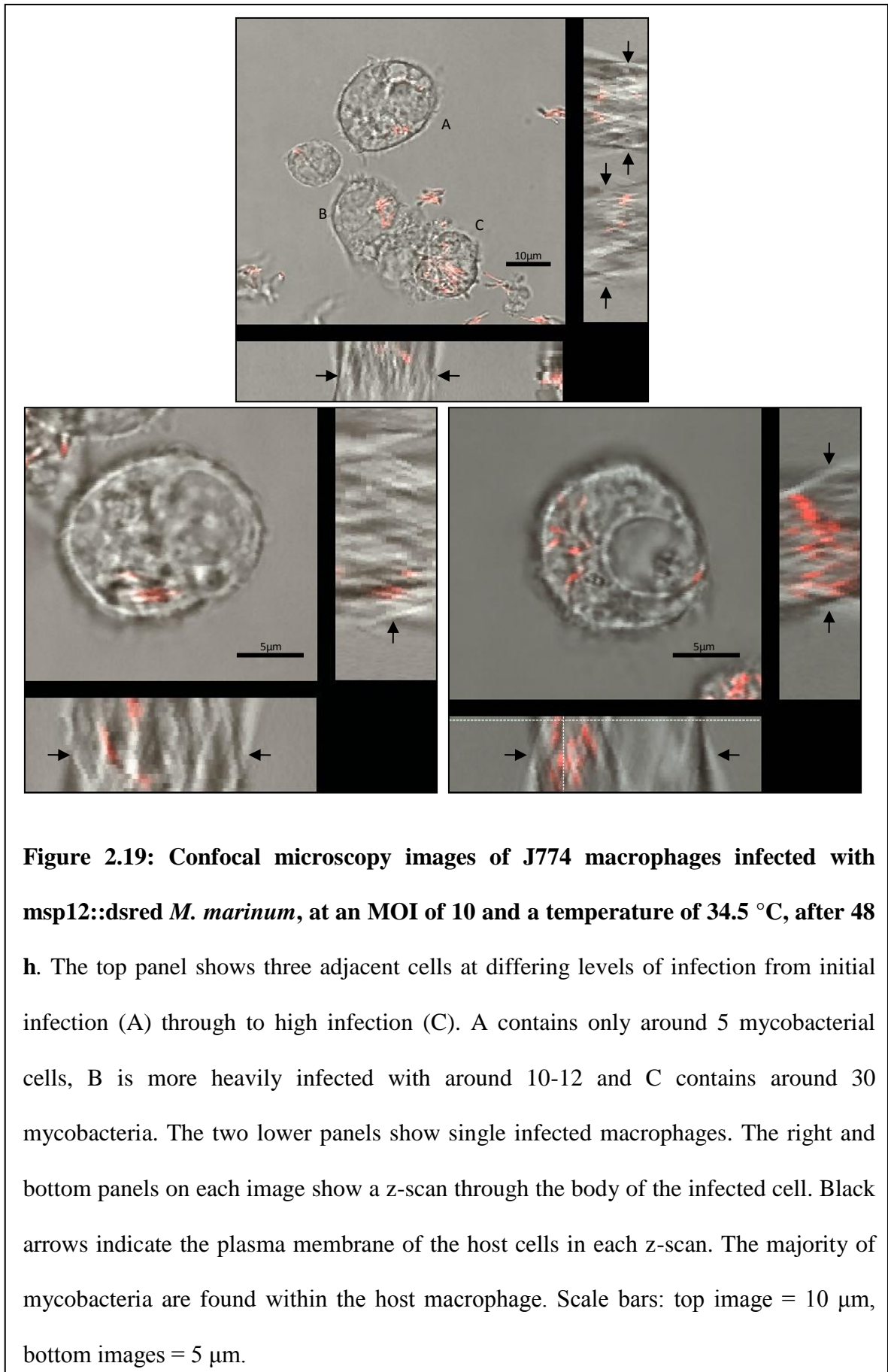


Figure 2.18: Example images for infection conditions tested in a 4 day time-course at 34.5 °C. The images show examples of infected cells at 24 hpi, with MOIs of 1 (A), 10 (B) and 30 (C). The initial MOI therefore dictates the speed of infection, as at a MOI of 1 (A), very few cells are infected at 24 hpi. A MOI of 30 (B) shows many cells heavily infected after 24 h, which would not survive a full 72 h infection time-course. Size bars = 20 μm .



Characterisation of the infection under different conditions indicated that using an MOI of 10 and a temperature of 34.5°C, a 4 day infection course could be studied. This should allow for stages of infection associated with low and high mycobacterial infection to be observed without host cell lethality, which should allow the expression of MPM70 tracking experiments in infected macrophages using the anti-MPM70 polyclonal antibody 4061.

2.4 Discussion

This chapter has outlined the optimisation of a mycobacterial infection model using *Mycobacterium marinum* in the murine macrophage J774 and the cloning, expression and purification of MPB70 and MPM70 proteins. Two populations of polyclonal antibodies against the *M. marinum* protein MPM70 were raised in rabbits (4060 and 4061), and IgGs from resulting sera were purified using a Protein A column. The polyclonal IgGs were analysed using immunological tests including ELISA, dot blot and Western blot to characterise their sensitivity and specificity.

In order to produce the conformational, native MPM70-specific antibodies, cloning and purification of the mycobacterial virulence factors MPB70 and MPM70 had to be achieved. Prior to these experiments MPB70 purification was achieved via a non-inducible system using *E. coli* DH5 α transformed with pBluescript KS⁺ containing the full coding sequence of MPB70 (Hewinson *et al.*, 1996; Bloemink *et al.*, 2001). This had a low yield (around 0.5 mg protein per litre *E. coli* culture) and also meant that expressed soluble protein was lost through the secA secretion machinery that is shared between mycobacteria and *E. coli* (Hewinson *et al.*, 1996). pLEICS-05 constructs for both MPB70 and MPM70 were optimised in order to maximise the soluble protein yield, as initial expression trials (37°C, 0.45mM IPTG, 4 h expression) gave very little soluble protein, but very high levels of protein in non-soluble inclusion bodies. Mature MPB70 or MPM70 cannot be purified from inclusion bodies because the N-terminal signal sequence would not be cleaved off, as N-terminal signal cleavage only occurs when the protein reaches the periplasm. In order to optimise the soluble protein yield, expression trials were performed at temperatures of 37°C, 25°C and 15°C, and IPTG concentrations of 0.45mM and 0.045mM. Testing combinations of these expression

conditions led to the discovery that a 15°C overnight expression at an IPTG concentration of 0.045mM was optimal for high levels of soluble MPB70 and MPM70. The new MPB70 and MPM70 constructs were further optimised in that they were expressed with a cleavable C-terminal His tag, allowing for a straightforward two-step purification (Ni-NTA followed by Sephadex gel filtration), as outlined in the results section 2.2.6. Furthermore, they allow a minimum of 8mg of purified protein yield per litre culture of *E. coli* grown. The double peak observed during Sephadex gel filtration of MPM70 was unexpected. The protein in the first peak eluted at an unexpected volume; representative of a larger or improperly folded protein. SDS-PAGE analysis revealed no significant size difference between species from the two eluted MPM70 peaks. The second peak, at the expected elution volume, contained protein that was of the correct mass, confirmed by Electrospray Mass Spectroscopy. This protein was pooled and prepared for polyclonal antibody production.

Both purified MPB70 and MPM70 proteins were shown to be properly folded using 1D NMR spectroscopy. Following the removal of the His tag by TEV protease, the protein was over 99 % pure, confirmed by SDS-PAGE analysis. This highly purified, natively folded MPM70 was used to inoculate rabbits, allowing for the production of a custom polyclonal antibody. Experimental data described in this chapter confirms that the custom antibodies 4060 and 4061 are suitable for a number of different applications; including ELISA, Western blotting and immunofluorescence. In all tests, polyclonal antibody 4061 was shown to have a higher sensitivity than 4060, and was therefore used for the experimental investigation described in Chapter 3. The antibodies were applied to the *Mycobacterium marinum*: J774 macrophage infection model for MPM70 detection via immunofluorescence and Western blot.

The infection model used in these experiments has required characterisation in order to produce a 4 day infection time-course with both low and high mycobacterial counts to observe. This includes applying the correct MOI in order for a 4-day time course infection to proceed with a high percentage of host cells infected, without risking host cell lethality due to mycobacterial overload. A point to note is the variation in speed of the infection as a result of the initial bacterial load (MOI). Such an effect has not been alluded to before, but may account for variations in the results seen in previous publications, where MOIs of 1, 10 and 4-12 (Stamm *et al.*, 2003, Lasunskaja *et al.*, 2006, Collins *et al.*, 2009) have been used. This could alter the course of events during an infection time-course; for example, recent studies using a MOI of 1, actin tail formation was observed at 48 hpi, and a MOI of 3 allowed actin tails to be observed as early as 24 hpi (Stamm *et al.*, 2003, Stamm *et al.*, 2005), showing that initial mycobacterial density can affect the time-point at which specific events can be observed in a macrophage infection model. It should be stressed that time-points are somewhat arbitrary in the mycobacterial infection model due to the general heterogeneity of the system (see Figure 2.19) and the global rate of infection can vary based upon the initial MOI. Therefore, a system based upon per-cell bacterial load should be used to determine the course of infection in individual host cells. A system based upon per-cell mycobacterial load is used for characterisation of a 72 h infection process and MPM70 expression in Section 3.3.3. Neighbouring cells can be observed at varying levels of infection at any time-point, from no infection at all, to large bacterial counts of 50 cells or more. For example, at an MOI of 1 the infection proceeds slowly, and many host cells remain uninfected throughout the 4-day infection course. At 72hpi, the average bacterial load per cell would be around 20. However, at an MOI of 20, many J774 cells would die by the 72hpi point and any host cells left would be overloaded with

mycobacterial counts of 40-50 or more. The heterogeneity in this infection model may be inherent to the method itself, as the addition of mycobacteria to host cells in sterile PBS allows free mycobacteria to remain within the system. This means that they be phagocytosed at any point over the 72 h time-course by the macrophages, which introduces heterogeneity to the infection model as seen. Furthermore, dead mycobacteria will also be uptaken and remain as single cells within the macrophages, unable to grow until they are successfully killed in a mature lysosome. One way to address this heterogeneity would be to add the mycobacteria at the desired MOI for a short space of time (1 h only) to allow uptake of an initial load of mycobacteria by the host cells, at which point the excess media and free mycobacteria are removed and the cells washed in fresh sterile DMEM media, before fresh media is added. The infection of the remaining host cells could then continue over the 72 h time-course, and the spread of the infection should be limited to mycobacterial cell-cell spread or mycobacteria released into the surrounding media by host cell death and lysis.

The contents of this Chapter show that it is possible to create an inducible expression system for MPB70 and MPM70, and that the proteins can be purified using a two-step purification method. The antibodies 4060 and 4061 were purified and shown to have high specificity to purified MPM70 in a number of immunological tests. Due to its higher sensitivity, antibody 4061 was chosen for use in the experiments tracking MPM70 expression and localisation in Chapter 3. Also outlined is the setup and optimisation of the *M. marinum*:J774A.1 macrophage infection model into which the 4061 antibody will be applied.

Chapter 3

Localisation and quantification of MPM70 expression during infection

3.1 Introduction

This chapter describes the use of the murine macrophage infection model and *Mycobacterium marinum* to track the expression and localisation of MPM70 *in vitro* via confocal immunofluorescent microscopy and Western blotting. The results show that the majority of secreted MPM70 appears to be localised to the mycobacterial surface. MPM70 is expressed after mycobacteria have escaped the phagosome into the host cell cytoplasm and expression of the protein seems to be independent of intracellular mycobacterial density.

3.2 Methods

3.2.1 J774A.1 macrophage infections with fluorescent *Mycobacterium marinum*

J774A.1 mouse macrophages were seeded onto coverslips at 1×10^5 cells/ml or into 75 cm² flasks at 1×10^5 cells/ml and infected at an MOI of 10 for all the experiments in this Chapter. Infections were carried out as detailed in section 2.2.13.

3.2.2 Western blot analysis of the expression of MPM70 in *Mycobacterium Marinum* in infected macrophages

50 ml of J774A.1 macrophages at 2×10^5 cells/ml were grown for 4 days, and infected with *M. marinum* at an MOI of 10 (see section 2.2.13). These cells were then harvested by mechanical scraping and centrifugation at 2000 x g, and the pellet lysed using 1ml RIPA buffer (50 mM Tris-HCl, 150 mM NaCl, 10 mM MgCl₂, 1% NP40, 0.1% SDS) for 20 mins on ice. The samples were sonicated using a Misonix Sonicator 3000 for 2 mins, in cycles of 20 secs on, 20 secs off before being centrifuged for 20 mins at 4000 xg. The soluble fraction was taken and the A₂₈₀ measured. Samples were normalised by protein content and the constituent proteins separated by SDS-PAGE gel electrophoresis.

Western blots were used to track global MPM70 expression in infected J774A.1 macrophages at different time-points. The cell lysate protein content was separated by SDS-PAGE (section 2.2.3), and proteins transferred from the SDS-PAGE gel to nitrocellulose membrane (Invitrogen) at 30 V and 110 mA for 1 h using a transfer buffer of 12.5 mM Tris-HCl, 100 mM glycine, 20 % (v/v) methanol. The molecular weight markers used were Novex Prestained Protein markers (Invitrogen).

The nitrocellulose membrane was blocked using 5% Calbiochem BLOT-Quickblocker™ Reagent in PBS-Tween for 1 h and washed three times with PBS-Tween. The primary antibody was 4061 (purified from sera from rabbit 4061, as detailed in Section 2.3.6) applied at a 1:1000 (v/v) dilution in PBS-Tween with 1% Quickblocker™ Reagent for 1 h at 4°C, washing three times with PBS-Tween before adding the secondary antibodies. The secondary antibody was goat anti-rabbit IgG (H+L) with an HRP conjugate (Invitrogen Molecular Probes) used at a 1:2500 (v/v) dilution diluted in PBS-Tween with 1% Quickblocker™ Reagent. The secondary antibody was applied for 1 h at room temperature then washed three times with PBS-Tween. Protein bands were visualised using GE Healthcare ECL plus Western Blot Detection kit.

3.2.3 Confocal fluorescence imaging of MPM70 expression during infection

To visualise intracellular membranes, J774A.1 macrophages were allowed to uptake the lipophilic membrane marker DiIC₁₈(5)-DS (Invitrogen Molecular Probes) for 1.5 h at 34.5°C prior to fixation. This marker is highly fluorescent and photostable when incorporated into membranes.

For fixation, media was removed, and the cells washed three times in PBS before adding 1 ml 4% paraformaldehyde in PBS for 10 minutes. The coverslips were again washed three times in PBS and the cells were permeabilized using ice-cold 0.2% Triton X-100 in PBS for five minutes. The cells were then washed with PBS three times and blocked for 1 h at 4°C with 5% BSA (Sigma) in PBS before being washed in PBS to remove any excess blocking buffer.

Primary antibodies, such as anti-MPM70 4061 (Cambridge Research Biochemicals), and monoclonal 1D4B rat anti-mouse LAMP-1 (BD Biosciences) were then added at their specific dilutions in 1% BSA in PBS (see Figure 3.1). When labelling more than one protein, primary antibodies were added together in the 1% BSA PBS solution for 1 h at 4°C, before being removed and the slides washed in PBS three times. For multiple labelling, fluorescently-labelled secondary antibodies were applied together, such as goat anti-rabbit IgG (H+L) conjugated with AlexaFluor 488 (Invitrogen Molecular Probes). Slides were prepared by washing the coverslips three times in PBS, air-drying and mounting using ProLong[®] Gold anti-fade reagent (Invitrogen). Mounted slides were allowed to dry for 24 h before being imaged on a Leica Confocal Scanning Laser Microscope. The infected cells were studied at 63x magnification using an oil immersion lens.

Bacterial Strain	Excitation/Emission (nm)	Protein	Primary Antibody (dilution)	Secondary Antibody (dilution)	Excitation/Emission (nm)
<i>M. marinum</i> (DsRed)	561 / 583	MPM70	Rabbit anti-MPM70 4061 (1:500)	Goat anti-rabbit IgG + AlexaFluor 488 (1:1000)	495 / 519
<i>M. marinum</i> (DsRed)	561 / 583	LAMP-1	1D4B rat anti-mouse LAMP-1 (1:30)	Goat anti-rat IgG + AlexaFluor 633 (1:1000)	632 / 647
<i>M. marinum</i> ΔRD1 (GFP)	488 / 509	MPM70	Rabbit anti-MPM70 4061 (1:500)	Donkey anti-rabbit IgG + AlexaFluor 633 (1:1000)	555 / 565

Figure 3.1: Summary of the fluorophores used for fluorescent confocal microscopy. The table above contains the excitation and emission wavelengths (nm) for every fluorophore used in immunofluorescence experiments in this Chapter, and also details the primary and secondary antibodies used.

3.2.4 Quantification of MPM70 expression from fluorescent microscope slides

In order to characterise the mycobacterial infection and MPM70 expression, immunofluorescent slides were produced as in Section 3.2.3. Three infection experiments were performed at a MOI of 10, and slides prepared for infection time-points of 3, 24, 48 and 72 h. Fluorescent markers used were DiIC₁₈(5)-DS (Invitrogen Molecular Probes) for host cell membrane detection, and anti-MPM70 antibody 4061 and Goat anti-rabbit IgG conjugated with AlexaFluor 488 (Invitrogen Molecular Probes) for MPM70 detection.

Six representative z-stacked images were taken from each slide using a Leica Confocal Scanning Laser Microscope with an oil-immersion x40 objective lens. Cells were numbered in each image (Figure 3.7) and scored by infection level, based upon mycobacterial counts per host cell (Figure 3.8). DiIC₁₈(5)-DS staining was used to determine mycobacterial localisation as phagosomal or non-phagosomal, and MPM70 expression was scored by eye as Low, Medium or High based upon the area covered by MPM70 expression (the amount of coverage of intracellular mycobacteria) and the green fluorescence intensity observed.

3.2.5 Immobilised MPB70/MPM70-based screens for host cell interaction targets

NHS-activated Sepharose beads (GE Healthcare) were prepared by equilibrating in 5 x 0.5 ml washes of 1 mM HCl. MPB70 or MPM70 were bound to the 50 % bead slurry by adding 1 mg/ml protein in 25 mM Na₂HPO₄, 100 mM NaCl, and adjusting to pH 7.5. This mixture was incubated on a turntable overnight at 4 °C and the supernatant was removed by centrifugation. Any unbound interaction sites on the beads were blocked with 0.1 M Tris, pH 8.5 at room temperature for 4 h. Non-MPB70/MPM70 bound

control beads were prepared by adding 0.1 M Tris, pH 8.5 to 50 % bead slurry at room temperature for 4 h.

For NHS-activated sepharose-immobilised MPB70/MPM70 pull-down experiments, the soluble protein fraction from U937 monocyte cells was prepared by taking 600 ml of cells at 1×10^6 cells/ml. The cells were removed from the media by centrifugation at $2500 \times g$ for 10 mins at 25 °C. The pellet was lysed into 25 mM Na_2HPO_4 , 200 mM NaCl, 100 μM AEBSF, 25 μM EDTA, 10 mM AEBSF, pH 7.5. Cells were lysed by sonication and the non-soluble material is removed by centrifugation at $4000 \times g$, for 10 mins at 4°C. The cell lysate was mixed with 200 μl of 50% slurry beads, MPB70 NHS beads and blocked NHS control beads in the same buffer. These were incubated on a turntable at 4°C overnight. The beads were then washed with 5 x 1ml of the lysis buffer to wash off any excess WCL and the results analysed via SDS PAGE and silver stained with SilverXpress Silver staining Kit (Invitrogen). Any bands present on the gel from the preparation of MPB70-bound beads, and not found in the preparation of the unbound control beads, represented a potential MPB70 interaction partner.

For Ni-NTA immobilised MPB70/MPM70 pull-down experiments, the soluble protein fraction from U937 monocyte cells was prepared by taking 600 ml of cells at 1×10^6 cells/ml. The cells were removed from the media by centrifugation at $2500 \times g$ for 10 mins at 25 °C. These cells were then resuspended in 4 ml of Ni-NTA lysis buffer; 50 mM tris-HCl, 30 mM imidazole, 150 mM NaCl, 1 mM AEBSF, pH 8.0. Cells were lysed by sonication and the non-soluble material was removed by centrifugation at $4000 \times g$, for 10 mins at 4 °C. A 1ml Ni-NTA matrix was equilibrated with a base buffer of 20mM tris-HCl, 30 mM imidazole, 150 mM NaCl, pH8.0. cHis MPB70 is used at 20 μM , and 1ml was applied to the column to allow it to bind, washed with 5 column

volumes (CV) of base buffer. 4 ml of soluble U937 cell lysate was then washed down the column, collected in 1 ml fractions. Excess cell lysate was washed from the column with 5 CV of the base buffer before a 5-step concentration gradient was applied to the column. The increasing step-wise gradient consisted of a 20 mM tris-HCL, 150 mM NaCl, pH8.0 buffer with 50, 100, 150, 200 or 500 mM imidazole respectively. The aim of this is to displace the MPB70 and any binding partners still bound after the wash steps, and 1ml fractions were collected in Eppendorf tubes so that the A_{280} can be measured. Any significant peaks in the A_{280} were analysed by SDS-PAGE and the results visualised using an Invitrogen SilverXpress silver staining kit.

3.3 Results

3.3.1 Global MPM70 expression in *Mycobacterium marinum* infected macrophage cells

In order to quantify global MPM70 expression in *M. marinum* infected macrophage cells, a Western blot was performed on samples obtained from 50 ml cultures of infected J774A.1 macrophages at an MOI of 10. Samples were prepared at 3, 24, 48 and 72 hpi (Hours Post Infection). The expression of MPM70 is observed as early as 3 hpi and is upregulated over 24 and 48 hpi, before expression levels drop at 72 hpi. MPM70 is only expressed inside infected macrophages, as Western blots performed from samples of 7H9 cultured *M. marinum* did not detect the protein (data not shown.)

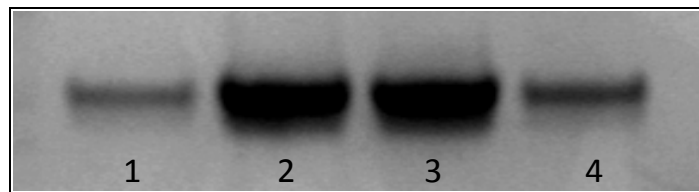


Figure 3.2: Global MPM70 expression in *M. marinum* infected macrophage cells over a 72 h time-course infection at a MOI of 10. Lanes 1-4 show MPM70 expression at 3, 24, 48 and 72 hpi, respectively. MPM70 expression is lowest at 3 hpi, is highest at 24 and 48 hpi and expression levels drop at 72 hpi.

A similar, but not identical situation is seen when the same time points of infection are studied via confocal microscopy. Although the global picture of the mycobacterial infection remains the same, there is a great deal of heterogeneity within the infection, even in neighbouring cells. An example of this is shown in Figure 3.3, where a group of neighbouring cells which have all been exposed to single-cell suspension msp12::dsred *M. marinum* for 24 h at an MOI of 10. The cell labelled A is uninfected. B shows a cell

infected with 3-5 mycobacteria (red), which are producing a high level of MPM70 (green), which appears to be closely associated with the mycobacterial surface. This low level of infection and high MPM70 staining are also seen in the cell directly below cell B. Cell C shows a higher level of infection, where some MPM70 expression is still present but it is not as high in relation to the mycobacterial number, which is around 20-30. Cell D shows a very highly infected cell in which no MPM70 expression is seen, and the mycobacterial count is 50+. The heterogeneity in this infection model is discussed in Section 2.4, and may be so heterogeneous because of dead mycobacteria present in the media, phagocytosed and unable to grow and infect, as well as free live mycobacteria in the media, which may be uptaken by host cells at any point during the 72 h infection course.

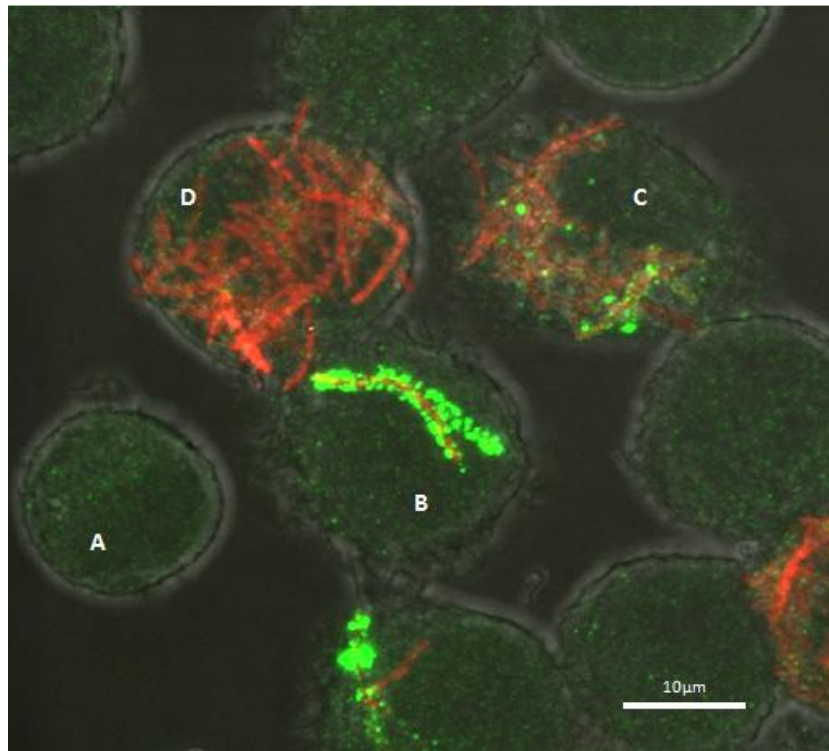


Figure 3.3: Heterogeneity in the *Mycobacterium marinum* J774A.1 mouse macrophage infection model, with regard to MPM70 expression. Cells A-D are neighbouring but at different levels of *M. marinum* infection and MPM70 expression. *M. marinum* cells are red, as the cells constitutively express DsRed. MPM70 is labelled with AlexaFluor 488 (green). Scale bar: 10 µm.

3.3.2 MPM70 expression is localised closely to the outer surface of *Mycobacterium marinum*

The localisation of MPM70 was found to be closely associated with the mycobacterial surface. This is shown in Figure 3.4 below, where the DsRed expressing *Mycobacterium marinum* (red) are surrounded by a non-uniform coating of MPM70, visualised with AlexaFluor 488 (green). The MPM70 is not expressed by all

mycobacteria in the infected cell, which appears to be another facet of the heterogeneous mycobacterial infection model.

The row A images in Figure 3.4 shows a macrophage after 3 h infection. It is infected with two single *M. marinum* cells, one of which is heavily expressing MPM70 (right) and the other is not expressing MPM70 (left). The second line of images shows two mycobacterial cells (end-to-end) that are expressing high levels of MPM70 24 h post-infection. The irregular patterning of the MPM70 expression gives it a ‘beaded’ or ‘studded’ appearance along the outside of the mycobacterial surface. The third line of images shows a very densely infected cell at 72 h post-infection, with 30+ mycobacteria and minimal MPM70 expression is detected.

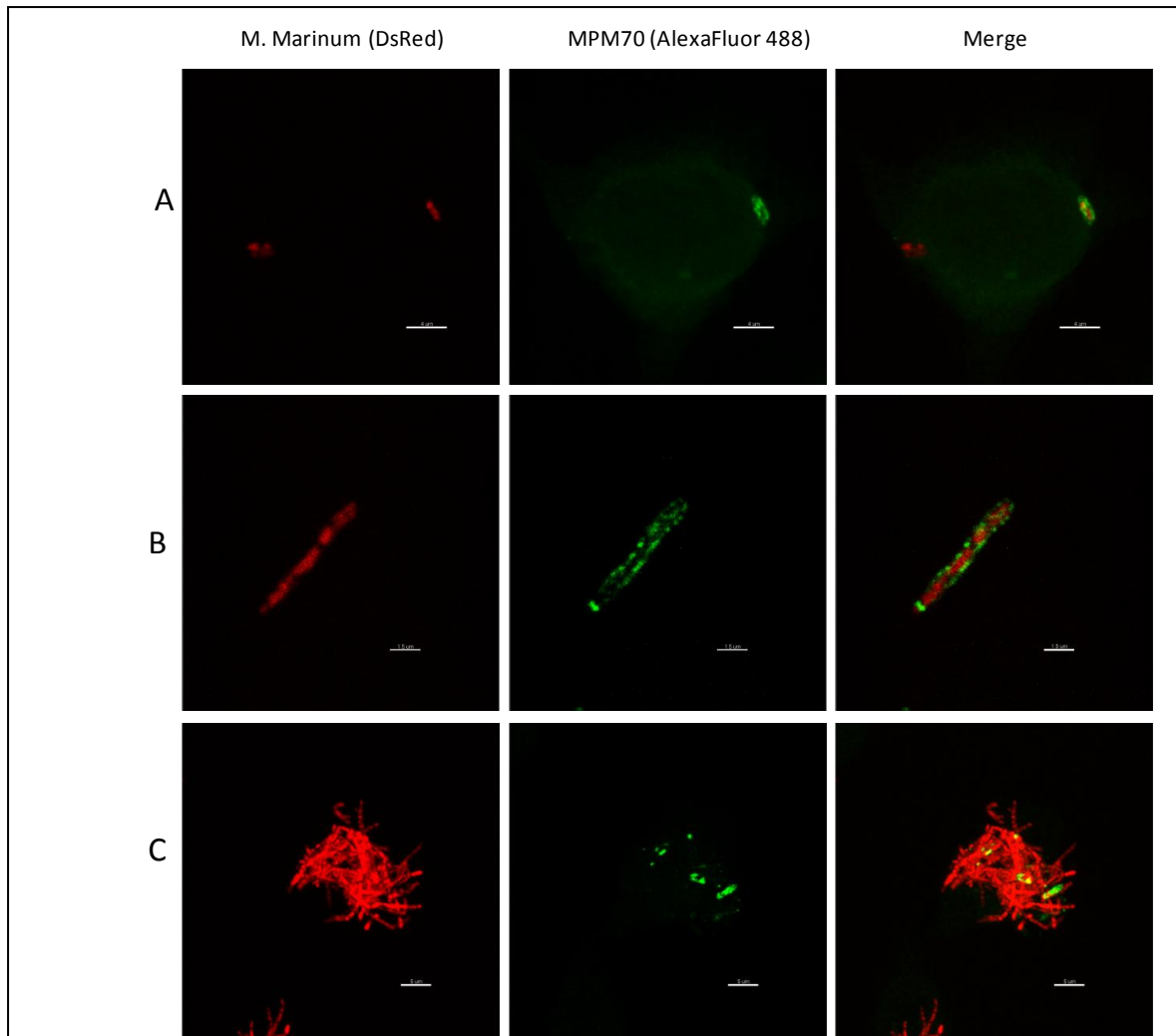
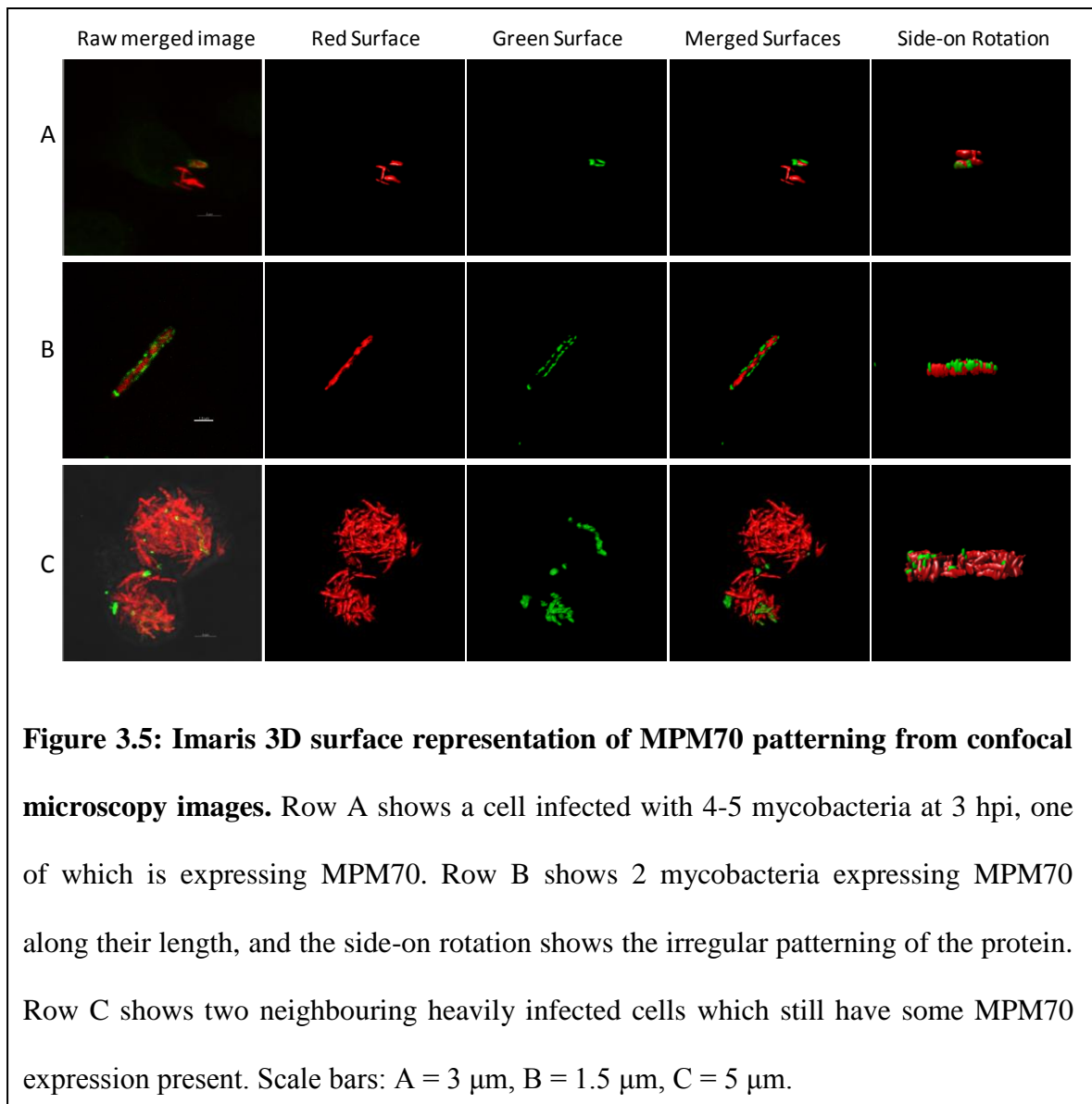


Figure 3.4: MPM70 expression at different mycobacterial densities. Row A shows two mycobacterial cells (red) infecting a single J774A.1 macrophage. Only the *M. marinum* cell on the right is expressing MPM70. Row B shows 2 mycobacterial cells growing end-to-end, with the MPM70 expressed in a non-uniform beaded formation along the mycobacterial length. Row C shows a dense bundle of mycobacteria consisting of 30+ cells; a few of which are still expressing MPM70. Scale bars: top row = 4 μm , middle = 1.5 μm , bottom = 5 μm



Using z-scan data from the confocal microscope, it was possible to reconstruct the raw image data and manipulate it with the Imaris software package (Bitplane). This allowed real-time rotation of the full z-scan in three dimensions, confirming that MPM70 was indeed localised around the surface of the mycobacterial cells. Furthermore, the software can build a three-dimensional surface representation, which allows clearer study of the patterning of MPM70 on the mycobacterial surface. This patterning is ‘beaded’ or ‘studded’ along the outside of the mycobacteria in a non-uniform fashion,

and examples at different time-points and mycobacterial densities can be seen in Figure 3.5.

A rare event observed was a trail of MPM70 sometimes left behind in the patterning of a nearby cell expressing the protein, as seen in Figure 3.6. Just below the mycobacterial wall-associated MPM70 is a trail with a strikingly similar pattern at almost 90°, almost as if a trail of the protein has been left behind. This suggests that the protein is not simply anchored to the mycobacterial surface, but to another host cell component too. These trails may be left behind by movement of the mycobacterial cell which can break the anchoring of the protein at the mycobacterial side.

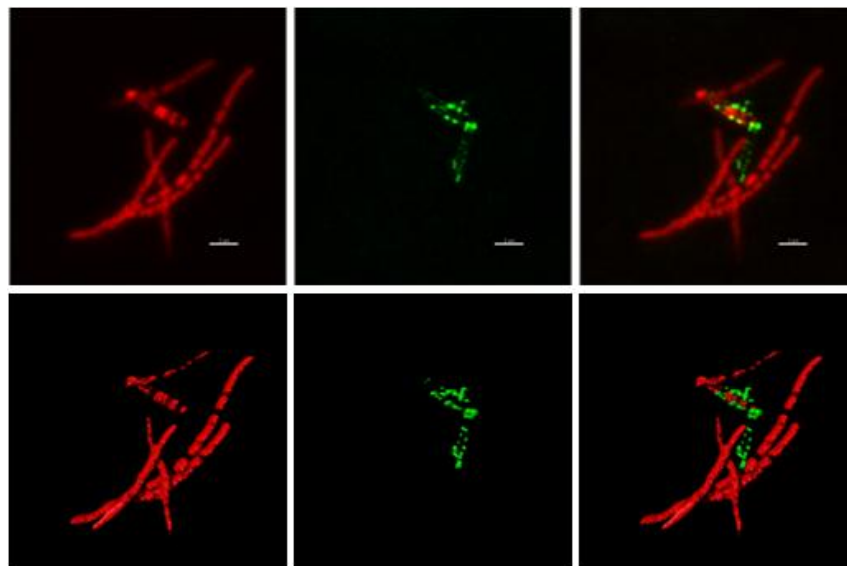


Figure 3.6: Trails of MPM70 left behind by expressing *M. marinum* cells. The top row shows the raw pixel data of *M. marinum* cells (red), one of which is expressing MPM70 (green). The lower row is the same image, with surface rendered 3D to show the patterning more clearly. Scale bar = 2 μm .

3.3.3 Characterisation of the *M. marinum*:J774A.1 macrophage infection model and MPM70 expression

Semi-quantification studies were performed on J774A.1 cells infected at a MOI of 10. Confocal microscope images were collected at 3, 24, 48 and 72 hpi, with each individual whole cell numbered. A representative image is shown in Figure 3.7. The infection process was characterised by grouping individual cells into one of 6 groups; Uninfected, Low (1-5 mycobacteria), Medium-Low (6-15 mycobacteria), Medium (16-25 mycobacteria), High (26-35 mycobacteria) and Very High (35+ mycobacteria). Mycobacterial co-localisation with the lipophilic membrane marker DiIC₁₈(5)-DS was used to determine whether mycobacteria were contained within the host cell phagosome. Cells were recorded as 'Phagosomal mycobacteria' only when all mycobacteria were co-localised to the lipophilic membrane dye. Representative examples of cells at these infection densities are shown in Figure 3.8. Infected cells were scored as being positive or negative for MPM70 expression. At 3 hpi, 90% of cells were infected at a Low level (1-5 mycobacteria per cell). At 48 and 72 hpi, cells were infected over the full range of mycobacterial densities, reflecting the heterogeneity of this infection model. At 3 hpi, 60% of cells contained phagosomal mycobacteria only. At 48 and 72 hpi, almost 98% of cells contained mycobacteria which were cytoplasmically localised.

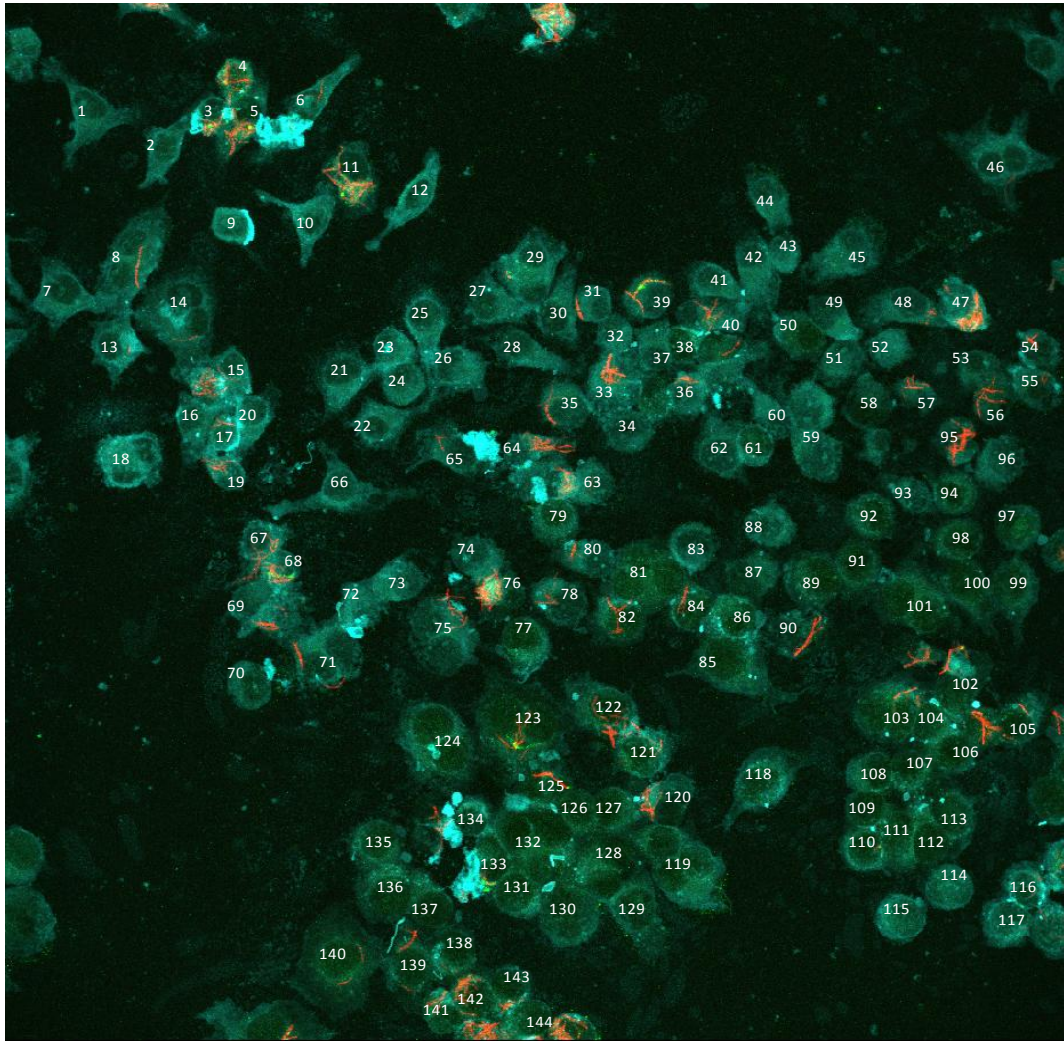


Figure 3.7: A representative image used for quantification of *M. marinum* infection and MPM70 expression. Whole cells contained within the image are numbered and infection levels are scored based upon mycobacterial numbers within a host cell. Low Infection = 0-5, Medium-Low Infection = 6-15, Medium Infection = 16-25, High Infection = 26-35, Very High Infection = 36+ mycobacteria per host cell. MPM70 expression is detected by anti-MPM70 antibody 4061 and Goat anti-rabbit IgG conjugated with AlexaFluor 488. MPM70 expression (if observed) was scored as positive or negative for each infected cell. Mycobacterial localisation is deemed as phagosomal or non-phagosomal based upon co-localisation with the host cell membrane marker DiIC₁₈(5)-DS (light blue).

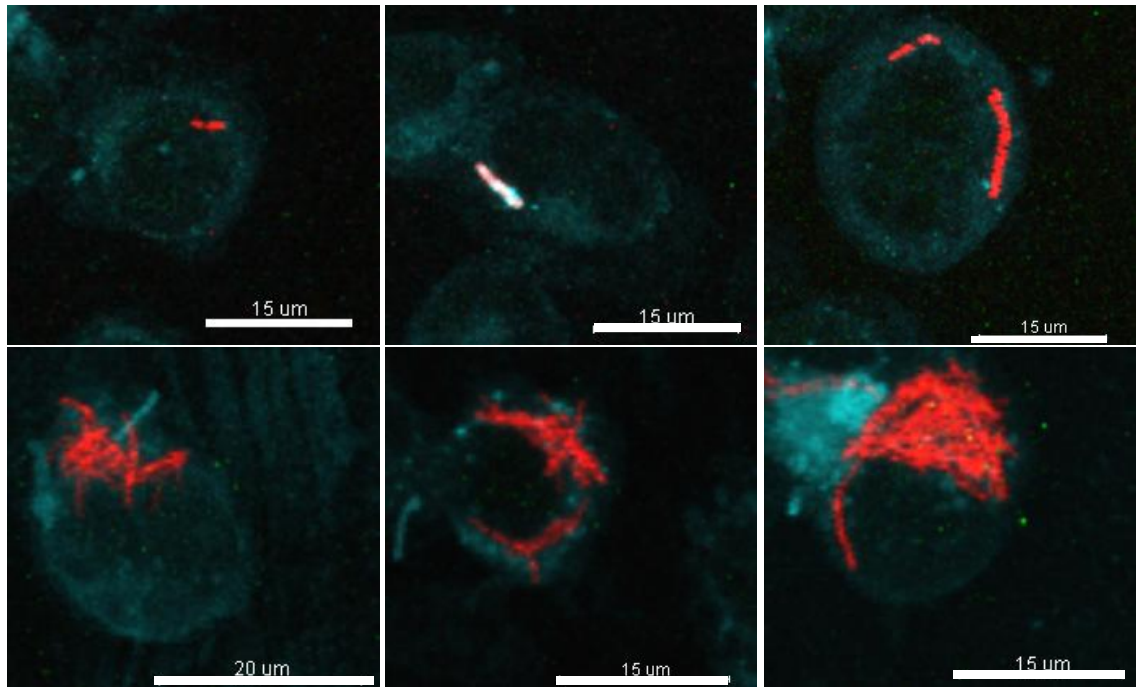


Figure 3.8: Typical examples of low-very high infection loads for fluorescence microscopy-based quantification of *M. marinum* infection and MPM70 expression.

The representative images show J774A.1 macrophage cells containing the full range of mycobacterial loads quantified in this experiment. Top row - low infection with cytoplasmic mycobacteria (left), low infection with phagosomal mycobacteria, where red mycobacteria co-localise with the light blue DiIC₁₈(5)-DS membrane staining (centre), medium-low infection (right). Middle row - Medium infection (left), high infection (centre), very high infection (right). Infected J774s were scored as positive or negative for MPM70 expression for semi-quantification (Figure 3.10).

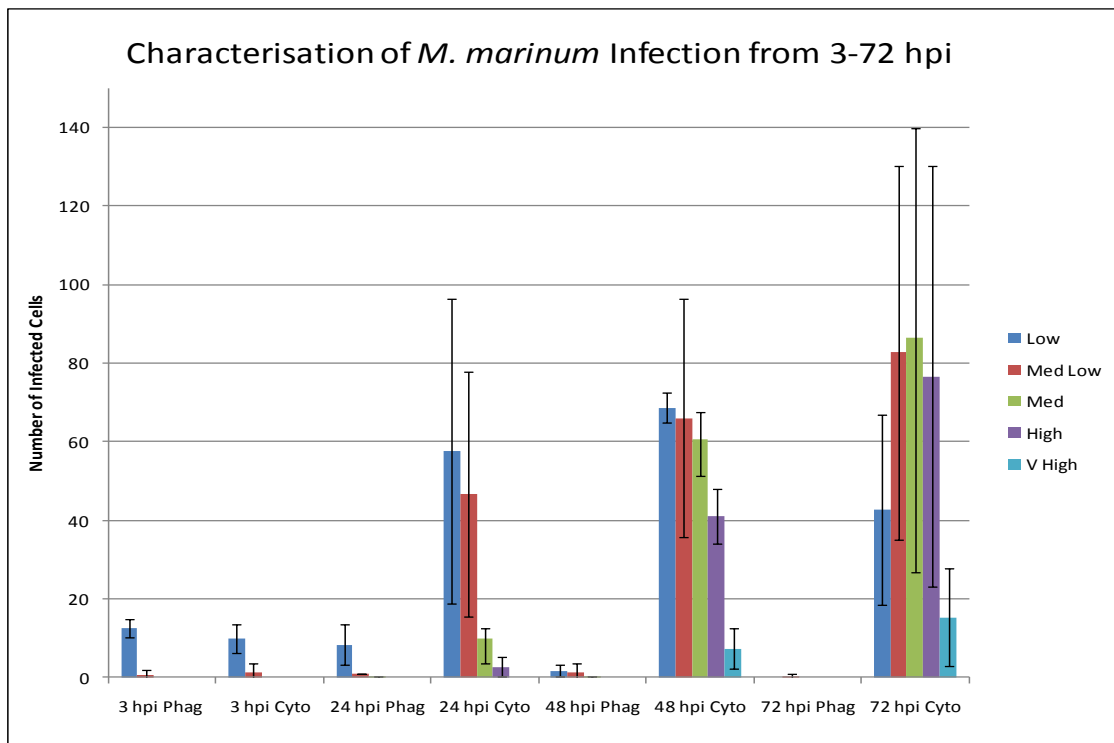


Figure 3.9: *Mycobacterium marinum* localisation during infection from 3-72 hpi.

The graph shows the number of J774 macrophages infected with different mycobacterial loads from confocal microscope images taken at 3, 24, 48 and 72 h infection. Mycobacterial localisation was recorded as phagosomal (all mycobacteria co-localised to DiIC₁₈(5)-DS) or cytoplasmic (at least one mycobacteria not localised to DiIC₁₈(5)-DS). The infection shifts from 90% Low infection (3 hpi) to a range of mycobacterial densities at 72 hpi, showing the heterogeneous nature of the mycobacterial infection. At 3 hpi, over 60% of cells were infected with phagosomal mycobacteria only. At 48 and 72 hpi, almost 98% of cells contained mycobacteria which had moved into the host cytoplasm. Blue – Low infection (1-5 mycobacteria), Red – Medium-Low infection (6-15 mycobacteria), Green – Medium infection (16-25 mycobacteria), Purple – High infection (26-35 mycobacteria), Teal – Very High infection (35+ mycobacteria). The error bars represent the standard deviation from 3 infection experiments.

The data in Figure 3.9 shows that at 3 hpi, around 60% of mycobacteria at Low infection levels are phagosomal. This may explain why MPM70 expression increases steeply when mycobacteria reach a Medium-Low infection level; as the mycobacteria leave the phagosome and express MPM70. Figure 3.10 shows that MPM70 expression is rarest in the Low group of infected cells, but rapidly increases in the Medium-Low group. MPM70 expression then plateaus between Medium, High and Very High infection levels with an average of 20% of the total infected cells having MPM70 expressed within them. MPM70 expression was on cytoplasmic mycobacteria in over 99% of cases, where 367 host cells were recorded as containing MPM70 expressing mycobacteria (data not shown). The results in Figure 3.10 indicate that MPM70 expression is lowest in the cells that have Low infection (1-5 intracellular mycobacteria) and increases quickly in Medium-Low infected cells (6-15 mycobacteria). The overall trend for MPM70 expression is an initial increase in expression at Medium-Low infection levels and a plateau in cells infected at all levels from Medium to Very High. This implies that MPM70 expression is not dependent upon mycobacterial density. This may mean that expression is transient, and may occur in all cells. Expression appears to be on a subset of mycobacteria within the intracellular population, and a cytoplasmic host cell factor contacting this subset of infecting mycobacteria may act as the trigger for MPM70 expression.

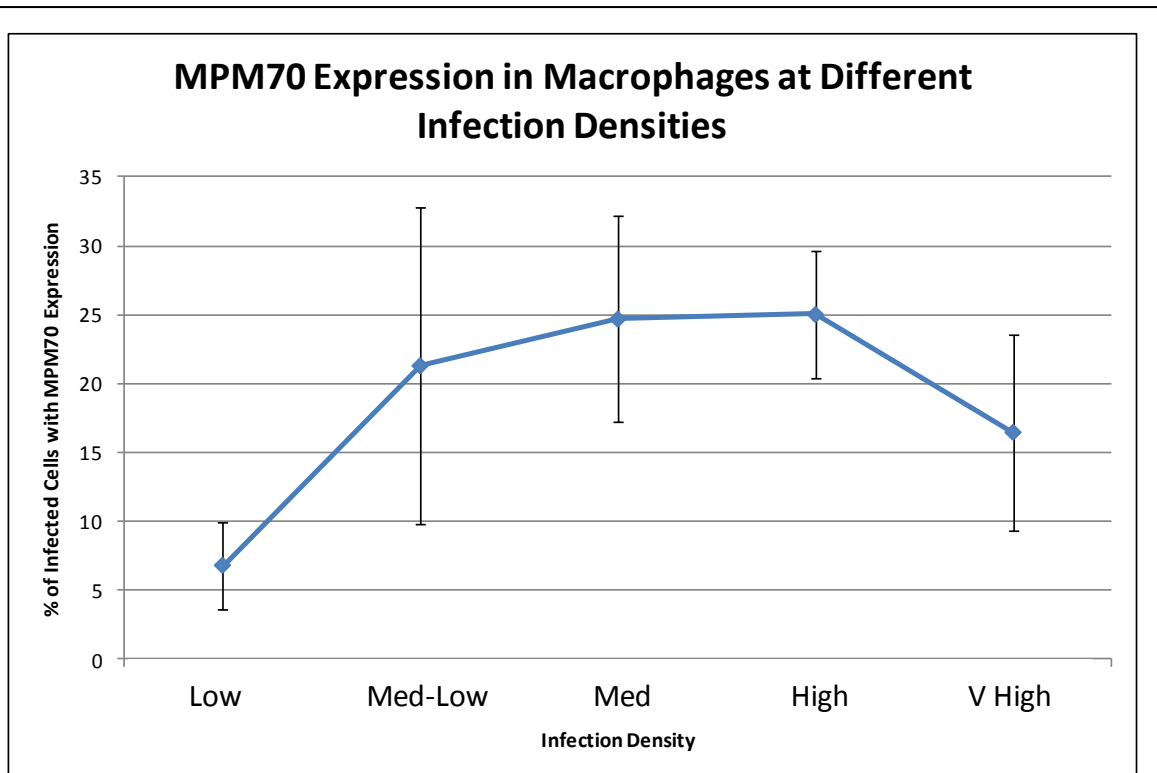
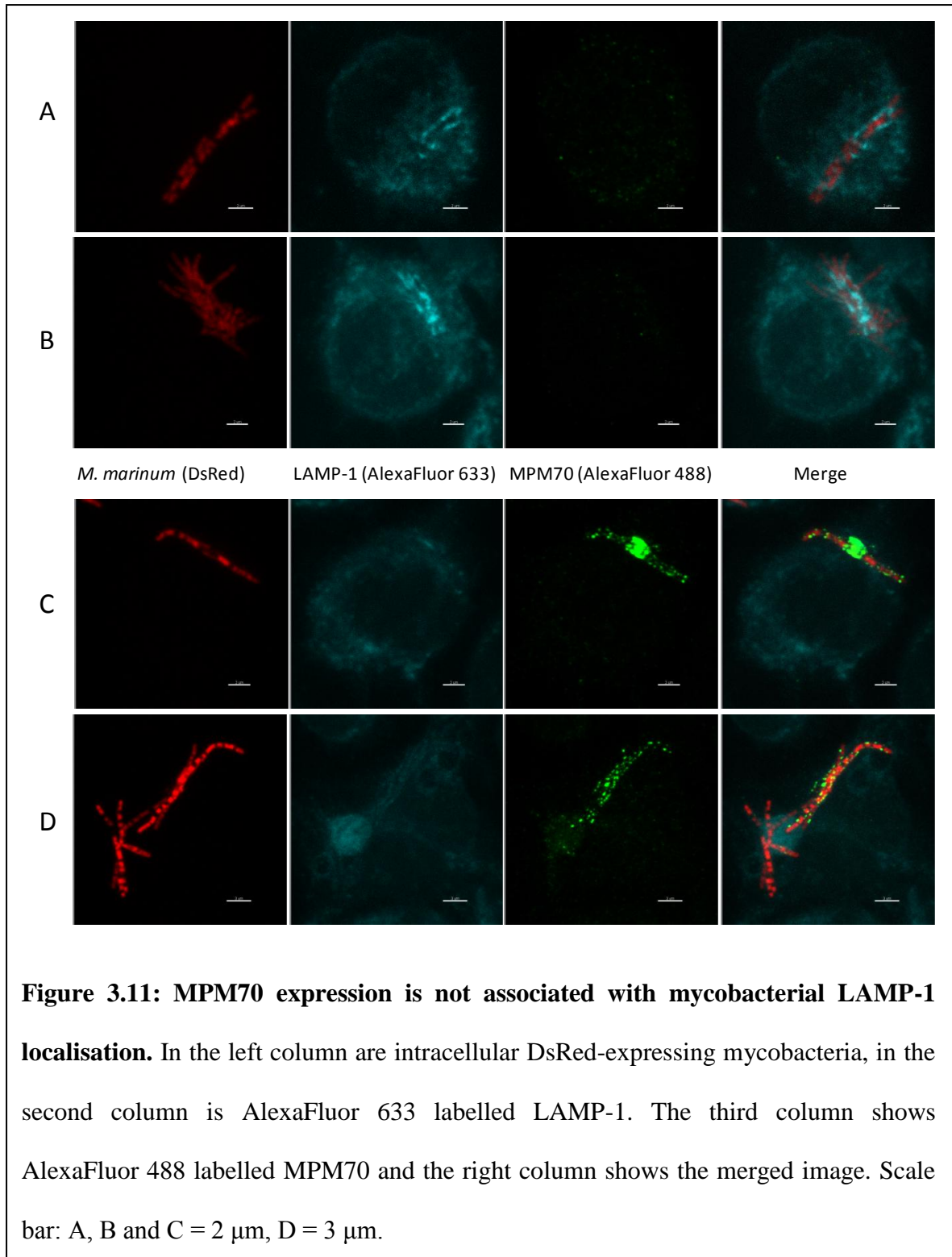
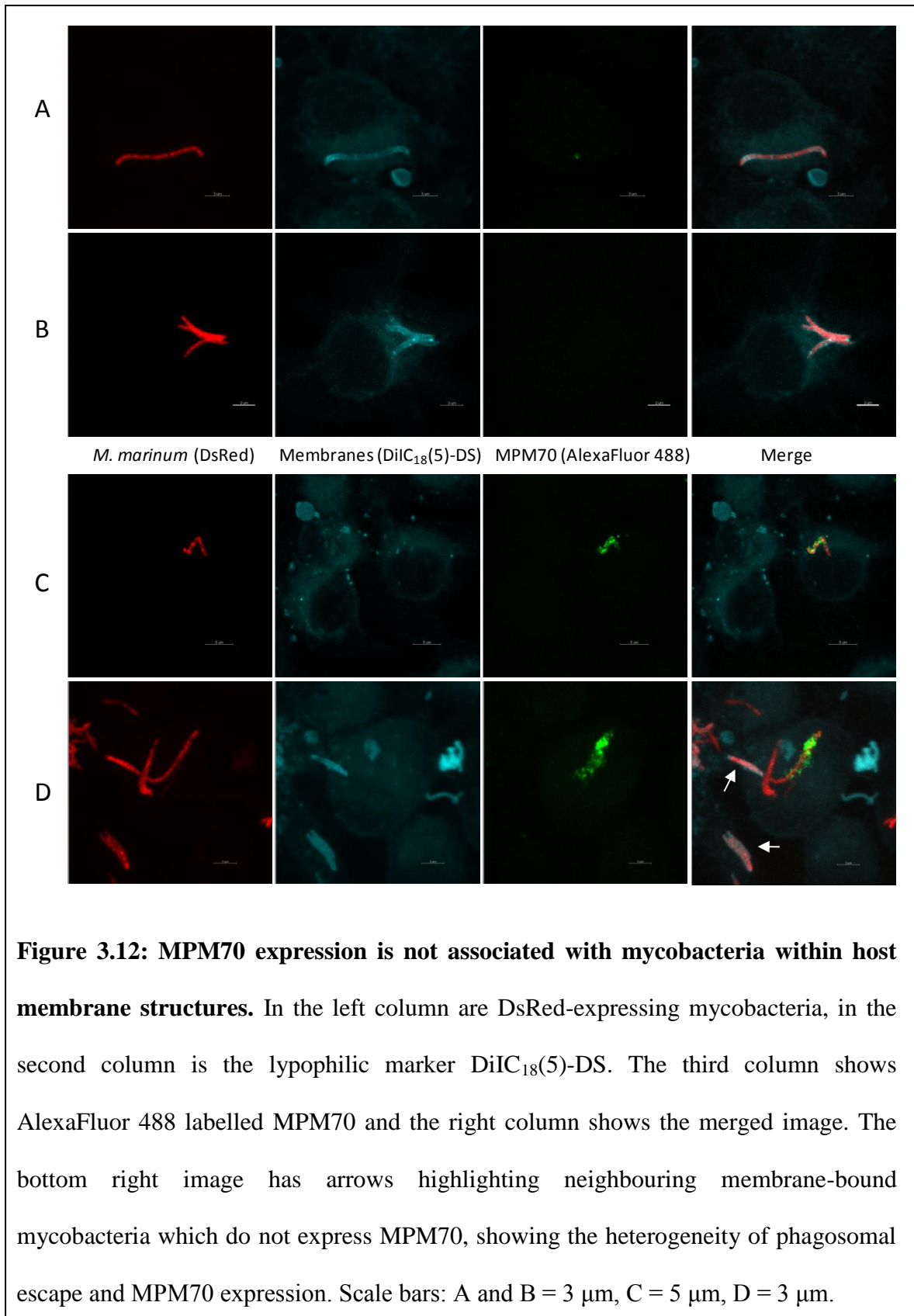


Figure 3.10: Characterisation of MPM70 expression levels in *Mycobacterium marinum* infected macrophages, over 72 h. The graph shows percentages of infected host cells containing MPM70 expressing mycobacteria, as scored from confocal microscope images in J774 cells scored at different infection levels (Low-Very High). Percentages are calculated from the total number of cells infected at each mycobacterial density. MPM70 expression increases greatly between cells infected in the Low and Medium-Low infection range. Globally, MPM70 expression increases (at Low, Medium and High expression levels) dramatically once cells reach a Medium-Low infection level, and is then seen at all infection levels in around 20% of cells, indicating that MPM70 expression is not mycobacterial density dependent. The error bars represent the standard deviation from 3 infection experiments.

3.3.4 MPM70 expression is not associated with phagolysosomal *Mycobacterium marinum*

In order to assess whether the expression of MPM70 was by phagolysosomal *M. marinum* or those that had escaped into the host cell cytoplasm, two experiments were performed. Firstly, the lysosomal marker LAMP-1 was used to show that when high levels of MPM70 were being expressed by the mycobacteria, they were not within a LAMP-1-associated membrane (Figure 3.11). Rows A and B show LAMP-1 associated *M. marinum* which clearly do not express MPM70. Rows C and D show examples of high MPM70 expression by mycobacteria which are not LAMP-1 associated. This implied that the bacteria had escaped the phagolysosome before expressing the protein. This was confirmed in the second experiment, where the lipophilic membrane marker DiIC₁₈(5)-DS (Invitrogen Molecular Probes) was applied. This showed that mycobacteria that were fully contained within the phagosome did not produce high levels of MPM70, and only those not co-localised with the lipophilic membrane marker had high levels of MPM70 expression (Figure 3.12). The top two rows show membrane-bound *M. marinum* which do not express MPM70. The bottom two rows show examples of high MPM70 expression by mycobacteria which are not contained within a host cell membrane structure.





3.3.5 MPM70 expression is not associated with actin polymerisation

Section 3.3.1 and 3.3.2 showed that MPM70 expression is localised to the mycobacterial surface and only highly expressed by mycobacteria that were in the host cell cytoplasm. In order to assess whether MPM70 was associated with actin polymerisation and tail formation, phalloidin conjugated with the dye AlexaFluor 633 (Invitrogen Molecular Probes) was used to stain F-actin. It was observed that actin polymerisation was only seen at very high mycobacterial densities and there was no co-localisation with MPM70 expression (Figure 3.13). It must be noted that long actin ‘tails’ were not seen in this infection model, but actin polymerisation can clearly be seen in tubular structures surrounding a subset of the mycobacteria at high growth densities.

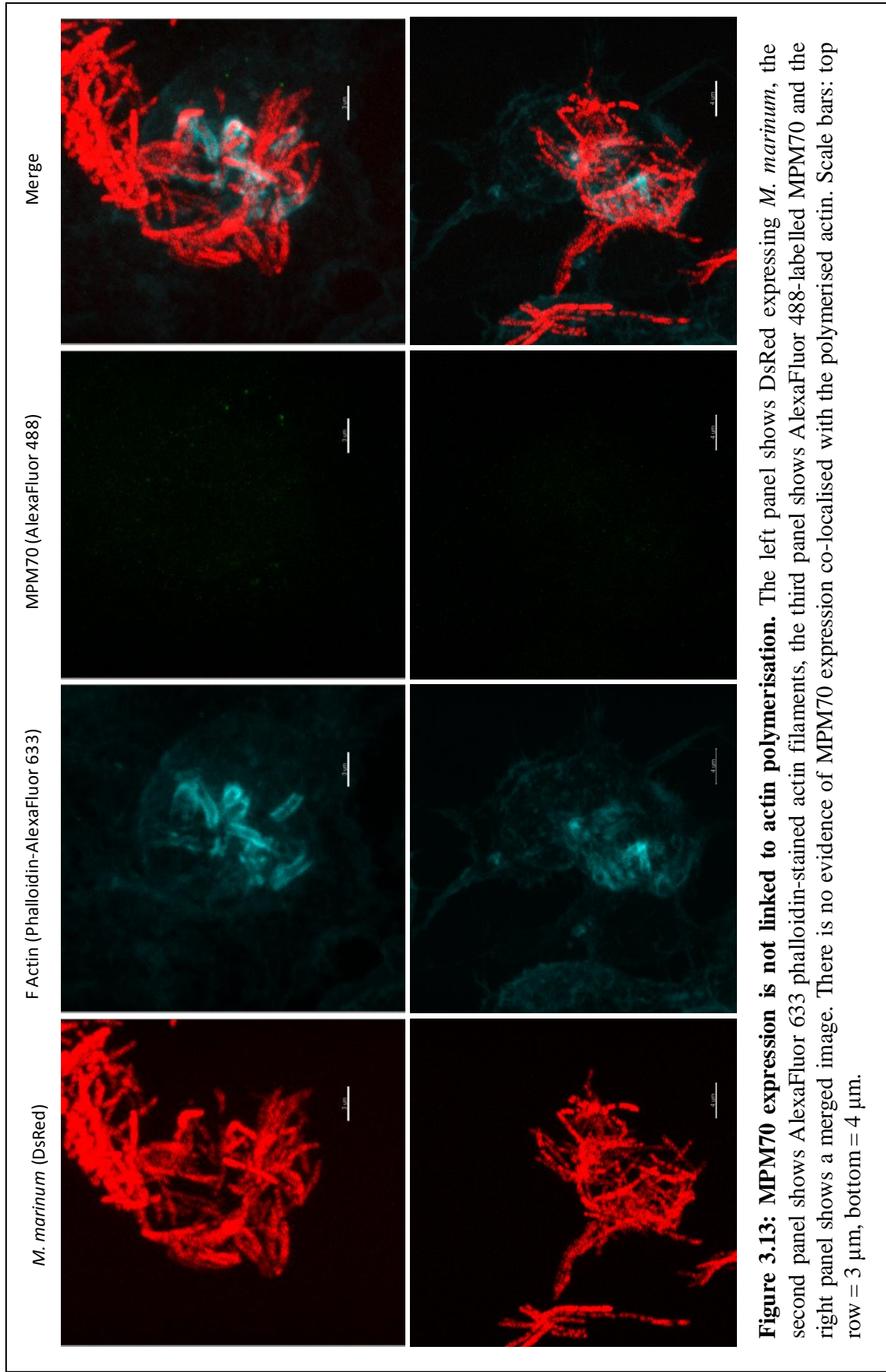
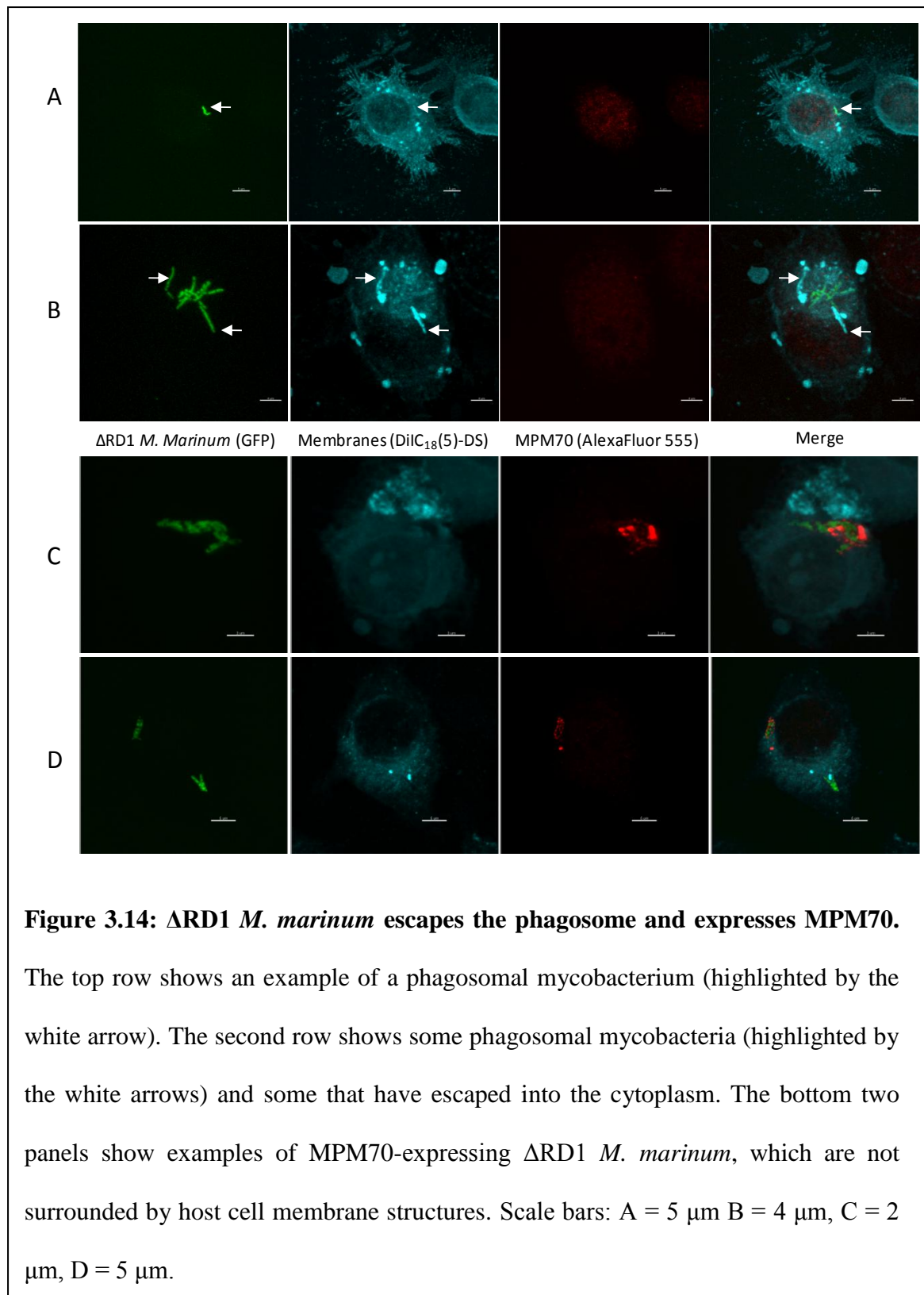


Figure 3.13: MPM70 expression is not linked to actin polymerisation. The left panel shows DsRed expressing *M. marinum*, the second panel shows AlexaFluor 633 phalloidin-stained actin filaments, the third panel shows AlexaFluor 488-labelled MPM70 and the right panel shows a merged image. There is no evidence of MPM70 expression co-localised with the polymerised actin. Scale bars: top row = 3 μm, bottom = 4 μm.

3.3.6 Phagosomal escape and MPM70 expression are RD1 independent in *Mycobacterium marinum*

In *Mycobacterium tuberculosis*, RD1 mutant strains (carrying truncated *cfp10* or *espA* genes) were shown to be unable to escape the host cell phagosome, even at 7 days post-infection. In order to assess whether an RD1 deletion would interfere with phagosomal escape and MPM70 production in *Mycobacterium marinum*, a Δ RD1 strain of *M. marinum* was acquired (courtesy of Thierry Soldati, University of Geneva) and tested with the DiIC₁₈(5)-DS lipophilic membrane marker, as well as the rabbit anti-MPM70 polyclonal antibody 4061. The results clearly show that not only do Δ RD1 *M. marinum* escape the phagosome (see Figure 3.14, second row of images) but they do indeed produce MPM70 to high levels when they are not bound within the phagosome, as with the wild-type strain (Figure 3.14, both lower rows of images). However, this MPM70 expression seems to be less, although this may be a facet of the Δ RD1 strain's attenuated growth and otherwise impaired virulence.



3.3.7 Immunoprecipitation confirms that MPM70 is strongly associated with the mycobacterial surface

With the 4061 polyclonal antibody working well for visualisation of MPM70 via confocal microscopy, its function was also assessed in immunoprecipitation experiments. This was done using a method modified from AbCam. However, using gentle lysis procedures to obtain the soluble fraction of infected cells meant that the *M. marinum* infecting the host cells was not lysed (they must be boiled at 95 °C for at least 5 mins). This may have meant the MPM70 bound to the mycobacterial surface was not present in the final soluble fraction, as the non-soluble pellet would contain intact mycobacteria with the protein still localised to the mycobacterial cell wall. However, it is most likely that immunoprecipitation lacks the sensitivity to pick up the low levels of MPM70 seen in these infection experiments, and therefore this result may not be completely reliable.

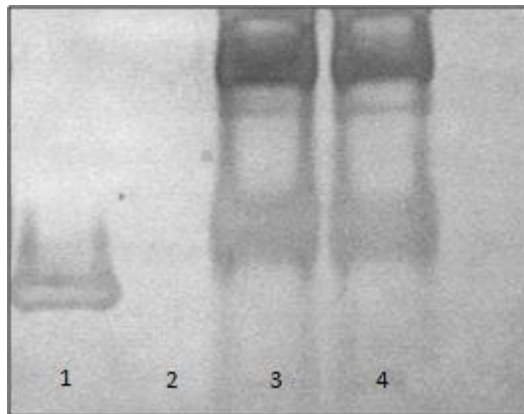


Figure 3.15: Western blot immunoprecipitation results for MPM70 during infection. Lane 1 shows purified MPM70, lane 2 is blank. Lane 3 contains protein A control beads with IgGs from the pre-bleed sera of rabbit 4061. Lane 4 shows polyclonal antibody 4061-bound test beads which have failed to immunoprecipitate MPM70 from the cell lysate of infected cells.

3.3.8 Assessment of pull-down experiments to identify MPB70 and MPM70 binding targets

With immunoprecipitation unable to identify MPM70s binding target, pull-downs against immobilised purified proteins MPM70 and MPB70 were attempted in two different ways. Firstly, the proteins were attached onto NHS-activated sepharose beads via their N-terminal lysine residues. This allowed U937 human monocyte whole cell lysate (WCL) to be washed over the beads, and any binding targets of either MPM70 or MPB70 should remain bound. The SDS-PAGE results did not reveal any significant binding targets, as identical bands were observed in pull-downs on blocked control beads and MPB70/MPM70-bound beads (Figure 3.16). Lane 6 (MPB70-immobilised NHS sepharose beads) in Figure 3.16 (below) shows a darker band present at around 14 kDa when compared to non-MPB70 bound control beads (lane 4), which would appear to be a positive result for a pull-down experiment. Mass spectroscopy analysis revealed this protein to be Macrophage Migratory Inhibitory Factor (MIF), a cytokine. However, subsequent experimentation by a range of methods, including analytical gel filtration and pull-down experiments using purified MIF and MPB70 proteins, showed these proteins do not interact (data not shown).

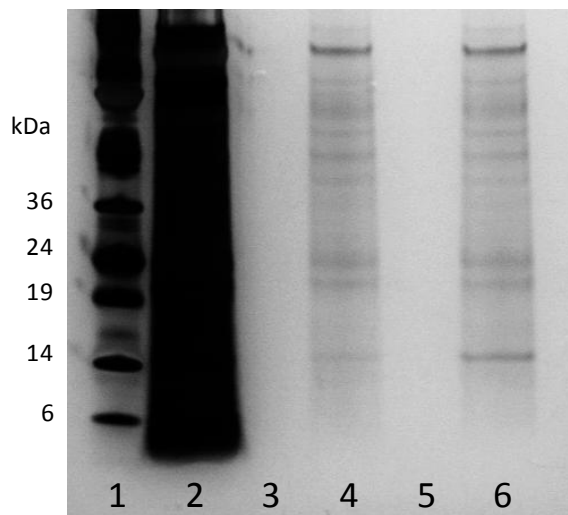


Figure 3.16: NHS-activated sepharose pull-downs do not identify an MPB70 binding target. Lane 1 shows Wide Range Molecular Weight Markers (Sigma), lane 2 contains U937 whole cell lysate used in the pull-down experiment. Lanes 3 and 5 are blank. Lane 4 shows control NHS-activated sepharose beads blocked with 0.1 M Tris, pH 8.5. Lane 6 shows beads coupled to 1 mg/ml MPB70 via the proteins N-terminus. Although lane 6 shows a darker band, and therefore a potential interaction, at around 14 kDa (identified as Macrophage Migratory Inhibitory Factor, MIF, by mass spectroscopy) than in control beads, MIF was cloned and purified, and any interaction with MPB70 was subsequently disproven using analytical gel filtration and pull-down experiments with purified MIF and MPB70 proteins (data not shown).

The second pull-down method employed the purified proteins with the C-terminal His tag intact. This allowed immobilisation of the proteins into Ni-NTA resin where the proteins could once again be exposed to U937 monocyte lysate. The resulting SDS-PAGE analysis did not yield any potential binding targets for either protein, when compared to unbound control beads (Figure 3.17).

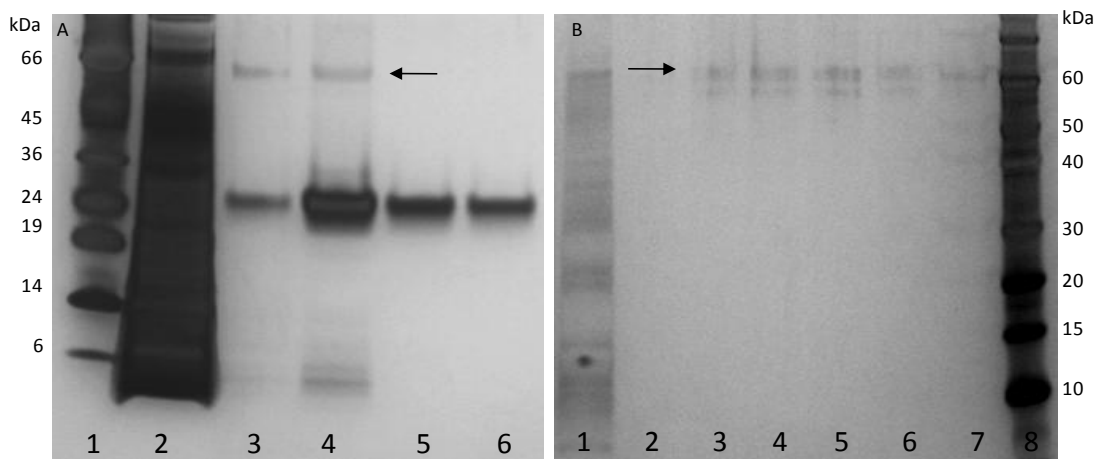


Figure 3.17: Ni-NTA matrix pull-downs do not identify an MPB70 binding target. Image A shows an example of a cHis MPB70-bound Ni-NTA pull-down experiment. Lane 1 shows Wide Range Molecular Weight Markers (Sigma), lane 2 contains U937 whole cell lysate used in the pull-down experiment. Lanes 3, 4 5 and 6 show the eluate at 30, 50, 100 and 150 mM imidazole, respectively. One high molecular weight protein (~60 kDa) and one low molecular weight protein (~4 kDa) elute with the His-tagged MPB70 protein. The 60 kDa protein is also observed in the control (non MPB70-bound) experiment seen in image B. At 100 and 150 mM imidazole concentrations, clean MPB70 is eluted from the Ni-NTA resin. Image B (Kirsty Lightbody, personal communication) shows a control experiment using Ni-NTA resin alone. Lanes 1 and 2 show the eluate from control beads at 30 and 100 mM imidazole, respectively. Lanes 3-6 show four elutions at 200 mM imidazole, and lane 7 shows the eluate at 500 mM imidazole. Lane 8 contains Novex[®] Sharp Prestained Protein Markers (Invitrogen). The arrow in both images highlights a non-specifically binding protein around 60 kDa in size. Results were similar for MPM70.

The pull-down results shown here were reproducible for both MPB70 and MPM70, and show that pull-downs are not an effective strategy to study the interaction partners of these proteins during infection. Both NHS-activated sepharose and Ni-NTA resin pull-downs were also performed with J774A.1 cells infected at an MOI of 10 for 48 h, but results did not show any potential host protein interactions (data not shown).

3.4 Discussion

This chapter describes the application of the anti-MPM70 polyclonal rabbit antibody 4061 for tracking MPM70 expression in the *M. marinum*:J774A.1 macrophage infection model. Global expression trends for MPM70 were observed using Western blots and specific protein localisation was visualised in individual cells using confocal microscopy.

Fluorescence microscopy studies showed that MPM70 formed buttress-like structures along the length of the mycobacterial cell, which rather than having a uniform pattern, can vary, even in neighbouring cells. This variability may be another facet of the general heterogeneity within the mycobacterial infection, as seen and discussed in Chapter 2. It appears that not all host cells are infected at the same level at the same time, and that some host cells may remain uninfected whilst adjacent cells become may be infected with a wide range of intracellular mycobacterial densities. Semi-quantification analyses of confocal microscope images indicate that throughout a 72 h infection, 59% of cells are infected at Low and Medium-Low levels (1-15 mycobacteria per host cell), and only 16.67% are infected in the Very High range (35+ mycobacteria per host cell). MPM70 expression in these cells is lowest in the Low group of infected cells, but rapidly increases in the Medium-Low (6-15 mycobacteria per host cell) group. MPM70 expression plateaus between Medium, High and Very High infection levels, with 7% of infected cells having MPM70 expressed within them. MPM70 expression was on cytoplasmically-localised mycobacteria in over 99% of infected host cells. This may explain why MPM70 expression increases steeply when mycobacteria reach a Medium-Low infection level; as this may be the point at which mycobacteria escape the phagosome, and phagosomal escape seems to be a prerequisite for MPM70 expression.

MPM70, once expressed, has been shown to localise to the mycobacterial surface. Variability in the 'beaded' MPM70 patterning on the mycobacterial wall may be linked to either the patterning of an as-yet unknown mycobacterial anchor protein, or the cytoplasmic host protein which MPM70 may be binding to. It appears that MPM70's role may be to act as an intermediate between the mycobacterial surface (via an as-yet unknown mycobacterial anchor protein) and host cell cytoplasmic proteins. This may be analogous to the bridging function of fasciclin and β ig-H3, which bind eukaryotic cell surface proteins (NCAMs and integrins, respectively) and components of the extracellular matrix such as collagen and fibronectin (Kim *et al.*, 2002; Kim *et al.*, 2008). MPM70 binding to ECM components seems unlikely because the expression of its *M. tuberculosis* homologue, MPT70, is greatly upregulated when mycobacteria are inside infected macrophages (Schnappinger *et al.*, 2003; Charlet *et al.*, 2005). Also; observations in this study show MPM70 expression occurs only in mycobacteria that are in the host cell cytoplasm. Consideration of the positions of conserved residues from MPB70, MPB83, fasciclin and the mutated residues in β ig-H3 within patients with corneal dystrophy suggests two distinct functional sites on the surface of MPT70 (Carr *et al.*, 2003). This suggests that MPM70 may act as an intermediate between two binding partners; one being a protein found within the mycobacterial wall, the other being a host cell protein or protein complex.

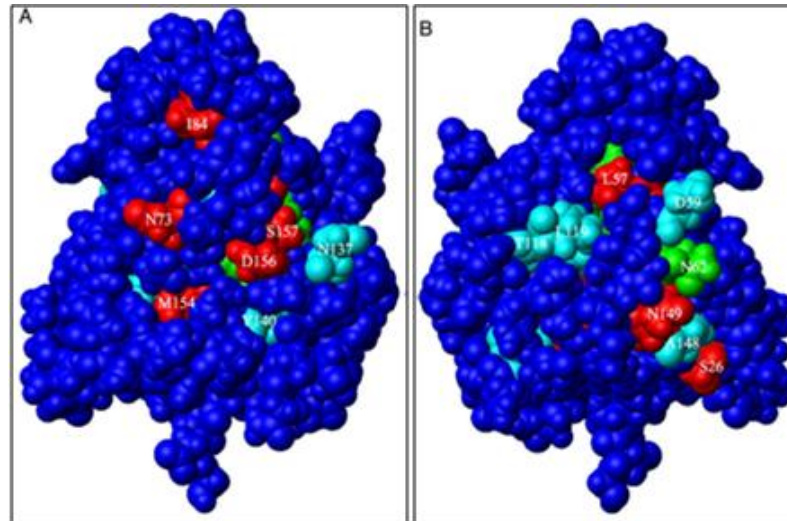


Figure 3.18: Structure of MPB70 and comparison to related proteins MPB83, fasciclin and β ig-H3. Images A and B show two opposite faces of a filled-space model of MPB70. The green residues are those that are identical in MPB70, MPB83, fasciclin and β ig-H3, and the cyan residues are conserved to type. The red residues are those that are mutated in β ig-H3 in patients that have corneal dystrophy. The localisation of these strongly conserved residues and those associated with the correct function of β ig-H3 reveals two potential protein binding sites on opposite faces of MPB70. This suggests that MPB70 may be an intermediate between two binding partners; one being a component of the mycobacterial cell surface and the other a cytoplasmic host cell protein. This may be analogous to the way that fasciclin and β ig-H3 act as intermediates between eukaryotic cell surface proteins (integrins and NCAMs, respectively) and the extracellular matrix (with permission, Carr *et al.*, 2003) .

The mutated residues are concentrated in two patches on opposite sides of the protein, suggesting that MPM70/MPB70 may act as an intermediate between two interacting proteins. The MPM70 ‘footprints’ observed in this Chapter may support this theory, as

the patterning of the protein looks strikingly similar to that of MPM70 on nearby mycobacterial cells. This implies that, either due to host cell or bacterial cell movement, MPM70 has dissociated from the mycobacterial surface and has been left attached to the host cell target. This may also further indicate that MPM70 binds more tightly to its host cell target than the mycobacterial anchor protein. In *M. bovis* and *M. tuberculosis*, MPT83 has an N-terminal glycolipid that covalently binds the protein to the mycobacterial surface. There is no MPT83 homologue in *M. marinum* (Stinear *et al.*, 2008), and the high homology between MPT70 and MPT83 suggests that MPT83 arose because of a gene duplication event. The findings here indicate that instead of MPT70 and MPT83 having distinct roles due to their differing localisations as previously thought, they may actually share the same function as a mediator between the mycobacterial surface and a host cytoplasmic protein. MPT83 is less likely to detach from the mycobacterial surface because it has an N-terminal glycolipid anchor, meaning that the mycobacteria may remain bound to the host cell target (Harboe *et al.*, 1998).

The results in this Chapter show that MPM70 expression occurs in mycobacteria that have escaped the phagosome, and is RD1 independent. However, in *M. tuberculosis*, it has been shown that a Δ RD1 mutant is unable to escape from the phagosome at 7 days post-infection, and this is also shown in *M. bovis* BCG. (van der Wel *et al.*, 2007). Phagosome escape still occurs in Δ RD1 *M. marinum* (Hagedorn *et al.*, 2009), and this is supported by the findings in this chapter. It may be that *M. marinum* has more than one mechanism for phagosomal escape which *M. tuberculosis* has subsequently lost due to genome downsizing and host specification.

Although MPM70 expression is shown to occur only in mycobacteria that are in the host cytoplasm, results using AlexaFluor Phalloidin staining shows that it is not

associated with actin polymerisation or tail formation. Modulation of host cell actin has been shown to be important in the motility of mycobacterial cells, where it forms long polymerised tails using host factors such as ARP2/3 and WASP (Stamm *et al.*, 2003, Stamm *et al.*, 2005). Host actin can also allow mycobacteria to move between neighbouring cells via ejectosomes at the host plasma membrane (Collins *et al.*, 2009; Hagedorn *et al.*, 2009). In this study neither long tails nor ejectosomes were observed, but actin polymerisation formed tube-like structures around mycobacterial cells. This may be a characteristic of the J774A.1 macrophage infection model, as the actin polymerisation observed can vary between infected host cells. For example, ejectosome structures are formed in *Dictyostelium* but actin tails cannot be seen (Soldati 2009, personal communication).

Attempts to use the 4061 antibody in immunoprecipitation experiments have not yet yielded any specific host targets for MPM70. In terms of immunoprecipitation, this is most likely due to the mycobacterial localisation of the MPM70 protein. Sample preparation for immunoprecipitation must not disrupt protein-protein interactions, and therefore the buffers used must not be over-stringent. The extraction of a soluble lysate would leave intact mycobacteria in the insoluble pellet, which may retain the majority of MPM70 immobilised to the mycobacterial wall. This is supported by the final silver-stained gel results which do not show a band where MPM70 should be. Using a crude lysate produced from sonication of the infected cells may be able to remedy this, as it would include both soluble and insoluble protein components from the cell lysis. It may also be the case that immunoprecipitation is simply not sensitive enough to pull out such small amounts of MPM70 as seen in the microscopy results in Chapter 3, along

with the fact that MPM70 expression is only observed in around 20 % of total infected macrophages (Section 3.3.3), regardless of its localisation.

Pull-downs were also used to alleviate the problem of MPM70s mycobacterial wall localisation, but once again did not yield any significant results. Potential interactions were studied against both the MPB70 C-terminal (by immobilising the N-terminal of the protein to NHS-activated sepharose) and the N-terminal (by immobilising the C-terminal His-tagged protein to Ni-NTA resin) but no significant binding of host cell target proteins were discovered when MPB70/MPM70 bound beads were compared to control beads which were not MPB70/MPM70 bound. This may be because MPM70 and MPB70 do not form tight enough complexes with their host cell targets, or complexes formed are transient in nature. Localisation and structural evidence suggest that MPB70/MPM70 may be bound to the mycobacterial wall via an as-yet unknown mycobacterial protein, and this may be required for complex formation with the host cell target. Therefore, pull-downs with purified MPB70/MPM70 are not sufficient to find the binding targets of these proteins.

Chapter 4

Conclusions and future work

4.1 Conclusions

4.1.1 Cloning of MPB70, MPM70 and the production of anti-MPM70 polyclonal antibodies

The results in this thesis show the optimisation of MPB70 and MPM70 purification, allowing for much greater protein yields. Previously, constitutive, non-inducible expression led to low protein yields and MPB70 leaching into the surrounding media through the SecA secretion machinery. Newly-constructed expression systems for MPB70 and MPM70 allowed IPTG induction of the proteins and final yields of around 8 mg protein per litre of *E. coli* culture. Furthermore, the addition of a cleavable His tag means that a simple two-step purification can be employed. Firstly, a Ni-NTA column yielded MPB70/MPM70 with very few contaminants due to the specificity of the His-tag for the column. A gel filtration step removed any high and low molecular weight contaminants to give proteins pure enough for polyclonal antibody production. Prior to immunisation, the His-tag was cleaved from MPM70 to ensure that antibodies were raised against the fully-folded protein and would not cross-react to His-tagged proteins. Rabbit polyclonal antibodies were raised in two rabbits, 4060 and 4061, over the course of 11 weeks. Test bleeds were assessed for their reactivity in a range of immunological tests. IgGs were purified from the final bleeds using a prepacked Protein A column. These polyclonal antibodies (4060 and 4061) were then tested for sensitivity and specificity via dot blot, Western blot and ELISA. Polyclonal antibody 4061 was deemed more sensitive and was selected for experiments tracking MPM70 expression in the *Mycobacterium marinum*:J774A.1 macrophage infection model.

4.1.2 Characterisation of the *Mycobacterium marinum*:J774A.1 macrophage infection model.

In order to track the expression of MPM70 by *M. marinum* during infection, an infection model in the murine macrophage line J774 was established and characterised. This allowed a four day time-course to be followed with low, medium and high intracellular mycobacterial counts observed. Multiplicity of Infection (MOI) was shown to greatly influence the course of infection, globally, and in microscopy studies of single infected cells. A low MOI (MOI = 1) results in a slow infection in which late-stage events cannot be observed over a 72 h infection course. A high MOI (MOI = 20) results in over-infection and high rates of host cell death at 48-72 h post-infection (hpi). It was found that an MOI of 10 gave a 72 h infection time-course that allowed for early and late-stage events to be observed within host cells, and this is consistent with existing published work using similar infection models (Stamm *et al.*, 2003; van der Wel *et al.*, 2007; Collins *et al.*, 2009). Further optimisation was needed in the form of a temperature balance between host cells and *M. marinum* cells, and 34.5°C was found to be optimal for infection. This is also consistent with previously published results using *M. marinum* as a model for *M. tuberculosis* infection (Ramakrishnan *et al.*, 1994). Once these infection conditions were optimised, the infection model could be used with the 4061 antibody in order to track MPM70 expression during infection in the J774 macrophage.

Semi-quantification of confocal microscope images allowed representative groups of individual cells to be assessed according to the number of intracellular *M. marinum* cells. Infection groups were defined as: Low (0-5 mycobacteria per cell), Medium-Low (6-15), Medium (16-25), High (26-35) and Very High (36+). Cells were determined to

contain phagosomal mycobacteria only if all of the intracellular mycobacteria co-localised with the membrane marker DiIC₁₈(5)-DS. At 3 hpi, 90% of cells were infected at a Low level (1-5 mycobacteria per cell). At 48 and 72 hpi, cells were infected over the full range of mycobacterial densities, reflecting the heterogeneity of the infection model. At 3 hpi, 62.5% of cells contained phagosomal mycobacteria only, and at 48 and 72 hpi, almost 98% of cells contained mycobacteria which had escaped into the host cell cytoplasm.

These observations show that at a MOI of 10 and a temperature of 34.5°C, a stable 72 h infection experiment can be performed. Early and late stages of infection can be studied, allowing the observation of phagosomal mycobacteria and those that have escaped into the host cytoplasm. It also allows the study of cells infected with a wide range of mycobacterial densities, from single mycobacteria to dense bundles of 40-50 cells. This means that MPM70 expression can be correlated with the intracellular localisation of mycobacteria as well as their density inside the host macrophage.

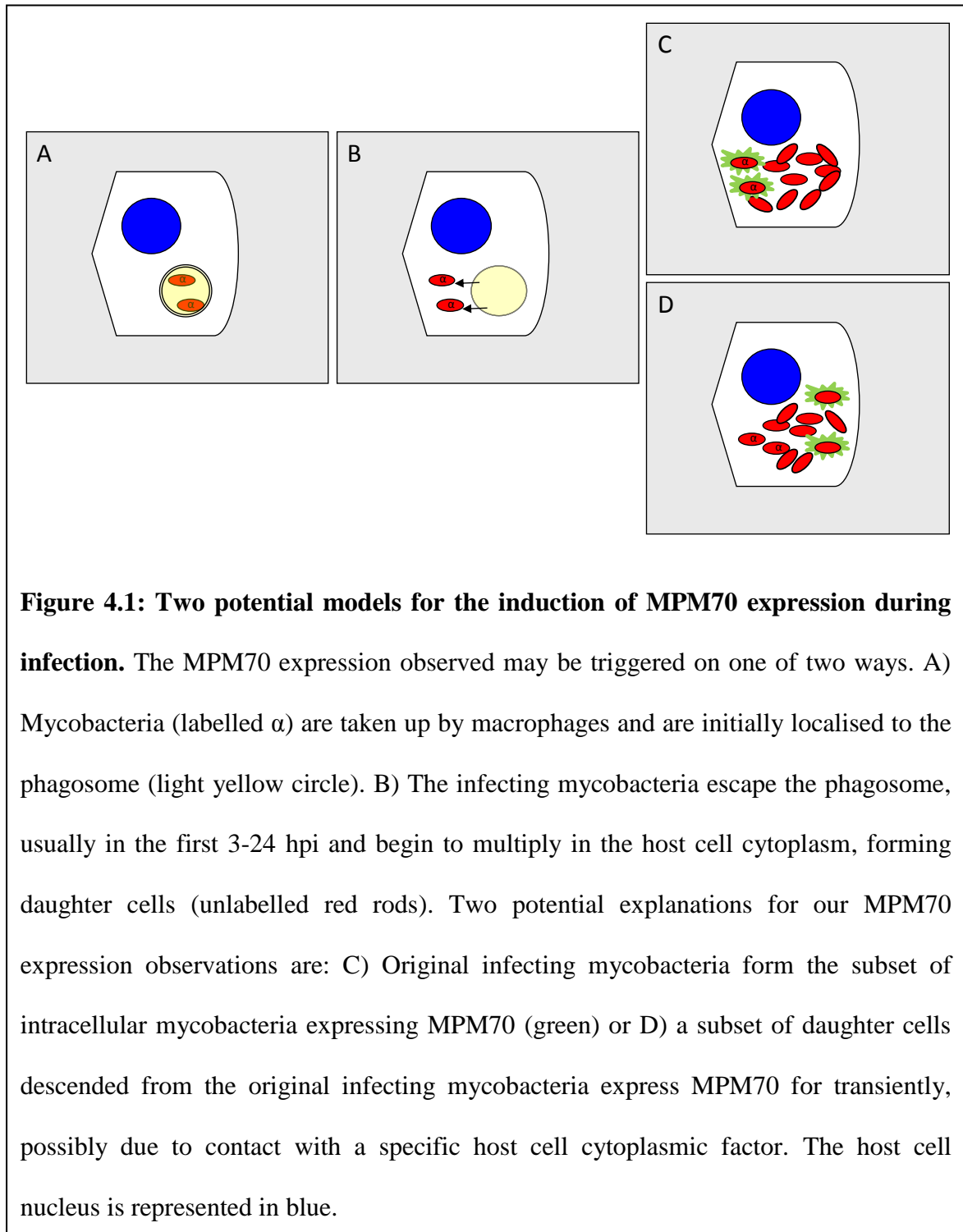
4.1.3 Characterisation of MPM70 expression and localisation during infection

Polyclonal antibody 4061 proved to be sensitive to MPM70 both in Western blots and for immunofluorescence studies, allowing the expression to be tracked both on a global scale, and in individual cells. At a MOI of 10, Western blots detected a low average MPM70 expression at 3 hpi, with the highest levels occurring at 24 and 48 hpi. Lower levels of expression were observed at 72 hpi.

Semi-quantification by confocal microscopy allowed individual infected cells to be grouped from Low to Very High infection according to the intracellular mycobacterial

load. MPM70 expression is lowest in the Low group of infected cells, but rapidly increases in the Medium-Low group (6-15 mycobacteria per host cell). MPM70 expression plateaus between Medium, High and Very High infection levels with an average of 20.5 % of cells having MPM70 expressed at any level (Low, Medium or High) within them. Fluorescence microscopy studies showed that MPM70 expression is linked to the localisation of individual mycobacteria within the host cell. MPM70 seems to be expressed only by *M. marinum* cells which have escaped the host phagosomal compartment. This was shown using the monoclonal anti-LAMP-1 antibody ID4B and the lipophilic membrane dye DiIC₁₈(5)-DS. The mycobacterial cells showing high levels of MPM70 expression were not associated with either of these host cell markers, leading to the conclusion that expression of the protein only occurs after phagosomal escape. MPM70 expression was on cytoplasmic mycobacteria in over 99% of cases, and the sharp increase in MPM70 expression in cells with Medium-Low infection levels may reflect the mycobacteria escaping the phagosomal environment.

Figure 4.1 outlines two potential models to explain the MPM70 expression observations during the semi-quantification experiment in Section 3.3.2. It has been shown that *Mycobacterium marinum* must escape the host cell phagosome in order for MPM70 to be expressed. Only a subset of mycobacteria within the infecting population express MPM70, and this could either be limited to the original mycobacteria infecting the host cell, which escape the phagosome and express MPM70 constitutively, or a subset of the daughter mycobacteria which express MPM70 for a short time, perhaps due to contact with a host cell cytoplasmic factor. The latter of these two is more likely, as MPM70 expression is observed at a wide range of mycobacterial densities and is most likely expressed in all infected cells at varying times during infection.



Surprisingly, MPM70 expression was found to be localised to the mycobacterial surface, but the rare observation of ‘MPM70 footprints’ in infected cells implies that MPM70 may also bind to a host cell cytoplasmic protein. The patterning of non-

mycobacterial associated MPM70 in the footprints was very similar to that on neighbouring mycobacterial cells, implying that the mycobacterium may have been anchored to a host cytoplasmic component using MPM70 as an intermediate. Movement of either the mycobacteria or motility of the host cell may have torn the mycobacterial cell from where it was bound (using MPM70 as an intermediate), leaving a similar pattern of MPM70 behind. This type of bridging role for MPB70 is supported by the structure of MPB70 and its homologues, fasciclin and β ig-H3 (Figure 3.18). Consideration of the positions of conserved residues from MPB70, MPB83, fasciclin and the mutated residues in β ig-H3 within patients with corneal dystrophy suggests two distinct functional sites on the surface of MPB70. This implies that it may act as an intermediate between two binding partners; one being a protein found within the mycobacterial wall, the other being a host cell protein or protein complex. This may be analogous to the bridging function of fasciclin and β ig-H3, which bind eukaryotic cell surface proteins (NCAMs and integrins, respectively) and components of the extracellular matrix such as collagen and fibronectin.

4.2 Future directions

In order to elucidate the precise role of MPM70 during infection, there are a number of directions in which this project could be developed. In order to identify the cytoplasmic host cell target of MPM70, a mammalian expression vector could be used. This could contain an antibody epitope (Flag, Myc or GFP) or affinity purification tags (TAP and hexa-histidine), to allow the isolation and identification of host cell interaction partners. These MPM70 constructs could be inducible with tetracycline, or purely constitutive in their expression, which would require the CMV promoter. J774 or U937 cells could be transiently transfected with mycobacterial protein expression vectors to allow expression of the MPM70. MPM70 could then be chemically cross-linked to any bound intracellular targets and extracted from the lysates using chromatography and the eluted fractions analysed by SDS-PAGE. SDS-PAGE bands corresponding to potential protein interaction partners would be excised, trypsin digested and identified by mass spectrometry. With untagged or antibody epitope-tagged proteins, well established immunoprecipitation protocols could be employed to extract MPM70 with any targets bound. As above, SDS-PAGE analysis would allow for target identification by mass spectrometry.

In order to identify the mycobacterial cell-wall associated protein that MPM70 may be binding to, a yeast two-hybrid screen could be employed against a *Mycobacterium marinum* or *Mycobacterium tuberculosis* library. Other two-hybrid models to be considered could include the *M. smegmatis* two-hybrid (mycobacterial protein fragment complement, or M-PFC). An advantage of the *M. smegmatis* two-hybrid system (Singh *et al.*, 2006) is that it allows for expression of MPM70/MPB70 and the anchor protein within a mycobacterial system, which may enhance the chances of an interaction, and

more positive results. However, there may be false positive results if MPM70 interacts with more than one mycobacterial wall component, which could also be present in *M. smegmatis*. Therefore, a combination of yeast and bacterial two-hybrid systems should be considered for the identification of the mycobacterial anchor for MPM70/MPB70.

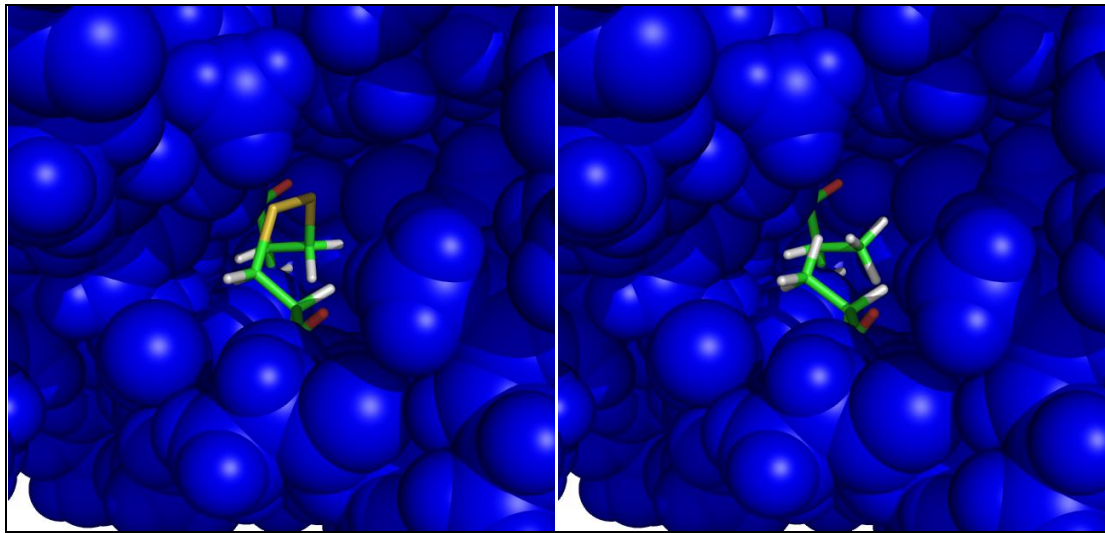


Figure 4.2: Alanine substitution mutation of the C8-C142 disulphide bridge in MPB70, using PyMol. The left image shows a filled-space model of the structure of wild type MPB70 (blue) with the C8 and C142 residues (green) forming a disulphide bridge (yellow). The image on the right shows MPB70 with C8A and C142A substitutions *in silico* (green). Other interacting structural residues should allow the protein to fold correctly without the disulphide bridge formed between the two cysteine residues (Václav Veverka, personal communication).

Mammalian transfection and yeast/bacteria two-hybrid experiments provide a problem for MPM70/MPB70 expression because of the reducing nature of their respective cytoplasmic environments. Using MPB70 as an example, this would not allow the disulphide bridge to form between residues C8 and C142, which may cause problems in

the folding and stability of the protein upon expression. In order to rectify this, the C8-C142 disulphide bridge must be removed from the protein prior to expression, and the residues mutated to amino acids that still form appropriate van der Waal's interactions, allowing the protein to fold stably within the cytoplasm. Structural analysis has shown that it should be possible to engineer MPM70 and MPB70 constructs which lack the disulphide bridge, and this should not be detrimental to the protein structure or folding (Václav Veverka, personal communication). Due to the number of remaining interacting structural residues still present, allowing cysteines 8 and 142 to be mutated without misfolding of the protein (Figure 4.2).

It may be possible to create MPM70 knockout mutants of *M. marinum*, which would allow direct comparison to the wild type strain in the mycobacterial infection model utilised within the work in this thesis, or using animal infection models. This could be done using homologous recombination, where the MPM70 gene, (*MMAR_1834*) is replaced within the genome by an antibiotic resistance cassette in order for mutants to be selected. A similar technique was used to create an ESAT-6 knockout strain of *M. tuberculosis* (Wards *et al.*, 2000), which showed attenuated virulence in a guinea pig infection model. Furthermore, it may be interesting to produce an MPM70 over-expressing *M. marinum* strain by using an extrachromosomal plasmid with a strong promoter like *msh12*, as used to previously create DsRed expressing fluorescent mycobacteria as used in Chapters 2 and 3 of this thesis (Valdavia *et al.*, 1996). This would allow for comparisons with wild type and MPM70 knockout strains to assess MPM70's role in virulence, within cell infection or animal infection models.

References

- Abdallah M.A., Gey van Pittius N.C., DiGiuseppe Champion P.A., Cox J., Luirink J., Vandenbrouke-Grauls C.M.J.E., Appelmelk B.J., and Bitter W. (2007) Type VII secretion - mycobacteria show the way. *Nat. Rev. Micro.* 5: 883-891.
- Allix-Beguec C., Fauville-Dufaux M., Stoffels K., Ommeslag D., Walravens K., Saegerman C., and Supply P. (2010) Importance of identifying mycobacterium bovis as a causative agent of human tuberculosis. *Eur. Respir. J.* 35: 692-694.
- Ala-aho R., and Kahari V.M. (2005) Collagenases in Cancer. *Biochimie.* 87: 273-286.
- Barker, L.P., George K.M., Falkow S., and Small P.L. (1997) Differential trafficking of live and dead *Mycobacterium marinum* organisms in macrophages. *Infect. Immun.* 65: 1497-1504.
- Behr M.A., Wilson M.A., Gill W.P., Salamon H., Schoolnik G.K., Rane S., Small P.M. (1999). Comparative Genomics of BCG Vaccines by Whole-Genome DNA Microarray. *Science.* 284, 1520-1523.
- Billings P.C., Whitbeck J.C., Adams C.S., Abrams W.R., Cohen A.J., Engelsberg B.N., Howard P.S., and Rosenbloom J.. (2002) The transforming growth factor-beta-inducible matrix protein beta ig-h3 interacts with fibronectin. *J. Biol. Chem.* 277: 28003-28009.
- Bloemink M.J., Kemmink J., Dentten E., Muskett F.W., Whelan A., Sheikh A., Hewinson R.G., Williamson R.A., and Carr M.D. (2001) Sequence-specific assignment and determination of the secondary structure of the 163-residue M-tuberculosis and M-bovis antigenic protein mpb70. *J. Biomol. NMR.* 20: 185-186.
- Bouley D.M., Ghori N., Mercer K.L., Falkow S., and Ramakrishnan L. (2001) Dynamic nature of host-pathogen interactions in *Mycobacterium marinum* granulomas. *Infect. Immun.* 69: 7820-7831.
- Braunstein M., Brown A.M., Kurtz S., and Jacobs W.R. Jr. (2001) Two nonredundant SecA homologues function in mycobacteria. *J. Bacteriol.* 183 (24): 6879-6990.
- Brosch, R., Gordon S.V., Garnier T., Eiglmeier K., Frigui W., Valenti P., Dos Santos S., Duthoy S., Lacroix C., Garcia-Pelayo C., Inwald J.K., Golby P., Garcia J.N, Hewinson R.G., Behr M.A., Quail M.A., Churcher C., Barrell B.G., Parkhill J., and Cole S.T. (2007). Genome plasticity of BCG and impact on vaccine efficacy. *PNAS.* 104 (13): 5596-5601.
- Carr M.D., Bloemink M.J., Dentten E., Whelan A.O., Gordon S.V., Kelly G., Frenkiel T.A., Hewinson R.G., and Williamson R.A. (2003) Solution structure of the mycobacterium tuberculosis complex protein MPB70 - from tuberculosis pathogenesis to inherited human corneal disease. *J. Biol. Chem.* 278: 43736-43743.

- Charlet D., Mostowy S., Alexander D., Sit L., Wiker H.G., and Behr M.A. (2005) Reduced expression of antigenic proteins MPB70 and MPB83 in mycobacterium bovis BCG strains due to a start codon mutation in sigK. *Mol. Microbiol.* 56: 1302-1313.
- Cole S.T., Brosch R., Parkhill J., Garnier T., Churcher C., Harris D., Gordon S.V., Eiglmeier K., Gas S., Barry C.E. 3rd, Tekaiia F., Badcock K., Basham D., Brown D., Chillingworth T., Connor R., Davies R., Devlin K., Feltwell T., Gentles S., Hamlin N., Holroyd S., Hornsby T., Jagels K., Krogh A., McLean J., Moule S., Murphy L., Oliver K., Osborne J., Quail M.A., Rajandream M.A., Rogers J., Rutter S., Seeger K., Skelton J., Squares R., Squares S., Sulston J.E., Taylor K., Whitehead S., and Barrell B.G. (1998). Deciphering the biology of *Mycobacterium tuberculosis* from the complete genome sequence. *Nature* 393, 537–544
- Collins C.A., De Maziere A., van Dijk S., Carlsson F., Klumperman J., and Brown E.J. (2009) Atg5-independent sequestration of ubiquitinated mycobacteria. *PLoS Pathog.* 5.
- Cosma C., Chan K., Humbert O., Davis J.M., Falkow S., and Ramakrishnan L. (2002) Identification and characterization of mycobacterium marinum genes expressed in vivo. *Abstracts of the General Meeting of the American Society for Microbiology* 102: 488.
- Cosma C.L., Humbert O., and Ramakrishnan L. (2004) Superinfecting mycobacteria home to established tuberculous granulomas. *Nat. Immunol.* 5: 828-835.
- Cosma C.L., Swaim L.E., Volkman H., Ramakrishnan L., and Davis J.M. (2006) Zebrafish and frog models of mycobacterium marinum infection. *Curr. Protoc. Microbiol.* Chapter 10: Unit 10B.2.
- Daniel T.M., and Janicki B.W. (1978). Mycobacterial antigens: A review of their isolation, chemistry, and immunological properties. *Microbiol. Rev.* 42 (1): 84-113.
- Davis J.M., and Ramakrishnan L. (2009) The role of the granuloma in expansion and dissemination of early tuberculous infection. *Cell.* 136: 37-49.
- Elkins T., Hortsch M., Bieber A.J., Snow P.M., and Goodman C.S. (1990) Drosophila fasciclin-i is a novel homophilic adhesion molecule that along with fasciclin-iii can mediate cell sorting. *J. Cell. Biol.* 110: 1825-1832.
- Escribano J., Hernando N., Ghosh S., Crabb J., and Cocaprados M. (1994) Cdna from human ocular ciliary epithelium homologous to beta-ig-H3 is preferentially expressed as an extracellular protein in the corneal epithelium. *J. Cell. Physiol.* 160: 511-521.
- Faik A., Abouzouhair J., and Sarhan F. (2006). Putative fasciclin-like arabinogalactan-proteins (FLA) in Wheat (*Triticum aestivum*) and Rice (*Oryza sativa*): Identification and bioinformatic analyses. *Mol. Genet. Genom.* 276 (5): 478-494.
- Fifis, T., Costopolous C., Corner L.A., and Wood P.R. (1992) Serological reactivity to *Mycobacterium bovis* protein antigens in cattle. *Vet. Microbiol.* 30: 343-354.

Fratti R.A., Chua J., Vergne I., and Deretic V. (2003) Mycobacterium tuberculosis glycosylated phosphatidylinositol causes phagosome maturation arrest. *Proc. Natl. Acad. Sci. USA.* 100: 5437-5442.

Garcia-Pelayo C., Uplekar S., Keniry A., Lopez M.P., Garnier T., Garcia J.N., Boschioli L., Zhou X., Parkhill J., Smith N., Hewinson G., Cole S.T., and Gordon S.V. A Comprehensive survey of Single Nucleotide Polymorphisms (SNPs) across *Mycobacterium bovis* strains and *M. bovis* BCG vaccine strains refines the genealogy and define a minimal set of SNPs that separate virulent *M. bovis* strains and *M. bovis* BCG strains. *Inf. Immun.* 77: 2230-2238.

Garnier T., Eiglmeier K., Camus J.C., Medina N., Mansoor H., Pryor M., Duthoy S., Grondin S., Lacroix C., Monsempe C., Simon S., Harris B., Atkin R., Doggett J., Mayes R., Keating L., Wheeler P.R., Parkhill J., Barrell B.G., Cole S.T, Gordon S.V., and Hewinson R.G. (2003). The complete genome sequence of *Mycobacterium bovis*. *PNAS.* 100 (13): 7877-7882.

Hagedorn M., Rohde K.H., Russell D.G., and Soldati T. (2009) Infection by tubercular mycobacteria is spread by nonlytic ejection from their amoeba hosts. *Science.* 323: 1729-1733.

Harboe M., Nagai S., Patarroyo M.E., Torres M.L., Ramirez C., and Cruz N. (1986) Properties of proteins Mpb64, Mpb70, and Mpb80 of mycobacterium-bovis bcg. *Infect. Immun.* 52: 293-302.

Harboe M., Wiker H.G., Ulvund G., Lund-Pedersen B., Andersen A.B., Hewinson R.G., and Nagai S. (1998) MPB70 and MPB83 as indicators of protein localization in mycobacterial cells. *Infect. Immun.* 66: 289-296.

Harboe M., Wiker H.G., Duncan J.R., Garcia M.M., Dukes T.W., Brooks B.W., Turcotte C., and Nagai S. (1990). Protein G-based enzyme-linked immunosorbent assay for anti-MPB70 antibodies in bovine tuberculosis. *J. Clin. Microbiol.* 28 (5): 913-921.

Hartmann G., Honikel K.O., Knusel F., and Nuesch J. (1967) The specific inhibition of DNA-directed RNA synthesis by rifamycin. *Biochim. Biophys. Acta.* 145: 843-844.

Hewinson R.G., Harris D.P., Whelan A., and Russell W.P. (1996) Secretion of the mycobacterial 19-kilodalton protein by escherichia coli, a novel method for the purification of recombinant mycobacterial antigens. *Clin. Diagn. Lab. Immunol.* 3: 23-29.

Hewinson R.G., and Russell W.P. (1993) Processing and secretion by *Escherichia coli* of a recombinant form of the immunogenic protein MPB70 of *Mycobacterium bovis*. *J. Gen. Microbiol.* 139: 1253-1259.

Horiuchi K., Amizuka N., Takeshita S., Takamatsu H., Katsuura M., Ozawa H., Toyama Y., Bonewald L.F., and Kudo A.. (1999) Identification and characterization of a novel protein, periostin, with restricted expression to periosteum and periodontal

ligament and increased expression by transforming growth factor beta. *J. Bone. Miner. Res.* 14: 1239-1249.

Huber O., and Sumper M. (1994). Algal-CAMs: Isoforms of a cell adhesion molecule in embryos of the alga *Volvox* with homology to *Drosophila* fasciclin I. *EMBO J.* 13 (18): 4212-4222.

Juarez M.D., Torres A., Espitia C. Characterization of the *Mycobacterium tuberculosis* region containing the *mpt83* and *mpt70* genes. (2001) *FEMS Micro. Lett.* 203; 95-102.

Jordao L., Bleck C.K., Moyarga L., Griffiths G., and Anes E. (2008). On the killing of mycobacteria by macrophages. *Cell. Microbiol.* 10: 529-548.

Junqueira-Kipnis A.P., Basaraba, R.J.; Gruppo, V.; Palanisamy, G.; Turner, O.C.; Hsu, T.; Jacobs, W.R.; Fulton, S.A.; Reba, S.M.; Boom, W.H.; and Orme, I.M. (2006) Mycobacteria lacking the RD1 region do not induce necrosis in the lungs of mice lacking interferon-gamma. *Immunology.* 119: 224-231.

Kannabiran C., and Klintworth G.K. (2006) TGFBI gene mutations in corneal dystrophies. *Hum. Mutat.* 27: 615-625.

Kaufmann S.H.E., and McMichael A.J. (2005) Annulling a dangerous liaison: Vaccination strategies against AIDS and tuberculosis. *Nat. Med.* 11: S33-S44.

Kelley V.A., and Schorey J.S. (2003) *Mycobacterium's* arrest of phagosome maturation in macrophages requires Rab5 activity and accessibility to iron. *Mol. Biol. Cell.* 14 (8): 3366-3377.

Kim H.J., and Kim I.S. (2008) Transforming growth factor-beta-induced gene product, as a novel ligand of integrin alpha(M)beta(2), promotes monocytes adhesion, migration and chemotaxis. *Int. J. Biochem. Cell. Biol.* 40: 991-1004.

Kim J.E., Jeong H.W., Nam J.O., Lee B.H., Choi J.Y., Park R.W., Park J.Y., and Kim I.S. (2002) Identification of motifs in the fasciclin domains of the transforming growth factor-beta-induced matrix protein beta ig-h3 that interact with the alpha v65 integrin. *J. Biol. Chem.* 277: 46159-46165.

Kim J.E., Kim S.J., Lee B.H., Park R.W., Kim K.S., Kim I.S. (2000). Identification of Motifs for cell adhesion within the repeated domains of transforming growth factor-beta-induced gene, betaig-h3. *J. Biol. Chem.* 275 (40): 30907-30915.

Klintworth G.K., Enghild J., and Valnickova Z. (1994) Discovery of a novel protein (beta-ig-H3) in normal human cornea. *Invest. Ophthalmol. Vis. Sci.* 35: 1938-1938.

Lasunskaja E.B., Campos M.N.N., de Andrade M.R.M., DaMatta R.A., Kipnis T.L., Einicker-Lamas M., and Da Silva W.D. (2006) Mycobacteria directly induce cytoskeletal rearrangements for macrophage spreading and polarization through TLR2-dependent PI3K signaling. *J. Leukoc. Biol.* 80: 1480-1490.

Leake E.S., Myrvik Q.N., and Wright M.J. (1984). Phagosomal membranes of *Mycobacterium bovis* BCG-immune alveolar macrophages are resistant to disruption by *Mycobacterium tuberculosis* H37Rv. *Infect. Immun.* 45 (2) 443-446.

Lightbody K.L., Ilghari D., Waters L.C., Carey G., Bailey M.A., Williamson R.A., Renshaw P.S., and Carr M.D. (2008) Molecular features governing the stability and specificity of functional complex formation by mycobacterium tuberculosis CFP-10/ESAT-6 family proteins. *J. Biol. Chem.* 283: 17681-17690.

Lightbody K.L., Renshaw P.S., Collins M.L., Wright R.L., Hunt D.M., Gordon S.V., Hewinson R.G., Buxton R.S., Williamson R.A., and Carr M.D.. (2004) Characterisation of complex formation between members of the mycobacterium tuberculosis complex CFP-10/ESAT-6 protein family: Towards an understanding of the rules governing complex formation and thereby functional flexibility. *FEMS Microbiol. Lett.* 238: 255-262.

Lind A. (1965). Immunologic analysis of mycobacterial antigens. *Am. Rev. Respir. Dis.* 92: 54-62

Lowrie D.B., Tascon R.E., Bonato V.L.D., Lima V.M.F., Faccioli L.H., Stavropoulos E., Colston M.J., Hewinson R.G., Moelling K., and Silva C.L. (1999) Therapy of tuberculosis in mice by DNA vaccination. *Nature.* 400: 269-271.

Malik Z.A., Denning G.M., and Kusner D.J. (2000) Inhibition of Ca²⁺ signaling by mycobacterium tuberculosis is associated with reduced phagosome-lysosome fusion and increased survival within human macrophages. *J. Exp. Med.* 191: 287-302.

Matsumoto S., Matsuo T., Ohara N., Hotokezaka H., Naito M., Minami J., Yamada T. (1995). Cloning and sequencing of a unique antigen MPT70 from *Mycobacterium tuberculosis* H37Rv and expression in BCG using *E.coli*-mycobacteria shuttle vector. *Scand. J. Immuno.* 41 (3): 291-287.

McDonough K.A., Kress Y., and Bloom B.R. (1993). Pathogenesis of tuberculosis: interaction of *Mycobacterium tuberculosis* with macrophages. *Infect. Immun.* 61: 2763-2773.

Miura K., Nagai S., Kinomoto M., Haga S., Tokunaga T. (1983) Comparative studies with various substrains of *Mycobacterium bovis* BCG on the production of an antigenic protein, MPB70. *Infect. Immun.* 39: 540-545.

Munier F.L., Korvatska E., Djemai A., LePaslier D., Zografos L., Pescia G., and Schorderet D.F. (1997) Kerato-epithelin mutations in four 5q31-linked corneal dystrophies. *Nat. Genet.* 15: 247-251.

Musser J.M., Kapur V., Williams D.L., Kreiswirth B.N., van Soolingen D., and van Embden J.D. (1996) Characterization of the catalase-peroxidase gene (katG) and inhA locus in isoniazid-resistant and -susceptible strains of *Mycobacterium tuberculosis* by automated DNA sequencing: restricted array of mutations associated with drug resistance. *J. Infect. Dis.* 173: 196-202.

- Myrvik Q.N., Leake E.S., and Wright M.J. (1984). Disruption of phagosomal membranes of normal alveolar macrophages by the H37Rv strain of *Mycobacterium tuberculosis*. A correlate of virulence. *Am. Rev. Respir. Dis.* 129: 322-328.
- Nagai S., Matsumoto J., and Nagasuga T. (1981). Specific skin-reactive protein from culture filtrate of *Mycobacterium bovis* BCG. *Infect. Immun.* 31 (1): 152-160.
- Panchuk-Voloshina N., Haugland R.P., Bishop-Stewart J., Bhargava M.K., Millard P.J., Mao F., Leung W.Y., and Haugland R.P. (1999) Alexa dyes, a series of new fluorescent dyes that yield exceptionally bright, photostable conjugates. *J. Histochem. Cytochem.* 47: 1179-1188.
- Pfyffer G.E., Auckenthaler R., van Embden J.D.A., and van Soolingen D. (1998) *Mycobacterium canettii*, the smooth variant of M-tuberculosis, isolated from a swiss patient exposed in africa. *Emerg. Infect. Dis.* 4: 631-634.
- Ramakrishnan L. (2004) Using *Mycobacterium marinum* and its hosts to study tuberculosis. *Curr. Sci.* 86: 82-92.
- Ramakrishnan L., and Falkow S. (1994) *Mycobacterium marinum* persists in cultured-mammalian-cells in a temperature-restricted fashion. *Infect. Immun.* 62: 3222-3229.
- Rattan A., Kalia A., Ahmad N. (1998). Multidrug-resistant *Mycobacterium tuberculosis*: Molecular perspectives. *Emerg. Infect. Dis.* 4: 195-209.
- Renshaw P.S., Panagiotidou P., Whelan A., Gordon S.V., Hewinson R.G., Williamson R.A., and Carr M.D. (2002) Conclusive evidence that the major T-cell antigens of the *Mycobacterium tuberculosis* complex ESAT-6 and CFP-10 form a tight, 1 : 1 complex and characterization of the structural properties of ESAT-6, CFP-10, and the ESAT-6-CFP-10 complex - implications for pathogenesis and virulence. *J. Biol. Chem.* 277: 21598-21603.
- Renshaw P.S., Lightbody K.L., Veverka V., Muskett F.W., Kelly G., Frenkiel T.A., Gordon S.V., Hewinson R.G., Burke B., Norman J., Williamson R.A., and Carr M.D. (2005) Structure and function of the complex formed by the tuberculosis virulence factors CFP-10 and ESAT-6. *EMBO J.* 24: 2491-2498.
- Russell D.G. (2007) Who puts the tubercle in tuberculosis? *Nat. Rev. Microb.* 5: 39-47.
- Sassetti C.M., Boyd D. H., Rubin E.J. (2003). Genes required for *Mycobacterium tuberculosis* growth defined by high-density mutagenesis. *Mol. Micro.* 48 (1): 77-84
- Schaible U.E., Collins H.L., and Kaufmann S.H. (1999) Confrontation between intracellular bacteria and the immune system. *Adv. Immunol.* 71: 267-377.
- Schaible U.E., Sturgill-Koszycki S., Schlesinger P.H., and Russell D.G. (1998) Cytokine activation leads to acidification and increases maturation of *Mycobacterium avium*-containing phagosomes in murine macrophages. *J. Immunol.* 160: 1290-1296.

Schnappinger D., Ehrh S., Voskuil M.I., Liu Y., Mangan J.A., Monahan I.M., Dolganov G., Efron B., Butcher P.D., Nathan C., and Schoolnik G.K. (2003) Transcriptional adaptation of mycobacterium tuberculosis within macrophages: Insights into the phagosomal environment. *J. Exp. Med.* 198: 693-704.

Singh A., Mai D., Kumar A., and Steyn A.J.C. (2006) Dissecting virulence pathways of mycobacterium tuberculosis through protein-protein association. *Proc. Natl. Acad. Sci. USA.* 103: 11346-11351.

Slayden R.A., Barry C.E. (2000) The genetics and biochemistry of isoniazid resistance in mycobacterium tuberculosis. *Microbes. Infect.* 2: 259-269.

Smith J., Manoranjan J., Pan M., Bohsali A., Xu J.J., Liu J., McDonald K.L., Szyk A., LaRonde-LeBlanc N., and Gao L.Y.. (2008) Evidence for pore formation in host cell membranes by ESX-1-secreted ESAT-6 and its role in mycobacterium marinum escape from the vacuole. *Infect. Immun.* 76: 5478-5487.

Smith N.H., Crawshaw T., Parry J., and Birtles R.J. (2009) Mycobacterium microti: More diverse than previously thought. *J. Clin. Microbiol.* 47: 2551-2559.

Sreevatsan S., Pan X., Stockbauer K.E., Connell N.D., Kreiswirth B.N., Whittam T.S., and Musser J.M. (1997) Restricted structural gene polymorphism in the mycobacterium tuberculosis complex indicates evolutionarily recent global dissemination. *Proc. Natl. Acad. Sci. USA.* 94: 9869-9874.

Stamm L.M., Pak M.A., Morisaki J.H., Snapper S.B., Rottner K., Lommel S., and Brown E.J. (2005) Role of the WASP family proteins for mycobacterium marinum actin tail formation. *Proc. Natl. Acad. Sci. USA.* 102: 14837-14842.

Stamm L.M., Morisaki J.H., Gao L.Y., Jeng R.L., McDonald K.L., Roth R., Takeshita S., Heuser J., Welch M. and Brown E.J.. (2003) Mycobacterium marinum escapes from phagosomes and is propelled by actin-based motility. *J. Exp. Med.* 198: 1361-1368.

Stevens M.P., Stevens J.M., Jeng R.L., Taylor L.A., Wood M.W., Hawes P., Monaghan P., Welch M.D., and Galyov E.E. (2005) Identification of a bacterial factor required for actin-based motility of burkholderia pseudomallei. *Mol. Microbiol.* 56: 40-53.

Stinear T.P., Seemann T., Harrison P.F., Jenkin G.A., Davies J.K., Johnson P.D.R., Abdellah Z., Arrowsmith C., Chillingworth T., Churcher C., Clarke K., Cronin A., Davis P., Goodhead I., Holroyd N., Jagels K., Lord A., Moule S., Mungall K., Norbertczak H., Quail M.A., Rabinowitsch E., Walker D., White B., Whitehead S., Small P.L.C, Brosch R., Ramakrishnan L., Fischbach M.A., Parkhill J., and Cole S.T. (2008) Insights from the complete genome sequence of mycobacterium marinum on the evolution of mycobacterium tuberculosis. *Genome Res.* 18: 729-741.

Tan T., Lee W.L., Alexander D.C., Grinstein S., and Liu J. (2006) The ESAT-6/CFP-10 secretion system of mycobacterium marinum modulates phagosome maturation. *Cell. Microbiol.* 8: 1417-1429.

- Taniguchi H., Aramaki H., Nikaido Y., Mizuguchi Y., Nakamura M., Koga T., Yoshida S. (1996) Rifampicin resistance and mutation of the *rpoB* gene in *Mycobacterium tuberculosis*. *FEMS Microbiol. Lett.* 144: 103-108.
- Tobin D.M., and Ramakrishnan L. (2008) Comparative pathogenesis of *Mycobacterium marinum* and *Mycobacterium tuberculosis*. *Cell. Microbiol.* 10: 1027-1039.
- Unlstrup J.C., Jeansson S., Wiker H.G., Harboe M. (1995). Relationship of secretion pattern and MPB70 homology with osteoblast-specific factor 2 to osteitis following *Mycobacterium bovis* BCG vaccination. *Infect. Immun.* 63 (2): 672-675.
- Valdivia R.H., Hromockyj A.E., Monack D., Ramakrishnan L., and Falkow S. (1996) Applications for green fluorescent protein (GFP) in the study of host-pathogen interactions. *Gene.* 173: 47-52.
- van der Wel N., Hava D., Houben D., Fluitsma D., van Zon M., Pierson J., Brenner M., and Peters P.J. (2007) *M. tuberculosis* and *M. leprae* translocate from the phagolysosome to the cytosol in myeloid cells. *Cell.* 129: 1287-1298.
- van Soolingen D., Hoogenboezem T., deHaas P.E.W., Hermans P.W.M., Koedam M.A., Teppema K.S., Brennan P.J., Besra G.S., Portaels F., Top J., Schouls L.M, and van Embden J.D.A. (1997) A novel pathogenic taxon of the *Mycobacterium tuberculosis* complex, *canetti*: Characterization of an exceptional isolate from Africa. *Int J. Syst. Bacteriol.* 47: 1236-1245.
- Vergne I., Chua J., and Deretic V. (2003a) *Mycobacterium tuberculosis* phagosome maturation arrest: selective targeting of PI3P-dependent membrane trafficking. *Traffic.* 4: 600-606.
- Vergne I., Fratti R.A., Hill P.J., Chua J., Belisle J., and Deretic V. (2003b) *Mycobacterium tuberculosis* phagosome maturation arrest: mycobacterial phosphatidylinositol analog phosphatidylinositol mannoside stimulates early endosomal fusion. *Mol. Biol. Cell.* 15 (2): 751-760.
- Volkman H.E., Pozos T.C., Zheng J., Davis J.M., Rawls J.F., and Ramakrishnan L. (2010) Tuberculous granuloma induction via interaction of a bacterial secreted protein with host epithelium. *Science.* 327: 466-469.
- Vordermeier H.M., Cockle P.J., Whelan A.O., Rhodes S., Chambers M.A., Clifford D., Huygen K., Tascon R., Lowrie D., Colston M.J., and Hewinson R.G. (2000) Effective DNA vaccination of cattle with the mycobacterial antigens MPB83 and MPB70 does not compromise the specificity of the comparative intradermal tuberculin skin test. *Vaccine.* 19: 1246-1255.
- Wards B.J., de Lisle G.W., and Collins D.M. (2000) An *esat6* knockout mutant of *Mycobacterium bovis* produced by homologous recombination will contribute to the development of a live tuberculosis vaccine. *Tuberc. and Lung Dis.* 80 (4-5): 185-189.

Welch M.D., Iwamatsu A., and Mitchison T.J. (1997) Actin polymerization is induced by Arp2/3 protein complex at the surface of *listeria monocytogenes*. *Nature*. 385: 265-269.

World Health Organisation. (2009) Global tuberculosis control 2009: Epidemiology, strategy, financing.

World Health Organisation. (2004) Global Tuberculosis Control – Surveillance, planning, financing.

World Health Organisation. (2006) WHO global task force outlines measures to combat XDR-TB worldwide.

Zhang Y., Heym B., Allen B., Young D., and Cole S. (1992). The catalase-peroxidase gene and isoniazid resistance of *Mycobacterium tuberculosis*. *Nature*. 358: 591-593.